becomes orthorhombic, nor in the FM region, where a increases linearly and b decreases. If the plot of a versus T below T_c is extrapolated back to T_N (see Fig. 1), a linear increase in a is predicted over the HM region. This increase approximates the experimental jump that occurs at the HM-FM transition. (The same may also be true for the decrease in b over the same regions, but the experimental scatter below T_c is too severe to permit much more than guesswork.) The above is suggestive that, in the HM region, there are missing basal strains somehow stored in the lattice, perhaps as torsional strains, and that these are released at the HM-FM transition. There are a number of conceivable configurations such strains might take, the most interesting possibility being a macroscopic twist about the c axis of a single crystal.

PHYSICAL REVIEW VOLUME 156, NUMBER 2 10 APRIL 1967

Theory of Critical-Point Scattering and Correlations. I. The Ising Model

MICHAEL E. FISHER*
Baker Laboratory, Cornell University, Ithaca, New York

AND

ROBERT J. BURFORD
Wheatstone Physics Laboratory, King's College, London, England

(Received 19 October 1966)

The theory of the correlations and critical scattering of two- and three-dimensional nearest-neighbor Ising models is discussed critically. A distinction is drawn between $\kappa(T)$, the true inverse range of exponential decay of the correlations, and $\kappa_1(T)$, the effective range determined from the low-angle scattering intensity. Ten to eleven terms of appropriate high-temperature series exapnsions for κ and κ_1 are determined for the square and simple cubic lattices, and shorter series are given for the triangular, fcc, and bcc lattices. For the former lattices, the complete correlation expansions are obtained to the same order. It is shown that κ and κ_1 vary as $(T-T_0)^\nu$ when $T\to T_c$, with $\nu=1$ for dimensionality $d=2$, but $\nu=0.6430\pm0.0025\simeq 9/14$ for $d=3$. The asymptotic decay of correlation *at* $T=T_c$ is found to be $1/r^{d-2+\eta}$, where η is related to the exponent γ of the divergence of the susceptibility by $(2-\eta)\nu=\gamma$, Numerical values are $\eta=\frac{1}{4}$ for $d=2$ and $\eta=0.056\pm0.008\simeq 1/18$ for $d=3$. The relative scattering intensity $\hat{\chi}$ as a function of wave number $\mathbf{k}$ is given to high accuracy for all $T\gtrsim T_c$ by

$$\hat{\chi}(\mathbf{k},T)\simeq\left(\frac{a}{r_1}\right)^{2-\eta}\frac{[(\kappa_1 a)^2+\phi^2 a^2K^2(\mathbf{k})]^{\eta/2}}{[(\kappa_1 a)^2+\psi a^2K^2(\mathbf{k})]},$$

where (i) a is the lattice spacing, (ii) $a^2K^2=2d[1-q^{-1}\sum\exp(i\mathbf{k}\cdot\mathbf{r})]\simeq(ka)^2$, the sum being over the q nearest-neighbor lattice sites, (iii) $r_1(T)$ is a slowly-varying decreasing function near T_c, (iv) $\psi=1+\frac{1}{2}\eta\phi^2$, and (v) $\phi(T)$ is slowly varying with a magnitude at T_c of 0.03 for $d=2$ and of 0.06 to 0.09 for $d=3$. Explicit formulas are given for κ_1, r_1, and ϕ as functions of T. The correlations and the scattering are isotropic near T_c. The critical scattering isotherm is curved for low k according to $\hat{\chi}^{-1}\sim k^{2-\eta}$ and it *intersects* the isotherms for $T>T_c$. Correspondingly, $\hat{\chi}(\mathbf{k},T)$ exhibits a maximum for fixed $\mathbf{k}$, at a temperature *above* T_c; for $d=2$ the maxima are very well marked, but for $d=3$ they are smaller and occur closer to T_c. The theory is compared favorably with recent neutron-scattering experiments on pure beta-brass.

1. INTRODUCTION

IN the vicinity of and just above the critical point of gas-liquid phase separation in a simple fluid one observes a striking increase in light scattering at low angles long known as the phenomenon of *critical opalescence*. Similar *critical scattering* is observed with light and x rays at upper and lower critical points for phase separation of binary fluid mixtures. The analogous phenomenon of the critical magnetic scattering of neutrons at a ferromagnetic critical (or Curie) point was first reported thirteen years ago. More recently, critical scattering has also been observed at *antiferromagnetic* critical points (or Néel points). With x rays and neutrons one may equally well observe critical scattering in binary metallic alloys at points of order-disorder transformation.[1]

Following the original suggestion of Smoluchowski, it is recognized in all these cases that the greatly enhanced scattering is due to the rapid increase in the spatial range of the inhomogeneity fluctuations occuring

* To whom requests for reprints should be sent.

[1] A useful review and survey of the background theory has been given by A. Münster, in *Fluctuation Phenomena in Solids*, edited by R. E. Burgess (Academic Press Inc., New York, 1965), Chap. 6.

within the medium as the critical point is approached. In single-component fluids the density fluctuations are the relevant quantity; for binary fluids and alloys composition fluctuations are principally responsible; while for ferromagnets and antiferromagnets the fluctuations of magnetization and sublattice magnetization, respectively, are the underlying cause of the scattering. The essential theoretical point in each case is that the scattering is proportional to the Fourier transform of an appropriate equilibrium pair correlation function (assuming that "multiple scattering" may be neglected or corrected for and that the static approximation is valid) so that a theoretical study of critical scattering reduces to an analysis of the appropriate correlation functions in the critical region.[1]

The first, and still fundamental, theoretical treatment is the famous work of Ornstein and Zernike (O.Z.).[2] This rests mainly on a crucial assumption concerning the finite range of the so-called *direct correlation function*, from which immediately follows the familiar prediction that the (net) correlation function *at* the critical point should decay asymptotically with distance as $1/r$ ($r\to\infty$). Many authors have sought to rederive the Ornstein-Zernike theory and to justify this underlying assumption. In recent years, however, it has been suggested that the O.Z. assumption may be incorrect and that the decay should rather be of the form $1/r^{1+\eta}$ with $\eta>0$.

The various derivations of the Ornstein-Zernike theory and the newer general theories have been reviewed critically quite recently.[3] The aim of the researches here reported was to calculate the correlation functions and thence the critical scattering as accurately as possible for specific many-body models. Until a rigorous general theory is found, this seems to be the best method of judging the validity of the Ornstein-Zernike and other approximate theories and, in as far as the models chosen are reasonably realistic, it also yields numerical predictions which may be usefully compared with experimental data in a variety of fields.

A rigorous mathematical treatment of one such model system has been presented by Uhlenbeck, Kac, and Hemmer[4] for the one-dimensional Van der Waals fluid in which the particles interact through forces of essentially infinite range. Their results are, in fact, in accord with the Ornstein-Zernike predictions. As has been argued previously, however, the critical-point behavior of most real systems is crucially dependent on the finite or relatively short-range character of the underlying interactions.[3,5] Consequently, the Van der Waals models, although of general theoretical interest, are not appropriate guides to the validity of the Ornstein-Zernike theory, in applications to real systems.

Essentially the only rigorous results for any model with short-range forces are various formulas obtained by Onsager and Kaufman[6,7] for the correlation functions of the two-dimensional square-lattice Ising model with nearest-neighbor interactions. As will be explained below they obtained, in particular, an explicit expression for the pair correlation function *at* the critical point which can be used to show that the Ornstein-Zernike theory and various other treatments cannot be correct in two dimensions.[8–10] Unfortunately, however, the available rigorous results do not extend to the complete scattering function of the plane Ising model, and no rigorous explicit formulas are known for the more interesting three-dimensional Ising lattices.

In the present paper we aim at the evaluation of the correlations and complete scattering functions for two- and three-dimensional Ising models in zero magnetic field for temperatures at and above critical. Our analysis is based on the extrapolation of extensive series expansions for the pair correlation functions and enables us to conclude with confidence that the Ornstein-Zernike theory is also incorrect in three dimensions. (Fairly simple explicit approximation formulas are obtained.) If, however, account is taken of the "nonclassical" behavior of the equation of state near the critical point,[3,5] the deviations from the Ornstein-Zernike predictions at small scattering angles turn out to be fairly small numerically since the parameter η appears to have a value of about $0.056\simeq 1/18$. At larger scattering angles, however, which are not discussed in the simple O.Z. theory, "structural" deviations occur whose magnitude may now be realistically assessed.

For convenience the Ising model is discussed below mainly in "magnetic language," the analysis applying both to ferromagnetic and antiferromagnetic interactions. As is well known, however, the Ising model is also equivalent to a lattice gas[11] and hence describes gas-liquid critical phenomena in single-component fluids. Furthermore the Ising model may equally be regarded as a model of a two-component fluid or a binary alloy.[11] Indeed it has often been felt that it should provide quite a realistic model of a binary alloy undergoing an order-disorder transition. Gratifyingly, recent accurate neutron scattering experiments on pure β-brass suggest an even closer correspondence with the properties of the three-dimensional Ising model than has been suspected.[12]

---

[2] L. S. Ornstein and F. Zernike, Proc. Acad. Sci. Amsterdam **17**, 793 (1914); Z. Physik **19**, 134 (1918); **27**, 761 (1926).

[3] M. E. Fisher, J. Math. Phys. **5**, 944 (1964).

[4] M. Kac, G. E. Uhlenbeck, and P. C. Hemmer, J. Math. Phys. **4**, 216 (1963); G. E. Uhlenbeck, P. C. Hemmer, and M. Kac, *ibid.* **4**, 229 (1963); **5**, 60 (1964).

[5] M. E. Fisher, in *Lectures in Theoretical Physics* (University of Colorado Press, Boulder, Colorado, 1965), Vol. VII C.

[6] L. Onsager, Phys. Rev. **65**, 117 (1944).

[7] B. Kaufman and L. Onsager, Phys. Rev. **76**, 1244 (1949).

[8] M. E. Fisher, Physica **25**, 521 (1959).

[9] F. H. Stillinger and H. L. Frisch, Physica **27**, 751 (1961).

[10] M. E. Fisher, Physica **28**, 172 (1962).

[11] See, for example, the reviews Ref. 5, Ref. 13, and C. Domb, Advan. Phys. **9**, 149 (1960).

[12] J. Als-Nielsen and O. Dietrich, Phys. Rev. **153**, 706 (1967); O. Dietrich and J. Als-Nielsen, *ibid.* **153**, 711 (1967); J. Als-Nielsen and O. Dietrich, *ibid.* **153**, 717 (1967).

The layout of the paper is as follows: In the next section the Ising model and its relevant properties are defined explicitly and the relation to the lattice gas and binary alloy models is sketched briefly for completeness. Various formal relations, definitions of moments and ranges of correlation, etc. are presented in Sec. 3. The standard approximate theories, mean field theory and the Elliott-Marshall-Bethe approximation, are reviewed in Sec. 4 in order to bring out clearly the difference between the "true" and "effective" ranges of correlation. The important exact results known for the plane Ising models are presented and analyzed in Sec. 5 to reveal the defects of the classical theories. The more general forms for the scattering that must be expected are described and discussed in Sec. 6 (which may be read as a summary of the general theoretical conclusions). The formulation of the high-temperature expansions and the techniques used to derive appropriately many terms are presented in Sec. 7. The resulting expansions, etc. are collected in the Appendices. Section 8 is devoted to numerical analysis of the series to obtain accurate estimates of the exponent η and the related exponent ν for the divergence of the range of correlation as $T-T_c$ vanishes. These results are summarized in Sec. 8.4. Explicit formulas for the evaluation of the effective and true correlation ranges are derived in Sec. 9. More detailed aspects of the correlation functions and the scattering are analyzed in Sec. 10. Finally in Sec. 11 the calculations are summarized, tested, and their consequences reviewed and compared briefly with the experiments on β-brass.[12] The reader uninterested in the details of the theory or calculations should skim through the definitions in Secs. 2 and 3, consult Sec. 6 and read Sec. 11, especially the concluding Secs. 11.5 and 11.6. A glossary of the principal symbols employed and their definitions is included (Appendix E) for ease of cross reference.

Preliminary reports of some of our work have been presented before.[3,13–15] The present paper largely supercedes an earlier tentative analysis[10] (which suggested rather larger deviations from the Ornstein-Zernike predictions in three dimensions). A following paper will be devoted to the Heisenberg model which should be a more realistic model for magnetic systems. In the future, it is hoped to discuss the Ising model at temperatures below the critical point and in general magnetic fields.

2. NOTATION

In this section we specify the model, namely the Ising model of a magnetic system, sketch its connection to the lattice gas and binary alloy models, and introduce the notation.[11]

2.1 Lattice

Let $i=1, 2, 3, \cdots N$ label the sites of a regular d-dimensional space lattice in which the position vector of the ith site is $\mathbf{r}_i$ and the volume per site is v_0. Each site (away from the edge) has a coordination number q and a set of equivalent nearest-neighbor lattice vectors $\boldsymbol{\delta}$ of length a. When convenient, the lattice will be regarded as wrapped on a torus so as to have no free edges. For the standard lattices we have

square	$d=2$,	$q=4$,	$v_0=a^2$,
triangular	$d=2$,	$q=6$,	$v_0=(3^{1/2}/2)a^2$,
sc	$d=3$,	$q=6$,	$v_0=a^3$,
bcc	$d=3$,	$q=8$,	$v_0(4/3^{3/2})a^3$,
fcc	$d=3$,	$q=12$,	$v_0=2^{-1/2}a^3$.

For the three cubic lattices the edge length of the cubic cell is

$$a'=(q/2d)^{1/2}a.$$

The fundamental nearest-neighbor Fourier transform (or lattice generating function) is defined by

$$\hat{q}(\mathbf{k})=q\hat{\gamma}(\mathbf{k})=\sum_{\mathbf{r}=\boldsymbol{\delta}} e^{i\mathbf{k}\cdot\mathbf{r}}$$
$$=q[1-(1/2d)k^2a^2+O(k^4a^4)], \qquad (2.1)$$

where the "momentum transfer" or wave vector $\mathbf{k}$ ranges over the appropriate Brillouin zone $[-(\pi/a)\leqslant k_x, k_y, k_z\leqslant(\pi/a)$ for the simple cubic lattice$]$. Because of the all-pervading nature of the lattice structure it is useful to define an *effective wave vector* $K(\mathbf{k})$ by

$$K^2(\mathbf{k})=2d[1-\hat{\gamma}(\mathbf{k})]/a^2$$
$$=k^2\{1+O(k^2a^2)\}, \qquad (2.2)$$

so that K becomes equal to k as $k\to 0$ (low angles).

2.2 Ising Model

The Hamiltonian of the spin-$\frac{1}{2}$ Ising model in a field H is

$$\mathcal{H}=-\sum_{(ij)} J(\mathbf{r}_{ij})s_is_j-mH\sum_{i=1}^{N} s_i, \qquad (2.3)$$

where the spin variables $s_i=2S_i^z$ take the values ± 1 and the first sum runs over all pairs of spins. The parameters $J(\mathbf{r})$ are the exchange integrals defined to be positive for ferromagnetic interactions but negative for antiferromagnetic interactions. In the nearest-neighbor model, which we shall consider, $J(\boldsymbol{\delta})=J$, but $J(\mathbf{r})=0$ if $\mathbf{r}$ is not a nearest-neighbor vector. The magnetic moment per spin of $\frac{1}{2}g\mu_B$ (in standard notation) is denoted by m. A convenient temperature variable is

$$v=\tanh(J/k_BT). \qquad (2.4)$$

[13] M. E. Fisher, in *Critical Phenomena*, edited by M. S. Green and J. V. Sengers (National Bureau of Standards, Washington, D. C., 1966).

[14] R. J. Burford, (a) in International Conference on Statistical Mechanics and Thermodynamics, Aachen, 1964 (unpublished); (b) Ph.D. thesis, University of London, 1966 (unpublished), available for loan or copying.

[15] M. E. Fisher, in *Proceedings of the International Conference on Magnetism, Nottingham, 1964* (The Institute of Physics and The Physical Society, London, 1965).

As T falls from ∞ to 0, the variable v runs from 0 to 1 for a ferromagnet but 0 to -1 for an antiferromagnet.

The reduced spin pair correlation function may be defined generally by

$$\Gamma(\mathbf{r})=[\langle s_0 s_r\rangle-\langle s_0\rangle^2]/[\langle s_0^2\rangle-\langle s_0\rangle^2], \qquad (2.5)$$

where s_0 denotes a typical spin (assuming translational invariance), s_r denotes the spin at relative separation $\mathbf{r}$, and the angular brackets indicate the thermodynamic expectation value in an infinite system. For $T\gtrsim T_c$ and $H=0$, one has, by symmetry and the absence of long-range order, $\langle s_0\rangle\equiv 0$ so that the correlation function reduces to

$$\Gamma(\mathbf{r})=\langle s_0 s_r\rangle, \quad (H=0,\ T\gtrsim T_c). \qquad (2.6)$$

The fluctuation theorem for the susceptibility per spin states that

$$\chi_T=(\partial M/\partial H)_T=m(\partial\langle s_0\rangle/\partial H)_T$$
$$=(m^2/k_B T)\sum_{\mathbf{r}}[\langle s_0 s_r\rangle-\langle s_0\rangle^2], \qquad (2.7)$$

so that in zero field above T_c we have

$$(k_B T/m^2)\chi_T=\chi_0=1+\sum_{\mathbf{r}=0}\Gamma(\mathbf{r}). \qquad (2.8)$$

If radiation of wavelength λ is scattered through an angle θ with change of wave number $\mathbf{k}$ so that for $d=3$, $|\mathbf{k}|=k=(4\pi/\lambda)\sin\frac{1}{2}\theta$, the diffuse magnetic scattering intensity (in the static approximation) is given by

$$I(\mathbf{k})/I_0(\mathbf{k})=\hat{\chi}(\mathbf{k})=1+\hat{\Gamma}(\mathbf{k}), \qquad (2.9)$$

where

$$\hat{\Gamma}(\mathbf{k})=\sum_{\mathbf{r}\neq 0} e^{i\mathbf{k}\cdot\mathbf{r}}\langle s_0 s_r\rangle, \qquad (2.10)$$

and $I_0(\mathbf{k})$ is the scattering from an ideal assembly of noninteracting spins. The result (2.9) indicates that $\hat{\chi}(\mathbf{k},T)$ is the function of principal theoretical interest. By virtue of (2.8) we have the important relation for zero-angle scattering, namely,

$$\lim_{k\to 0}\hat{\chi}(\mathbf{k})=\hat{\chi}(0)=\chi_0=(k_B T/m^2)\chi_T$$
$$=\chi_T/\chi_T^{\text{ideal}}. \qquad (2.11)$$

Finally, we remark that from the Hamiltonian (2.3) it is evident that the configurational energy U per spin in zero field satisfies

$$U=-\tfrac{1}{2}qJ\langle s_0 s_\delta\rangle, \qquad (2.12)$$

where s_δ denotes a near neighbor of s_0.

2.3 Lattice Gas

In the lattice-gas model the particles occupy the sites of the lattice and interact through a pair potential $\varphi(\mathbf{r})$ (defined only for the lattice vectors). Correspondence with the nearest-neighbor Ising model is obtained if

$$\varphi(\mathbf{r})=+\infty, \quad r=0$$
$$=-4J, \quad r=a$$
$$=0, \quad \text{otherwise}. \qquad (2.13)$$

On identifying an "up" spin $s_i=+1$ with a vacant site and a "down" spin $s_i=-1$ with an occupied site, the density ρ of the gas is seen to be related to the magnetization M of the magnet through

$$\rho/\rho_{\max}=[1-(M/m)]=\tfrac{1}{2}(1-\langle s_0\rangle), \qquad (2.14)$$

where $\rho_{\max}=1/v_0$. The restriction to zero field and $T>T_c$ thus corresponds to

$$\rho=\tfrac{1}{2}\rho_{\max}=\rho_c, \qquad (2.15)$$

i.e., to the critical isochore. The isothermal compressibility K_T is related to susceptibility via

$$4v_0\rho^2 K_T=(\chi_T/m^2), \qquad (2.16)$$

while the pair correlation function or radial distribution function $g_2(\mathbf{r})$ is related to the spin correlations by

$$\rho v_0 G(\mathbf{r})=\rho v_0[g_2(\mathbf{r})-1]=\Gamma(\mathbf{r}). \qquad (2.17)$$

The fluctuation relation (2.8) then reduces to the standard compressibility integral relation[3] with $\int d\mathbf{r}$ replaced by $\sum_{\mathbf{r}} v_0$ as is natural for a lattice gas. Similarly the Fourier transforms are related by

$$\rho\hat{G}(\mathbf{k})=\rho\sum_{\mathbf{r}\neq 0} v_0 e^{i\mathbf{k}\cdot\mathbf{r}}G(\mathbf{r})=\hat{\Gamma}(\mathbf{k}). \qquad (2.18)$$

Consequently (2.9) becomes the usual expression for the scattering in terms of the pair density correlations. Other useful relations between the lattice gas and Ising magnet have been tabulated in Ref. 13.

2.4 Binary Alloy

For a binary alloy model one represents one species, say A, by up spins and the other, say B, by down spins. The fractional composition variables are then

$$x_A=\tfrac{1}{2}[1+\langle s_0\rangle], \quad x_B=\tfrac{1}{2}[1-\langle s_0\rangle], \qquad (2.19)$$

and so the restriction to zero magnetic field corresponds to the symmetrical composition $x_A=x_B=\frac{1}{2}$. If the energies for neighboring AA, AB, and BB pairs are ϵ_{AA}, ϵ_{AB}, and ϵ_{BB} correspondence with the Ising model is obtained by setting

$$\epsilon=\epsilon_{AB}-\tfrac{1}{2}(\epsilon_{AA}+\epsilon_{AB})=J. \qquad (2.20)$$

Note that a tendency to ordering on alternate sublattices corresponds to $\epsilon<0$ and hence to antiferromagnetism. The short-range ordering may be described by specifying the fractions $x_{AA}(\mathbf{r})$, $x_{AB}(\mathbf{r})=x_{BA}(\mathbf{r})$, and $x_{BB}(\mathbf{r})$ of pairs of atoms occupying sites separated by a vector $\mathbf{r}$. These probabilities may be expressed in terms of a single order parameter which may be chosen

equal to the spin pair correlation function $\Gamma(\mathbf{r})$. Thus one finds

$$\begin{aligned} x_{AA}(\mathbf{r}) &= x_A{}^2[1+(x_B/x_A)\Gamma(\mathbf{r})], \\ x_{AB}(\mathbf{r}) &= x_A x_B[1-\Gamma(\mathbf{r})], \\ x_{BB}(\mathbf{r}) &= x_B{}^2[1+(x_A/x_B)\Gamma(\mathbf{r})]. \end{aligned} \tag{2.21}$$

The diffuse scattering from a crystal will then be given by the previous expression (2.9), where $I_0(\mathbf{k})$ is now the scattering intensity corresponding to a completely randomly mixed crystal.[1] (For the scattering to be observable the scattering powers of A and B atoms must, of course, be different.)

3. FORMAL RELATIONS

3.1 Antiferromagnetic Symmetry

For simple antiferromagnetic ordering to be possible under nearest-neighbor interactions, it is necessary for the lattice to be decomposable into two equivalent sublattices such that all the nearest-neighbor sites of a given site lie on the opposite sublattice. For such "loose-packed lattices" (which contain no polygons of odd order), the scattering function has a fundamental symmetry which may be established as follows. The Hamiltonian (2.3) in zero field is invariant under the transformation $J \rightarrow -J$ (or $v \rightarrow -v$) and $\{s_i^-\} \rightarrow \{-s_i^-\}$, where $\{s_i^-\}$ denotes the set of spins on the "odd" sublattice. Correspondingly the spin pair correlation functions transform as

$$\Gamma(\mathbf{r},v) = \langle s_0 s_r \rangle \rightarrow (-)^{\sigma(\mathbf{r})}\Gamma(\mathbf{r},-v), \tag{3.1}$$

where $\sigma(\mathbf{r})$ is an odd or even integer according to the (relative) parity of the site $\mathbf{r}$. By introducing the superlattice wave vector $\mathbf{k}_0$ where, using standard cubic (or square) cell coordinates,

$$\mathbf{k}_0 a = (\pi,\pi) \text{ (square)}, \quad \mathbf{k}_0 a = (\pi,\pi,\pi) \text{ (sc)}$$

or

$$\mathbf{k}_0 a' = (\tfrac{1}{2}\pi,\tfrac{1}{2}\pi,\tfrac{1}{2}\pi) \text{ (bcc)}, \tag{3.2}$$

we may write

$$(-)^{\sigma(\mathbf{r})} = e^{-i\mathbf{k}_0\cdot\mathbf{r}}. \tag{3.3}$$

Then by (2.9)

$$\begin{aligned} \hat{\chi}(\mathbf{k},-v) &= 1+\sum_{r\neq 0} e^{i\mathbf{k}\cdot\mathbf{r}}e^{i\mathbf{k}_0\cdot\mathbf{r}}\Gamma(\mathbf{k},v) \\ &= \hat{\chi}(\mathbf{k}+\mathbf{k}_0, v). \end{aligned} \tag{3.4}$$

This result may be rewritten as

$$\hat{\chi}_{\text{Anti}}(\mathbf{k}-\mathbf{k}_0; T) = \hat{\chi}_{\text{Ferro}}(\mathbf{k}; T), \tag{3.5}$$

which shows that the zero-field scattering from an Ising antiferromagnet measured with respect to the superlattice wave vector $\mathbf{k}_0$ is identical with the corresponding low-angle ($k \simeq 0$) scattering from the ferromagnet at the same temperature. (A similar result is valid for the Heisenberg model in the limit of infinite spin but does not hold for finite spin.)

We may notice that the basic lattice transform (2.2) for a loose-packed lattice satisfies

$$\hat{\gamma}(\mathbf{k}-\mathbf{k}_0) = -\hat{\gamma}(\mathbf{k}). \tag{3.6}$$

Consequently, *if* $\hat{\chi}(\mathbf{k},v)$ depends on $\mathbf{k}$ only through a dependence on $\hat{\gamma}(\mathbf{k})$ (as is found to be true in a fairly good approximation and might even be true generally in two dimensions) then $\hat{\chi}$ must be a function of $v\hat{\gamma}(\mathbf{k})$ and v^2 alone.

3.2 Moments

The spherical moments of the correlation functions may be defined formally by

$$\mu_t(v) = \sum_{\mathbf{r}\neq 0} (r/a)^t \Gamma(\mathbf{r},v). \tag{3.7}$$

For sufficiently high temperatures (in fact for $T > T_c$), the correlations will be bounded by an exponentially decaying function (see below) so the moments will exist for all t. Evidently by (2.8) one has

$$1+\mu_0(v) = \chi_0(v), \tag{3.8}$$

and from (2.9) and (2.10)

$$\hat{\chi}(\mathbf{k},v) = \chi_0(v) - (1/2d)\mu_2(v)k^2a^2 + O(k^4a^4). \tag{3.9}$$

To study the angular symmetry of the correlations (see Sec. 10.1) one may also define Cartesian moments on the simple cubic lattice by

$$\mu_{f,g,h}(v) = \sum_{\mathbf{r}} (x/a)^f (y/a)^g (z/a)^h \Gamma(\mathbf{r},v) \tag{3.10}$$

for integral f, g, and h and with a similar definition for the square lattice.

3.3 Inverse Scattering and "Direct" Correlations

Since the scattering intensity at low angles becomes indefinitely large near the critical point, it is useful both experimentally and theoretically to examine the inverse scattering intensity which may be written

$$1/\hat{\chi}(\mathbf{k}) = 1-\hat{H}(\mathbf{k}), \tag{3.11}$$

with

$$\hat{H}(\mathbf{k}) = \hat{\Gamma}(\mathbf{k})/[1-\hat{\Gamma}(k)]. \tag{3.12}$$

This latter function $\hat{H}(\mathbf{k})$ is the Fourier transform of a function[16] $H(\mathbf{r})$ which in lattice-gas terms is equal to $\rho v_0 C(\mathbf{r})$, where $C(\mathbf{r})$ is the *direct correlation function* as first defined by Ornstein and Zernike through the relation[2,3]

$$1+\rho\hat{G}(\mathbf{k}) = 1/[1-\rho\hat{C}(\mathbf{k})]. \tag{3.13}$$

For temperatures above T_c we expect to have ex-

[16] The usefulness of this function in the magnetic case has been pointed out by P. G. DeGennes, J. Phys. Chem. Solids **6**, 43 (1958).

pansions of the form

$$1/\hat{\chi}(\mathbf{k},v)=\chi_0^{-1}\{1+\Lambda_2(v)k^2a^2 -\Lambda_4(v)k^4a^4+\Lambda_6(v)k^6a^6-\cdots\} \quad (3.14)$$

or, equivalently

$$1/\hat{\chi}(\mathbf{k},v)=[\chi_0(v)]^{-1}+L_2(v)k^2a^2 -L_4(v)k^4a^4+L_6(v)k^6a^6-\cdots \quad (3.15)$$

valid at a fixed temperature for sufficiently small $(ka)^2$. From (3.9) we see that

$$\Lambda_2(v)=L_2(v)\chi_0(v)=\mu_2(v)/2d\chi_0(v). \quad (3.16)$$

The higher coefficients Λ_4, L_4, etc. will depend also on the direction $\mathbf{e}$ of the wave vector $\mathbf{k}=k\mathbf{e}$. For many purposes, however, only the spherical average of $[\hat{\chi}(\mathbf{k})]^{-1}$ is of interest so that $\Lambda_4, \Lambda_6, \cdots$ may be replaced by their spherical averages, $\bar{\Lambda}_4=\langle\Lambda_4\rangle_{\text{av}}$ etc.; specifically

$$\bar{\Lambda}_4=\bar{L}_4\chi_0=c_4\mu_4/(24\chi_0)-\Lambda_2^2, \quad (3.17)$$

where $c_4=\frac{3}{8}$ for $d=2$ and $c_4=\frac{1}{5}$ for $d=3$. It might be remarked that correct to order $(ka)^6$ the spherical average of the inverse scattering intensity is the same as the inverse of the spherically averaged scattering intensity (which is what would normally be observed directly); the leading term of the difference is proportional to $[\langle\Lambda_4^2\rangle_{\text{av}}-\bar{\Lambda}_4^2](ka)^8$.

There seems little doubt that it will prove possible to construct a rigorous mathematical proof that the expansions (3.14) and (3.15) are convergent for small enough $(ka)^2$ at sufficiently high temperatures, in view of the strictly finite range of the interactions.[17] The *Ornstein-Zernike hypothesis*, however, is equivalent to the assertion that *the expansion* (3.15) *remains valid right up to and at the critical point* in the sense of having a finite radius of convergence (or, at least, of being asymptotic so that the first terms represent the function accurately for small ka). If this is accepted then *at* $T=T_c$ we have

$$\hat{\chi}(\mathbf{k},v_c)\approx A/(ka)^2, \quad (k\to 0) \quad (3.18)$$

where $A=1/L_2(v_c)$ is finite. We will show that this hypothesis is untenable on the grounds that the coefficient $L_2(v)$ diverges to infinity as $T\to T_c$ while the scattering at $T=T_c$ (which will, of course, be finite for $k\neq 0$) does not have the form (3.18) but rather

$$\hat{\chi}(\mathbf{k},v_c)\approx\hat{D}/(ka)^{2-\eta}, \quad (k\to 0) \quad (3.19)$$

with a nonzero exponent η (and a finite amplitude $\hat{D}$).

[17] Comparable results have been obtained for the correlation functions of a continuum gas in the region of convergence of the virial expansion: See D. Ruelle, Ann. Phys. (N. Y.) **25**, 109 (1963); Rev. Mod. Phys. **36**, 580 (1964); O. Penrose, J. Math. Phys. **4**, 1312 (1963); **4**, 1488 (1963); J. Ginibre, *ibid.* **6**, 238 (1965); **6**, 252 (1965); **6**, 1432 (1965).

3.4 Effective Correlation Range

The coefficient Λ_2 in (3.14) determines a temperature-dependent length $\Lambda=1/\kappa_1$ through

$$\Lambda^2=\Lambda_2a^2 \quad \text{or} \quad (\kappa_1a)^2=1/\Lambda_2. \quad (3.20)$$

This length and the corresponding inverse range parameter $\kappa_1(T)$ will be referred to as the *effective* range (or inverse range) of correlation. The significance of this terminology is seen by the standard *approximate* argument[1-3] in which (3.14) is truncated after the quadratic term and the corresponding approximation for $\hat{\chi}(\mathbf{k})$ is Fourier inverted with the conclusion that $\Gamma(\mathbf{r})$ decays to leading asymptotic order as $\exp(-\kappa_1 r)$. [Note that in (3.20) we assume that Λ_2 is positive as will be the case for ferromagnetic interactions which we are principally considering. For antiferromagnetic coupling μ_2 and hence Λ_2 will be negative. In that case, however, interest centers on scattering near the superlattice vector $\mathbf{k}_0$ and we may use (3.5).]

Unless the inverse scattering intensity at $T=T_c$ varies *less* rapidly than $(ka)^2$ (which seems highly improbable *a priori* and even less probable *a posteriori*), the coefficient $\Lambda_2(T)$ should diverge to infinity as $T\to T_c$ at least as fast as the susceptibility $\chi_0(T)$. Consequently, $\kappa_1(T)$ will approach zero as $T\to T_c$ implying that the range of correlation becomes infinite. In fact we may write

$$\chi_0(T)\sim[1-(T_c/T)]^{-\gamma}, \quad (T\to T_c+) \quad (3.21)$$

where the exponent γ is defined more generally by

$$\gamma=-\lim_{T\to T_c+}\ln\chi_0(T)/\ln[1-(T_c/T)], \quad (3.22)$$

and similarly

$$\kappa_1(T)\sim[(T/T_c)-1]^{\nu_1}, \quad (T\to T_c+) \quad (3.23)$$

where ν_1 may be defined in an analogous way to (3.22). Evidently the Ornstein-Zernike hypothesis requires the finiteness of $L_2(T)$ at $T=T_c$ and hence that $2\nu=\gamma$. We shall, however, show that 2ν exceeds γ which is consistent with $\eta>0$ in (3.19).

[It should perhaps be stressed in writing (3.21), (3.23), and similar formulas that the presence of further, higher-order terms is *always* understood. The form of these terms, their magnitude and range of numerical significance can, however, only be gauged from more detailed calculations such as we shall present.]

3.5 True Correlation Range

The effective range parameter κ_1, which essentially determines *only* the second moment of the correlations and hence only the slope of an inverse scattering plot with k^2 at $k=0$, must be distinguished from the *true* (*inverse*) *range of correlation* $\kappa=\kappa_e(T)$ defined as follows[13]:

$$\kappa_e(T)=-\lim_{r\to\infty}\sup(1/r)\ln|\Gamma(r\mathbf{e})|, \quad (3.24)$$

where $\mathbf{e}$ is a unit vector. The existence of a nonzero

$\kappa_e(T)$ (which should be susceptible of rigorous proof,[17] see below) shows that the decay of the correlations as $\mathbf{r}\to\infty$ in the direction $\mathbf{e}$ is dominated by the exponential factor $\exp[-\kappa_e r]$.

From the general theory of the Fourier-Laplace transform, the value of κ_e is determined by the position of the singularities, $k_\alpha(\mathbf{e},T)$ of $\hat{\Gamma}(k\mathbf{e})$ or $\hat{\chi}(k\mathbf{e})$ which lie nearest the real axis in the complex k plane. Specifically we must have

$$\kappa_e(T)=|\operatorname{Im}\{k_\alpha(\mathbf{e};T)\}|. \tag{3.25}$$

By (3.11), the nearest singularities are either (a) zeros of

$$1-\hat{H}(k\mathbf{e})=0, \tag{3.26}$$

or (b) singularities (i.e., nonanalytical points) of the direct correlation transform $\hat{H}(k\mathbf{e})$ itself. In the former case which seems almost certain to hold at sufficiently high temperatures[3,13] and, by continuity, for all T *exceeding* T_c, the nearest singularities are poles of $\hat{\chi}(k\mathbf{e})$. It seems safe to assume that these poles are simple from which it follows (as in the standard Ornstein-Zernike argument) that the true asymptotic decay law is[3,10]

$$|\Gamma(r\mathbf{e})|\approx B_d\exp[-\kappa_e r]/r^{(d-1)/2}+\cdots,\quad(r\to\infty). \tag{3.27}$$

As argued previously,[3,5,10] this result should hold for all *fixed* temperatures *above* T_c. The distance for which the asymptotic law sets in, however, must depend on the position (and nature) of the more distant singularities of $\hat{\chi}(k\mathbf{e})$. If, as we will show, these singularities *close up* on the nearest singularity when $T\to T_c$ then (3.27) loses its validity for finite r and the Ornstein-Zernike arguments break down.

It will be demonstrated (Sec. 10.1) that the scattering becomes isotropic near T_c so that $\kappa_e(T)$ becomes independent of $\mathbf{e}$ and it is sufficient to consider one specific direction or the spherically averaged value κ. In as far as $\Lambda_2\to\infty$ in (3.13) when $T\to T_c$ and the higher terms of the expansion are not overwhelmingly important, the nearest zeros of (3.26) will be approximated by

$$k_\alpha a\simeq\pm i(\Lambda_2)^{-1/2}=\pm i\kappa_1 a,\quad(T\to T_c). \tag{3.28}$$

Consequently, as $T\to T_c$ we may expect $\kappa_1(T)$ to approximate $\kappa(T)$ or at least become proportional to it. Thus if we write, in analogy to (3.23),

$$\kappa(T)\sim[(T/T_c)-1]^{\nu},\quad(T\to T_c+) \tag{3.29}$$

we expect the equality of the exponents ν_1 and ν. Our calculations will in fact bear out these conclusions. One may note that the argument also indicates the approach to spherical symmetry near T_c since Λ_2 is independent of $\mathbf{e}=\mathbf{k}/k$. Away from T_c, however, κ_1 and κ will certainly differ and, moreover, the difference increases with T and soon becomes very large (as will be seen explicitly).

4. APPROXIMATE THEORIES

It is useful to survey briefly some of the fundamental approximate theories of scattering on an Ising model since, in the first place, this will reveal explicitly certain general features which apply also to the exact results and, secondly, it will form a basis for assessing the value of the more accurate calculations.

4.1 Mean Field Theory

The general result of mean field theory[18] is

$$\hat{\chi}(\mathbf{k})=\frac{1-\langle s_0\rangle^2}{1-(1/k_BT)\hat{J}(\mathbf{k})(1-\langle s_0\rangle^2)}, \tag{4.1}$$

where $\langle s_0\rangle=M/m$ is the reduced magnetization per spin and where $\hat{J}(\mathbf{k})$ is the transform of the exchange integral $J(\mathbf{r})$. In zero field above T_c we have $\langle s_0\rangle\equiv 0$ and (4.1) may be derived, as will be shown, by expanding the direct correlation function, Eq. (3.11), in powers of $(1/k_BT)$ and retaining only the zeroth- and first-order terms. (A similar, but *not* equivalent, approximation for a gas is obtained by retaining only the first virial coefficient in the expansion of the direct correlation function.) For nearest-neighbor interactions and $H=0$, Eq. (4.1) reduces to

$$\hat{\chi}(\mathbf{k})=1/[1-(qJ/k_BT)\hat{\gamma}(\mathbf{k})]. \tag{4.2}$$

As $k\to 0$ this reproduces the standard Curie-Weiss law

$$\chi_0(T)=[1-(T_c/T)]^{-1} \tag{4.3}$$

with

$$kT_c=qJ, \tag{4.4}$$

corresponding to an exponent $\gamma=1$ in Eq. (3.21). By rewriting (4.2) in terms of the effective wave vector $K(\mathbf{k})$, defined in (2.2), we obtain

$$\hat{\chi}(\mathbf{k},T)=r_1^{-2}[\kappa_1^2+K^2(\mathbf{k})]^{-1}, \tag{4.5}$$

which closely resembles the familiar Ornstein-Zernike approximation and indeed is equivalent to it near T_c. In this case, the effective correlation range parameter is

$$\kappa_1 a=(2d)^{1/2}[(T/T_c)-1]^{1/2}, \tag{4.6}$$

so that the exponent ν_1 in (3.21) has the classical value $\frac{1}{2}(=\frac{1}{2}\gamma)$ independent of dimensionality. The "effective range of direct interaction" $r_1(T)$ is given by

$$(r_1/a)=(2d)^{-1/2}(T_c/T)^{1/2}, \tag{4.7}$$

and is evidently slowly varying near T_c.

4.2 True Correlation Range

By solving Eq. (3.26), it is also possible to calculate the *true* range of correlation appropriate to the approximation (4.2). For simplicity consider the decay of

[18] See, for example, R. Brout, *Phase Transitions* (W. A. Benjamin, Inc., New York, 1965).

correlation along an axis of the square ($d=2$) and simple cubic ($d=3$) lattices and introduce the *decay factor*

$$\omega_x=\exp(-\kappa_x a). \tag{4.8}$$

On making the substitution $k_x=i\kappa_x$ in (4.2), the equation determining the poles of $\hat{\chi}(k)$ becomes simply

$$1-(T_c/T)(2d)^{-1}[2(d-1)+\omega_x+\omega_x^{-1}]=0 \tag{4.9}$$

with solution

$$\omega_x=1-[2d\tau+d^2\tau^2]^{1/2}+d\tau, \tag{4.10}$$

where

$$\tau=(T/T_c)-1. \tag{4.11}$$

Thus the true range of correlation is given by

$$\kappa_x a=\ln\{1+(2d)^{1/2}\tau^{1/2}[1+\tfrac{1}{2}d\tau]^{1/2}+d\tau\} \tag{4.12}$$

$$=(2d)^{1/2}[(T/T_c)-1]^{1/2} \times\{1+(d/2)^{1/2}\tau^{1/2}+O(\tau)\}, \tag{4.13}$$

and the correlations on this approximation will decay as in (3.27). Comparison with (4.6) shows that κ_1/κ approaches unity as $T\to T_c$ as was anticipated in the previous section. In particular the exponents ν and ν_1 are identical. On the other hand as T becomes large, $\kappa_1(T)$ varies as $(2d)^{1/2}(T/T_c)^{1/2}$ whereas $\kappa(T)$ increases only as $\ln 2d(T/T_c)$. Since (4.2) is asymptotically correct when $T\to\infty$, this high-temperature behavior of $\kappa_1(T)$ and $\kappa(T)$ is an *exact* property of the Ising model.

It is equally straightforward to evaluate the true correlation range along a major diagonal ($x=y=z$) of the simple cubic or square lattices. One finds

$$\kappa_{\text{diag}}a=d^{1/2}\ln\{1+2^{1/2}\tau^{1/2}[1+\tfrac{1}{2}\tau]^{1/2}+\tau\} \tag{4.14}$$

$$=(2d)^{1/2}[(T/T_c)-1]^{1/2} \times\{1+2^{-1/2}\tau^{1/2}+O(\tau)\}. \tag{4.15}$$

Evidently κ_x and κ_{diag} become equal as $T\to T_c$ confirming the asymptotic symmetry of the correlations near the critical point. It is significant, however, that the correction terms in the expressions (4.13) and (4.15) for κ vary as $(T-T_c)^{1/2}$ rather than linearly with T_c as might have been expected. For large T one finds that $\kappa_{\text{diag}}\approx d^{1/2}\kappa_x$ which demonstrates the anisotropic decay of the correlations away from T_c.

More generally one easily sees that *whenever the scattering has the form* (4.5) the effective and true correlation range parameters κ_1 and κ must be related by

$$(\kappa_1 a)^2=1/\Lambda_2'(\kappa a), \tag{4.16}$$

where, for appropriate directions $\mathbf{e}$,

$$\Lambda_2'=1/(\kappa_1' a)^2=f^2/(\omega+\omega^{-1}-2)=f^2\omega/(1-\omega)^2 \tag{4.17}$$

with

$$\omega=\exp(-f\kappa_e a). \tag{4.18}$$

The values of the factor f for various symmetric directions in the standard lattices are given in Appendix A. Whenever these relations apply $\kappa_1/\kappa\to 1$ as $T\to T_c$ (and hence $\nu=\nu_1$).

4.3 Elliott-Marshall-Bethe Approximation

Elliott and Marshall[19] adapted the Bethe-Peierls cluster approximation to treat the "propagation of order" from site to site of the lattice along the lines originally conceived by Zernike.[20] In a certain approximation they derived a linear difference equation for the correlations whose solution they constructed. In zero field their result may be written

$$\hat{\chi}(\mathbf{k},v)=\frac{1-v^2}{1+(q-1)v^2-qv\hat{\gamma}(\mathbf{k})}, \tag{4.19}$$

which is again of the precise form (4.5) but with

$$\tanh(J/kT_c)=v_c=1/(q-1), \tag{4.20}$$

and

$$(\kappa_1 a)^2=(2d/q)(1-v)v^{-1}[1-(v/v_c)], \tag{4.21}$$

$$(r_1/a)^2=(q/2d)v/(1-v^2). \tag{4.22}$$

These formulas can be derived directly from the high-temperature expansion (see below) if all closed circuits of three or more lines are ignored (as appropriate on a Bethe lattice or infinite Cayley tree[21]). Consequently $\hat{\chi}(\mathbf{k},v)$ becomes the generating function for random walks on the lattice which make no immediate reversals. This restricted random walk problem has been solved generally.[22] This derivation proves that the Bethe approximation is always correct to order $1/T^2$ at high temperatures and is correct to order $1/T^3$ for loose-packed lattices (without triangles).

Near T_c one finds

$$(\kappa_1 a)^2=d(q-2)^2(q-1)^{-1}\ln[q/(q-2)] \times[(T/T_c)-1]\{1+O(\tau)\} \tag{4.23}$$

and

$$(r_1/a)^2=[(q-1)/2d(q-2)]\{1-O(\tau)\}, \tag{4.24}$$

which are equivalent to the mean field results although numerically somewhat different. Notice the correction terms for $(\kappa_1 a)^2$ are linear in τ.

As for the mean field approximation one may again calculate explicitly the *true* range of correlation for

---

[19] R. J. Elliott and W. Marshall, Rev. Mod. Phys. **30**, 75 (1958).

[20] F. Zernike, Physica **7**, 565 (1940). One might also cite various related and more or less equivalent, if more complicated, approximations developed by J. M. Cowley, Phys. Rev. **77**, 669 (1950); **120**, 1648 (1960); **138**, A1384 (1965); D. O. Christy and G. L. Hall, *ibid.* **132**, 1959 (1963); P. C. Clapp and S. C. Moss, *ibid.* **142**, 418 (1966); and other authors.

[21] One must not, however, measure "distance" on the Bethe lattice (or Cayley tree) by the contour length along its branches (as suggested misleadingly in Ref. 10) but rather by mapping the Bethe lattice into a regular space lattice (of the same coordination number) with the systematic neglect of all overlaps.

[22] C. Domb and M. E. Fisher, Proc. Cambridge Phil. Soc. **54**, 48 (1958).

symmetric directions from (4.16) to (4.18) with essentially equivalent results. In particular, the correction terms to κ near T_c vary as $\tau^{1/2}$ rather than as τ.

5. EXACT RESULTS

In this section we survey the available exact results on the Ising-model correlation functions and indicate their significance.

5.1 Plane Lattice Correlation Functions

The exact critical temperatures of the square and triangular nearest-neighbor Ising lattices are given by

$$v_c=\tanh(J/k_BT_c)=\sqrt{2}-1, \quad \text{square}$$
$$=2-\sqrt{3}, \quad \text{triangular}. \tag{5.1}$$

Onsager and Kaufman[7] showed how the correlation functions of the square lattice in zero field could be expressed as determinants of order proportional to the coordinates x and y, and formed with elements which can be expressed as elliptic integrals in the appropriate temperature variables. Montroll, Potts, and Ward[23] simplified the calculations and Stephenson[24] extended them to the triangular lattice. Near the critical point one finds generally[7,8]

$$\Gamma(\mathbf{r},T)=\Gamma_c(\mathbf{r})+E(\mathbf{r})[(T/T_c)-1]\ln|(T/T_c)-1|+\cdots, \tag{5.2}$$

so that the temperature derivative of $\Gamma(\mathbf{r},T)$ for *all* $\mathbf{r}$ is logarithmically divergent as $T\to T_c$. On the square lattice the first few critical-point values are

$$\begin{aligned}&\Gamma_c(a,0)=\tfrac{1}{2}\sqrt{2}\simeq 0.707107,\\ &\Gamma_c(a,a)=(2/\pi)\simeq 0.636620,\\ &\Gamma_c(2a,0)=1-(4/\pi^2)\simeq 0.594715,\\ &\Gamma_c(2a,a)=(4/\pi^2)\sqrt{2}\simeq 0.573159,\\ &\Gamma_c(2a,2a)=16/3\pi^2\simeq 0.540380.\end{aligned} \tag{5.3}$$

Numerical values for the triangular lattice and further values for the square lattice have been tabulated by Stephenson.[24] Contrary to what might at first be expected, the amplitudes $E(\mathbf{r})$ of the singular term increase with $\mathbf{r}$. Thus

$$\begin{aligned}&E(a,0)=E_1=(2/\pi)\ln(1+2^{1/2})\simeq 0.561100,\\ &E(a,a)=2^{1/2}E_1,\\ &E(2a,0)=(4/\pi)2^{1/2}E_1, \quad E(2a,a)=2E_1.\end{aligned} \tag{5.4}$$

However, the higher-order terms, of the general form $(T-T_c)^{n+m}(\ln|T-T_c|)^n\, n$, $m=0, 1, 2,\cdots$, also become more important as $\mathbf{r}$ increases.

The correlations along the diagonal (la,la) at the critical point can be expressed as a single $l\times l$ determinant[24] with elements of the simple form $c_{ij}=1/\pi(i-j+\frac{1}{2})$. This determinant was evaluated exactly by Onsager and Kaufman[7,25] and yields

$$\Gamma_c(la,la)=\prod_{t=1}^{l}\frac{\Gamma(t)\Gamma(t)}{\Gamma(t-\frac{1}{2})\Gamma(t+\frac{1}{2})}, \tag{5.5}$$

where $\Gamma(z)$ is the gamma function. A straightforward asymptotic analysis then yields[8]

$$\Gamma_c(la,la)\approx D_0 l^{-1/4}\{1-\tfrac{1}{64}l^{-2}+O(l^{-3})\}, \tag{5.6}$$

where

$$D_0=\tfrac{3}{4}\exp\{-\tfrac{1}{4}C_E-\sum_{m=1}^{\infty}[\zeta(2m+1)-1]/(m+1)4^{m+1}\}$$
$$\simeq 0.645002, \tag{5.7}$$

in which C_E is Euler's constant and $\zeta(z)$ is the Riemann zeta function. The variation of the correlations along a row is similar[24,25] except that the amplitude has an extra factor of magnitude about $2^{1/8}$ which means that the decay is essentially spherically symmetric, i.e.,

$$\Gamma_c(\mathbf{r})\approx D(a/r)^{1/4}, \quad (r\to\infty) \tag{5.8}$$

with

$$D=2^{1/8}D_0\simeq 0.703380. \tag{5.9}$$

Comparison with the exact values in (5.3) shows that even at the nearest sites to the origin (5.8) is accurate to 1.5% or better. (See also Sec. 10.2 below.) Stephenson[24] has verified (5.8) numerically on the triangular lattice with the conclusion that $D\simeq 0.66865$.

By taking the Fourier transform of (5.8), we find[26] for small ka

$$\hat{\chi}(\mathbf{k},v_c)\approx\hat{D}/|ka|^{7/4}, \tag{5.10}$$

where

$$\hat{D}=2^{7/4}\sin(\pi/8)[\Gamma(\tfrac{7}{8})]^2D\simeq 1.07499D. \tag{5.11}$$

This shows that the Ornstein-Zernike conclusion (3.18) is false and that (3.19) holds with an exponent

$$\eta=\tfrac{1}{4}, \quad (d=2). \tag{5.12}$$

On this basis we must expect a similar breakdown of

[23] R. B. Potts and J. C. Ward, Progr. Theoret. Phys. (Kyoto) **13**, 38 (1955); E. W. Montroll, R. B. Potts, and J. C. Ward, J. Math. Phys. **4**, 308 (1963).

[24] J. Stephenson, J. Math. Phys. **5**, 1009 (1964); see also K. Kano, Progr. Theoret. Phys. (Kyoto) **35**, 1 (1966).

[25] Onsager and Kaufman published a calculation of the correlation functions along a *row* which expressed $\Gamma(0,la)$ as the sum of two determinants. They evaluated these determinants *approximately* at T_c, obtaining a result of the form (5.5) for the dominant term (after correction of some misprints). Onsager, however, showed (private communication) that (5.5) was *exact* for the diagonal correlations. The only published derivation of this result, however, is by Stephenson (Ref. 24). It might be mentioned that Potts and Ward (Ref. 23) obtained a rigorous expression for the row correlations as a *single* determinant but since its elements are not quite as simple even at T_c, it has not been expressed in more explicit form or completely analyzed for large r. Undoubtedly, however, the asymptotic behavior along the rows is similar to (5.6) as indicated by the calculations of Onsager and Kaufman. (See also the papers cited below in Ref. 30, especially Wu.)

[26] For example, by the techniques of B. R. A. Nijboer and F. W. DeWette [Physica **23**, 309 (1957)] or by approximating the Fourier sum by an integral which is justified for small $\mathbf{k}$.

the Ornstein-Zernike hypothesis in three dimensions with an exponent probably satisfying $\frac{1}{4}>\eta>0$ (on the grounds that deviations from "classical" critical-point theories seem to be smaller in three than in two dimensions[3,5]).

5.2 True Correlation Range

Onsager's original paper[6] contained an exact evaluation of the true correlation range κ_x although this was not, perhaps, very explicit.[3,8] The result is stated below in Eqs. (5.22) to (5.25). To demonstrate it, the spin pair correlation functions must be expressed in terms of the fundamental matrix $\mathbf{V}$ of order $2^n\times 2^n$, which adds an extra column of n sites to a lattice of n rows (and finite length).[11,27] In terms of $\mathbf{V}$ the partition function of a finite lattice of m columns with periodic boundary conditions is

$$Z_{nm}=\mathrm{Tr}\{\mathbf{V}^m\}. \tag{5.13}$$

Similarly the correlation function for a spin at $\mathbf{0}=(0,0)$ and one at $\mathbf{r}=(la,ja)$, i.e., at a spacing of l columns at j rows, is[7,11,27]

$$\Gamma_{nm}(\mathbf{r})=\langle s_{00}s_{lj}\rangle=Z_{nm}^{-1}\,\mathrm{Tr}\{\mathbf{s}_0\mathbf{V}^l\mathbf{s}_j\mathbf{V}^{m-l}\}, \tag{5.14}$$

where $\mathbf{s}_0$ and $\mathbf{s}_j$ are spin matrices for the rows 0 and j. (Note by translational invariance $\mathbf{0}$ is a typical site.)

The 2^n eigenvalues λ of $\mathbf{V}$ may be labeled conveniently by a *band index* $t=0,\ 1,\cdots n$ and an internal index

$$u=1,\ 2,\cdots\binom{n}{t}.$$

Since $\mathbf{V}$ is real and may be chosen symmetric it can be expanded in terms of its eigenvectors $|t,u\rangle$ and their conjugates (row) vectors $\langle t,u|$. On substitution in (5.13) and (5.14) and taking the trace in the diagonal representation we find

$$\Gamma_{nm}(\mathbf{r})=\Big[\sum_{t,u}\langle t,u|\,\mathbf{s}_0\mathbf{V}^l\mathbf{s}_j\,|t,u\rangle\lambda^{m-l}{}_{t,u}\Big]\Big[\sum_{t,u}\lambda^m{}_{t,u}\Big]^{-1}. \tag{5.15}$$

If $\lambda_{0,1}=\lambda_0=\lambda_{\max}$ is the largest eigenvalue and is nondegenerate, as is always the case for $T>T_c$, we may take the limit $m\to\infty$ by retaining only the first term in the sums over (t,u). Expressing $\mathbf{V}^l$ in terms of the eigenvectors then yields

$$\Gamma_{n\infty}(\mathbf{r})=\sum_{t',u'}\langle 0|\,\mathbf{s}_0\,|t',u'\rangle\langle t',u'|\,\mathbf{s}_j\,|0\rangle(\lambda_{t',u'}/\lambda_0)^l. \tag{5.16}$$

Now the eigenvectors are of odd or even parity under spin inversion according to the parity of t. Since the spin matrices are of odd parity the matrix elements in (5.16) thus vanish if t' is even (but they should not vanish otherwise).

In the limit $n\to\infty$ the lattice becomes infinite in both dimensions and the eigenvalues $\lambda_{t,u}$ within the bands $t=1,\cdots(n-1)$ close up to form continua.[6,28] If we set

$$\lambda_{tu}/\lambda_0=\exp[-P_n(t,u)], \tag{5.17}$$

we may define spectral densities and weights by the asymptotic formulas

$$\binom{n}{t}\mathcal{G}_t(p)dp\approx\text{number of values } u \text{ for which } p\leqslant P_n(t,u)<p+dp; \tag{5.18}$$

and

$$W_{t,j}(p)dp\approx\sum_{\substack{u\\ p\leqslant P_n(t,u)<p+dp}}\binom{n}{t}\langle 0|\,\mathbf{s}_0\,|t,u\rangle\langle t,u|\,\mathbf{s}_j\,|0\rangle. \tag{5.19}$$

Finally we obtain the limiting result

$$\Gamma(\mathbf{r})=\langle s_{00}s_{lj}\rangle=\sum_{t\ \mathrm{odd}}\int_{\xi_t}^{\infty}W_{t,j}(p)\mathcal{G}_t(p)e^{-pl}dp, \tag{5.20}$$

where the lower limit ξ_t of the tth integral is determined through (5.17) and (5.18) by the largest eigenvalue in the tth band; in particular $\exp(-\xi_1)\approx\lambda_{1,1}/\lambda_0$ where $\lambda_{1,1}=\lambda_{\max}{}^{(-)}$ is the *second* largest eigenvalue, and for $T>T_c$ we have $\xi_1<\xi_2<\xi_3\cdots$.

Now let us allow $\mathbf{r}$ to become large in the direction of the x axis, i.e., let $l\to\infty$, and examine the decay of the correlation. Unless $W_{1,j}(p)$ vanishes *identically* for an interval of p around $p=\xi_1$, the decay will be dominated by a factor $\exp(-\xi_1 l)$. Consequently, by definition (3.24) the true range of correlation is given generally by

$$\kappa_x a=\xi_1(T)=-\lim_{n\to\infty}\ln(\lambda_{1,1}/\lambda_0). \tag{5.21}$$

It is evident that this result is really quite independent of the lattice structure or the dimensionality if the matrix $\mathbf{V}$ is defined appropriately. A more general discussion of the result and its relation to other formulations is being prepared for separate publication.[29]

Since Onsager has calculated the spectrum exactly for the plane square lattice, we obtain immediately the explicit result

$$\kappa_x a=\ln\coth(J/kT)-2(J/kT), \quad (T>T_c) \tag{5.22}$$

which can also be written

$$\omega_x=\exp(-\kappa_x a)=v(1+v)/(1-v). \tag{5.23}$$

Near the critical point $\omega_x\to 1$ and we have

$$\kappa_x a=F[(T/T_c)-1]\{1-b\tau+O(\tau^2)\}, \tag{5.24}$$

where

$$F=2\ln(1+\sqrt{2})\simeq 1.762747,$$
$$b=1-2^{-3/2}\ln(1+\sqrt{2})\simeq 0.688387. \tag{5.25}$$

Consequently we see that for the square lattice the *exponent ν has the value unity* in contrast to the classical

[27] E. N. Lassettre and J. P. Howe, J. Chem. Phys. **9**, 747 (1941); J. Ashkin and W. E. Lamb, Jr., Phys. Rev. **64**, 159 (1943).

[28] B. Kaufman, Phys. Rev. **76**, 1232 (1949).

[29] M. E. Fisher (unpublished).

value $\frac{1}{2}$. The nonzero value of κ above T_c ensures the existence of the moments (3.7) and (3.10).

5.3 Details of Decay

From Onsager's calculation one finds easily that the "band edges" of the eigenvalue spectrum are given generally by

$$\xi_t(T)=t\xi(T)=i\kappa_x a, \quad t=0, 1, 2, 3\cdots. \tag{5.26}$$

Since $\xi(T)\to 0$ as $T\to T_c$ we see that all the "band edges" close up as T approaches T_c and, indeed, coalesce at $T=T_c$! *Above* T_c, however, it follows from (5.20) and the general theory of the Laplace transform that the details of the asymptotic decay will depend only on the behavior of $\mathcal{G}_1(p)$ and $W_{1,j}(p)$ as $p\to\xi+$. Without difficulty one finds from Onsager's results

$$\mathcal{G}_1(p)=(1/2\pi)[\sinh\tfrac{1}{2}(p-\xi)\sinh\tfrac{1}{2}(p+\xi)]^{-1/2}\sinh p \times[\cosh^2\tfrac{1}{2}\xi-\sinh^2\tfrac{1}{2}p]^{-1/2}, \tag{5.27}$$

which evidently has an inverse square root singularity at $p=\xi$. The higher densities $\mathcal{G}_2$, $\mathcal{G}_3$, etc. are essentially convolution powers of $\mathcal{G}_1$ and are less singular at the edge.

If it is now assumed that the weight function $W_{1,j}(p)$ approaches a positive limit $W_{1,j}(0)$ as $p\to\xi$ then it follows easily from (5.20) that the decay will be asymptotically of the form $Be^{-\kappa r}/r^{1/2}$, as anticipated in (3.27).[3,10] This would indicate that the Fourier transforms $\hat{\Gamma}(\mathbf{k})$ and hence $\hat{\chi}(\mathbf{k})$ have simple poles at $\kappa_\alpha=\pm i\kappa$ just as on the Ornstein-Zernike theory. However, the other band edges will *also* give rise to singularities at $k_\beta=\pm 3i\kappa$, $k_\gamma=\pm 5i\kappa$, etc. and these will *close up to the origin* as $T\to T_c$ in contrast to the classical expectations. [The necessity of some such behavior follows indeed from (5.10).]

Near T_c the expression (5.27) reduces to

$$\mathcal{G}_1(p)=(1/\pi)x(x^2-1)^{-1/2} \times\{1+\tfrac{1}{12}\xi^2(3x^2-2)+O(\xi^4)\}, \tag{5.28}$$

where $x=p/\xi$. Thus as $T\to T_c$ and $\xi\to 0$, $\mathcal{G}_1(p)$ and the higher-order densities become functions only of $(p/\kappa a)$. If the weights $W_{t,j}(p)$ remain slowly varying, or show a similar behavior, we may conclude that $\Gamma(\mathbf{r},T)$ will become asymptotically a function only of κr and, similarly, $\hat{\chi}(\mathbf{k},T)$ will approach a function of k/κ only. With this assumption and the rigorous result (5.8) we may write, using more general notation,[3,10]

$$\Gamma(\mathbf{r},T)\approx D(a/r)^{d-2+\eta}e^{-\kappa r}[1+Q(\kappa r)], \quad T\to T_c, \quad \kappa r \text{ fixed} \tag{5.29}$$

where the function $Q(x)$ must satisfy

$$Q(x)\to 0 \quad \text{as} \quad x\to 0, \tag{5.30a}$$

$$1+Q(x)\sim x^{-\frac{1}{2}(3-d)+\eta} \quad \text{as} \quad x\to\infty. \tag{5.30b}$$

Clearly this is correct at $T=T_c$ and as regards the dominant factors above T_c.

The complete analysis of the weight functions $W_{t,j}(p,T)$ required to justify these conclusions is not easy but has been substantially accomplished recently in important work by Kadanoff and independently by Wu and by Ryazanov.[30] In particular it has been shown (a) that for T fixed above T_c the asymptotic decay law (3.27) is valid, and (b) the form (5.29) is correct with, in fact,

$$D[1+Q(x)]\approx 2^{1/8}\pi^{-1/2}x^{-1/4}, \quad (x\to\infty) \tag{5.31}$$

confirming (5.30b).

5.4 Anisotropy of Correlation

In as far as the results (5.30b) and (5.31) indicate that $\hat{\chi}(\mathbf{k},T)$ has a simple pole we might hope that the generalized mean field approximation (4.5) would be fairly accurate above T_c if the appropriate value of κ_1' were substituted from (4.17) and (4.18). Thus we may expect $1/\hat{\chi}$ for the square lattice to have a factor

$$[1+\Lambda_2'(v)K^2(\mathbf{k})], \tag{5.32}$$

where, by (4.17) and the exact result (5.23) for κ_x, $\Lambda_2'(v)$ is given by

$$\Lambda_2'(v)=v(1-v^2)/(1-2v-v^2)^2 =v+4v^2+\cdots+2512v^8 \tag{5.33}$$

$$+6761v^9+18004v^{10}+47525v^{11}+\cdots, \tag{5.34}$$

which, of course, diverges at T_c as $(T-T_c)^{-2}$. It will be seen later (Sec. 8.3) that $\Lambda_2'(v)$ agrees with the true expansion coefficient $\Lambda_2(v)$ [defined in (3.14)] correct to order v^8 so that, in fact, (5.32) will be a surprisingly accurate approximation to the *total* function $\chi_0/\hat{\chi}(\mathbf{k})$! Clearly, however, in view of the critical-point result (5.10), it *cannot* be exact, and indeed the remaining factors must also be singular at $T=T_c$.

If, as seems very probable, the expression (5.32) is really a factor of $1/\hat{\chi}$, the true range of correlation in an arbitrary direction $\mathbf{e}=(\cos\vartheta, \sin\vartheta)$ follows from (3.25) and (3.26) as the root of

$$1-qB(v)\hat{\gamma}(i\kappa_{\mathbf{e}}\mathbf{e})=0, \tag{5.35}$$

where

$$qB(v)=2d\Lambda_2'/(1+2d\Lambda_2') \tag{5.36}$$

$$=v(1-v^2)(1+v^2)^{-2}, \tag{5.37}$$

which is nonsingular at $T=T_c$. This result may be rewritten, extending the analysis to different interactions

[30] L. P. Kadanoff, Nuovo Cimento 44, 276 (1966); G. V. Ryazanov, Zh. Eksperim. i Teor Fiz. 49, 1134 (1965) [English transl.: Soviet Phys.—JETP 22, 789 (1966)]; T. T. Wu, Phys. Rev. 149, 380 (1966).

J_x and J_y for horizontal and vertical bonds,[31] as

$$\cosh(2J_x/kT)\cosh(2J_y/kT) - \sinh(2J_x/kT)\cosh(\kappa\sin\vartheta) - \sinh(2J_y/kT)\cosh(\kappa\cos\vartheta) = 0, \quad (5.38)$$

which was first presented by Onsager on the basis of a "tentative" (and unpublished) calculation.[6]

For the principal diagonal $\vartheta=\pi/4$ one finds in place of (5.23)

$$\omega_{\text{diag}} = 2v/(1-v^2), \quad (5.39)$$

which by an analysis of the Toeplitz determinant referred to above is found to be exact. Thus even if the formula (5.35) is not completely correct it must be quite accurate for all directions even very close to T_c.[32] One easily sees from (5.35) that κ_e becomes independent of direction near T_c as in the approximate theories.

By related arguments (see also Sec. 7.2) one may surmise that for the triangular lattice in a direction normal to the bonds one has

$$\omega_y = 2v/(1-v)^2, \quad (5.40)$$

while along the bonds of the honeycomb lattice

$$\omega_x = 2v^2/(1-v^2). \quad (5.41)$$

In both cases the equation $\omega(v)=1$ yields the rigorously known critical points as it should. Furthermore the exponent ν is unity as expected for all plane Ising lattices. For the triangular lattice we obtain

$$\kappa a \approx 2[1-(v/v_c)] \quad \text{as} \quad T\to T_c, \quad (5.42)$$

and hence the amplitude

$$F = 1.9028538\cdots. \quad (5.43)$$

The effective reduced second moment for the triangular lattice following from (5.40) and (4.17) is

$$\tfrac{2}{3}\Lambda_2'(v) = v(1-v)^2/(1-4v+v^2)^2 \quad (5.44)$$

$$= v+6v^2+\cdots +2962v^6+12735v^7+53800v^8+\cdots. \quad (5.45)$$

6. FORM OF CRITICAL SCATTERING

In this section the conclusions following from the results for the plane square Ising lattice will be summarized and various approximate formulas embodying the most important features of the critical scattering will be advanced.

6.1 General Results

The principal conclusion about the square lattice correlation functions is the scaling relation (5.29) which states that near the critical point the scattering depends essentially on only the range parameter $\kappa(T)$, i.e., on only one temperature-dependent length.[3] Taking the Fourier transform of (5.29) for T near T_c (and hence small κ) yields for low k

$$\hat{\chi}(\mathbf{k},T) \approx X(k/\kappa)/\kappa^{2-\eta}, \quad (T\to T_c) \quad (6.1)$$

where the reduced scattering function $X(y)$ is related generally to the function $Q(x)$ by

$$X(y) = D(a^d/v_0)\int (e^{-x}/x^{d-2+\eta})[1+Q(x)]e^{ixy}d^dx. \quad (6.2)$$

It follows that, parallel with the expansion (3.14), we have

$$1/X(y) = X_0^{-1}\{1+\Delta_2 y^2+O(y^4)\} \quad \text{as} \quad y\to 0, \quad (6.3)$$

where $X_0=X(0)$, while, as a consequence of (3.19) or (5.10),

$$X(y) \approx \hat{D}/y^{2-\eta} \quad \text{as} \quad y\to\infty, \quad (6.4)$$

where, generally,

$$\hat{D}/D = 2^{2-\eta}\sin(\tfrac{1}{2}\pi\eta)[\Gamma(1-\tfrac{1}{2}\eta)]^2(a^2/v_0), \quad \text{for} \quad d=2$$
$$= 4\pi\cos(\tfrac{1}{2}\pi\eta)\Gamma(1-\eta)(a^3/v_0), \quad \text{for} \quad d=3 \quad (6.5)$$

[see also Eq. (5.11)].

Letting $k\to 0$ in (6.1) or integrating (5.29) directly yields the susceptibility as

$$\chi_0(T) \approx X_0/\kappa^{2-\eta}. \quad (6.6)$$

Now if, as established for the square lattice, we have

$$\kappa(T) \approx F[(T/T_c)-1]^{\nu}, \quad (T\to T_c) \quad (6.7)$$

it follows that

$$\chi_0(T) \approx C/[(T/T_c)-1]^{\gamma}, \quad (6.8)$$

where the exponent γ is related to ν and η by

$$\gamma = (2-\eta)\nu. \quad (6.9)$$

This important relation replaces the generalized Ornstein-Zernike relation $\gamma=2\nu$. The susceptibility amplitude in (6.8) is

$$C = X_0/F^{2-\eta}. \quad (6.10)$$

For the plane square lattice, the exact values $\eta=\frac{1}{4}$ and $\nu=1$ yield $\gamma=7/4$,[8] a result first discovered by numerical studies[33] and since confirmed in detail numerically for all plane lattices.[34,35] One should note that the exponent relation (6.9) does not depend on the existence of the amplitude F but follows merely from the existence of γ and ν defined as in (3.22).

---

[31] Equation (5.23) becomes $\omega_x = v_x(1+v_y)/(1-v_y)$.

[32] For $J_x\neq J_y$ there seems to be a difficulty when $\vartheta\neq 0$ or $\vartheta\neq\pi/2$ since the Toeplitz determinant indicates that $\omega_{\text{diag}} = [\sinh(2J_x/kT)\sinh(2J_y/kT)]^{1/2}$ which is *not* a solution of (5.38) when $\vartheta=\pi/4$.

[33] C. Domb and M. F. Sykes, Proc. Roy. Soc. (London) **A240**, 214 (1957); J. Math. Phys. **2**, 63 (1961).

[34] G. A. Baker, Jr., Phys. Rev. **124**, 768 (1961).

[35] M. F. Sykes and M. E. Fisher, Physica **28**, 919 (1962); **28**, 939 (1962).

Comparison of (6.3) and (3.14) yields

$$\Lambda_2(T)=1/(\kappa_1 a)^2\approx\Delta_2/(\kappa a)^2, \quad (T\to T_c). \quad (6.11)$$

It follows that the true and effective correlation ranges become proportional when $T\to T_c$ as anticipated originally. Thus

$$\nu=\nu_1, \quad (6.12)$$

and the corresponding amplitudes are related by

$$(\kappa/\kappa_1)^2\approx F^2/F_1{}^2=\Delta_2. \quad (6.13)$$

Similarly it is straightforward to see that the general correlation function moments (3.7) behave as

$$\mu_t(T)\approx M_t/[(T/T_c)-1]^{\gamma+t\nu}, \quad (T\to T_c). \quad (6.14)$$

Although the form of these results can only be regarded as fully established for the plane square lattice[6–8,30] we expect confidently that they will be valid also for other lattices in two or three dimensions. Our numerical calculations will lend support to this assumption by their internal consistency and their similarity to the rigorously known results. Our main approach will be to estimate the critical behavior of $\Lambda_2(T)$ and $\mu_2(T)$ as accurately as possible and hence to estimate ν. The susceptibility and the exponent γ are known accurately from previous work[33–35] and so the critical-point decay exponent η can be found from (6.9). We will also calculate the true correlation range κ and hence Λ_2' to verify the proportionality to κ_1 and Λ_2, respectively, and the identity (6.12). Separate estimation of the critical-point values of the correlation functions (Sec. 10.2) will also support (5.29).

6.2 Simple Approximants for the Scattering

It is appropriate at this stage to consider various approximate analytical expressions for the scattering intensity which embody some or all of the main features of the exact results and which serve as interpolation formulas for regions where exact results are not available.

Firstly it is instructive to examine the consequences of neglecting the function $Q(x)$ in the result (5.29). By (5.30b) this will lead to an incorrect form of decay in second asymptotic order away from T_c and this should yield an overestimate of $\Gamma(\mathbf{r},T)$ for large r in two dimensions but an underestimate in three. Neglecting $Q(x)$ we find in two dimensions

$$\hat{\chi}(\mathbf{k},T)\simeq\hat{D}P_{1-\eta}[\kappa/(\kappa^2+k^2)^{1/2}]/P_{1-\eta}(0)a^{2-\eta}(\kappa^2+k^2)^{1-\eta/2}, \quad (6.15)$$

where $P_l(z)$ is the Legendre function. At the critical point when $\kappa\to 0$ this becomes exact. Away from the critical point the approximation has a branch point at $k=\pm i\kappa$ of order $-(1-\frac{1}{2}\eta)$ rather than a simple pole. When $k\to 0$ we need the results

$$P_{1-\eta}(1)=1,$$
$$P_{1-\eta}(0)=\pi^{-1/2}\sin(\tfrac{1}{2}\pi\eta)\Gamma(1-\tfrac{1}{2}\eta)/\Gamma(\tfrac{3}{2}-\eta)$$
$$=\eta 2^{-\eta}/(1-\eta)\{1+O(\eta^2)\}. \quad (6.16)$$

[In fact for small η, $P_{1-\eta}(x)$ varies almost linearly with x and is quite analytic in the range 0 to 1.]

This leads to the *approximate* relation

$$C\simeq C'=2\pi\Gamma(2-\eta)(a^d/v_0)D/F^{2-\eta}, \quad (d=2) \quad (6.17)$$

for the susceptibility amplitude. Evaluation of the right-hand side for the square lattice, using (5.9) and (5.25), yields $C'=1.50620\cdots$, whereas the best numerical estimates[34,35] of the true behavior of the susceptibility give

$$C\simeq 0.96272, \quad \text{(square lattice)} \quad (6.18)$$

which is about 36% lower (see Table IX below). This large discrepancy indicates the importance of $Q(x)$ for the square lattice. (Notice the difference is in the expected direction.) The corresponding ratio C/C' for the triangular lattice is found to be identical to within 0.01% which is the probable limit of precision of the numerical estimates.

In three dimensions neglect of $Q(x)$ yields

$$\hat{\chi}(\mathbf{k},T)\simeq\frac{\hat{D}\sin[(1-\eta)\tan^{-1}(k/\kappa)]}{\cos(\frac{1}{2}\pi\eta)ka^{2-\eta}(\kappa^2+k^2)^{(1-\eta)/2}}, \quad (6.19)$$

which also has branch points at $k=\pm i\kappa$ rather than poles. At $T=T_c$ this again reduces to the correct form. For small η the formula may be simplified to

$$\hat{\chi}(\mathbf{k},T)\simeq\hat{D}'/a^{2-\eta}(\kappa^2+k^2)^{1-\eta/2}$$
$$\times\{1+\tfrac{1}{6}\eta(2-\eta)k^2/(\kappa^2+k^2)+\cdots\}, \quad (6.20)$$

where

$$\hat{D}'/\hat{D}=(1-\eta)/\cos\tfrac{1}{2}\pi\eta. \quad (6.21)$$

This is exactly equivalent to (6.19) for small k^2; furthermore the factor in braces is monotonic and never exceeds $\hat{D}/\hat{D}'$ which is always fairly close to unity when η is small.

For the susceptibility amplitude we obtain the approximation

$$C\simeq C'=4\pi\Gamma(2-\eta)(a^3/v_0)D/F^{2-\eta}, \quad (d=3). \quad (6.22)$$

At this stage we do not know the appropriate values of the parameters D and F and so cannot test for the importance of $Q(x)$ as before. We may anticipate our later results, however (see Tables VI and IX below), by stating that the estimates we will find for the right-hand side of (6.22) are only 13 to 14% *lower* (i.e., in the direction now expected) than the best estimates of C. Consequently $Q(x)$ is of less importance in three dimensions.

The relatively small variation of the correction factor in (6.20) suggests the following rough interpolation

formula[3] which embodies the principal differences from the Ornstein-Zernike mean field prediction (4.5):

$$\hat{\chi}(\mathbf{k},T)\simeq(1/r_1^{2-\eta})[\kappa_1^2+\psi K^2(\mathbf{k})]^{-1+(\eta/2)}, \quad (6.23)$$

where for given $\kappa_1(T)$ the length $r_1(T)$, the "effective interaction range," is now defined via

$$\chi_0(T)=1/(r_1\kappa_1)^{2-\eta}, \quad (6.24)$$

so that (6.23) is exact at $k=0$. By setting

$$\psi=1/(1-\tfrac{1}{2}\eta) \quad (6.25)$$

the approximation will also be correct at fixed T to first order in k^2. The variable $K^2(\mathbf{k})$ is used to take account of the lattice structure and to increase accuracy at higher values of k. Near T_c, the inverse ranges κ_1 and κ become proportional in accord with (6.13) and

$$F_1^2/F^2=\Delta_2\simeq\psi. \quad (6.26)$$

The behavior of (6.23) at $T=T_c$ is correct in *form* but as seen above, the amplitude will in general be in error although in three dimensions the deviation probably does not exceed about 15%. Furthermore, the singularity of (6.23) is *always* a branch point rather than a pole as required when $T>T_c$. Despite these defects (6.23) should be a useful first approximation both for the Ising model and for fitting experimental data.

6.3 A Better Approximant

To improve the approximants and allow for simple poles in $\hat{\chi}$ we may include a factor of the form (5.32) by writing

$$\hat{\chi}(\mathbf{k},T)\simeq\chi_0(T)\frac{[1+\phi^2\Lambda_2a^2K^2(\mathbf{k})]^{\eta/2}}{1+\psi\Lambda_2a^2K^2(\mathbf{k})}, \quad (6.27)$$

where ϕ and ψ may be functions of T. We suppose that accurate expressions for $\chi_0(T)$ and $\Lambda_2(T)$ or $\Lambda_2'(T)$ are available. If ψ is chosen so that

$$\psi(T)\Lambda_2(T)\approx\Lambda_2'(T) \quad \text{as} \quad T\to\infty, \quad (6.28)$$

the scattering function will have simple poles at $k_\alpha=\pm i\kappa$ corresponding correctly to the true range of correlation. As before the effective and true correlation ranges are related near T_c by (6.13) with $\Delta_2\simeq\psi_c=\psi(T_c)$. The exact behavior for small k^2 above T_c will be reproduced if $\phi(T)$ is now chosen so that

$$\psi(T)=1+\tfrac{1}{2}\eta\phi^2(T). \quad (6.29)$$

Evidently the *form* of the scattering at T_c will be correct while the amplitude will be approximated by

$$\hat{D}\simeq CF_1^{2-\eta}(\phi_c^\eta/\psi_c)\simeq CF^{2-\eta}(\phi_c/\psi_c^{1/2})^\eta, \quad (6.30)$$

where $\phi_c=\phi(T_c)$. Thus the critical value of ϕ can be chosen [possibly at some sacrifice of (6.28) near T_c] so that the *correct* value of D is given by the approximant.

By using the values (6.18), (5.11), and (5.25) we find for the square lattice

$$\begin{aligned}&\phi_c\simeq 0.0294,\\ &\psi_c\simeq 1.000108 \quad \text{(square lattice)}.\end{aligned} \quad (6.31)$$

We will find, furthermore, as already mentioned, that $\Lambda_2'-\Lambda_2=O(v^9)$ so that $\phi^2=O(v^8)$ for large T/T_c. Consequently, $\phi(T)$ must be small over its whole range and the departure of ψ from unity is always negligible for most practical purposes. This confirms the dominance of the exact pole terms in the scattering from the square lattice except rather close to T_c or, more specifically, except when $\phi k/\kappa\simeq k/35\kappa$ is of order unity or greater. For the triangular lattice the best estimate of the susceptibility amplitude C yields values of ϕ_c and ψ_c *identical* to (6.31).

It transpires that $\phi(T)$ is also rather small for the three-dimensional lattices ($\phi_c<0.1$, see Secs. 11.3 and 11.4) and is certainly always less than unity. Consequently the branch points $k_\beta'\simeq\pm i(\kappa/\phi)$ arising from the numerator of (6.27) are at least three times further from the real k axis than the zeros of the denominator, as is required generally. In fact these rather mild branch points mimic the effect of the presumably infinite sequence of singularities of the exact $\hat{\chi}(\mathbf{k})$ at $k_\beta=\pm 3i\kappa$, $k=\pm 5i\kappa,\cdots$, which are probably all weaker than poles (see Sec. 5.3). Like the true singularities the branch points k_β' close up on the poles as $T\to T_c$ in order to yield the appropriate behavior *at* T_c.

More elaborate approximation formulas than (6.27) are not justifiable without further detailed information about the correlations: This point is taken up briefly in Sec. 11.3. The remainder of the paper is chiefly concerned with obtaining accurate values of the exponents and other parameters needed for the approximation formulas and examining the numerical consequences.

7. HIGH-TEMPERATURE EXPANSIONS

7.1 Formulation

High-temperature expansions of the Ising-model correlation functions in zero field may be obtained in the standard way by writing the single-bond Boltzmann factor $\exp[(J/kT)s_is_j]$ as $\cosh(J/kT)[1+vs_is_j]$ and expanding all products.[11] The result is

$$\Gamma(\mathbf{r},T)=\sum_{n=1}^{\infty}v^nq_n(\mathbf{r}), \quad (\mathbf{r}\neq 0) \quad (7.1)$$

where

$$q_n(\mathbf{r})=\text{coefficient of } N^0 \text{ in } q_n(\mathbf{r};N) \quad (7.2)$$

and, in graphical terms,

$q_n(\mathbf{r};N)$ = number of configurations of n lines on a lattice of $N>n^d$ sites with periodic boundary conditions, in which (a) each bond of the lattice is used at most once, and (b) an even number of lines meet at each site other than the sites $\mathbf{0}$ and $\mathbf{r}$ where an odd number meet. (7.3)

This graphical prescription means essentially that one must have a self-avoiding *chain* of bonds (lines) running from site **0** to site **r** together with zero, one, or more polygons which may be quite separate or may touch the chain or one another at one or more vertices (although they must not have any lines in common). Some configurations, e.g., a theta graph,[36] can be decomposed into a chain and polygon in more than one way but must only be counted once.

Since it takes at least three bonds to close a polygon (or four on a loose-packed lattice) the first three (or four) coefficients will be given simply by the distributions on the lattice of random walks which make no immediate reversals.[22] The result may be written compactly in terms of the Fourier transforms $\hat{q}_n(\mathbf{k})$ for which

$$\hat{\Gamma}(\mathbf{k},T)=\sum_{n=1}^{\infty} v^n\hat{q}_n(\mathbf{k}). \tag{7.4}$$

Now the powers $[q\hat{\gamma}(\mathbf{k})]^n$ clearly generate the transforms of the unrestricted random walks. Thus by subtracting the immediate reversals and the triangular closure, we quite easily find

$$\hat{\chi}=1+q\hat{\gamma}v+(q^2\hat{\gamma}^2-q)v^2 +[q^3\hat{\gamma}^3-(2q-1)q\hat{\gamma}-6p_3]v^3+O(v^4), \tag{7.5}$$

where p_3 is the number of triangles per site of the lattice.[11] Inversion of this series yields

$$1/\hat{\chi}(\mathbf{k})=1-\hat{H}(\mathbf{k})=1-q\hat{\gamma}(\mathbf{k})v +qv^2-[\hat{\gamma}(\mathbf{k})+6p_3]v^3+O(v^4), \tag{7.6}$$

from which the statements of Sec. 4 regarding the degree of validity of the mean field and Bethe approximations may be checked directly. Notice that composite configurations of a chain and polygon can arise only in order $n=l+3$ (or $+4$), where l is the length of the shortest chain from **0** to **r**.

The expansions for the correlation moments (3.7) follow immediately from (7.1) to (7.3). In particular, in

$$\chi_0(T)=1+\mu_0=1+\sum_{n=0}^{\infty} m_n^{(0)}v^n, \tag{7.7}$$

the coefficient $m_n^{(0)}$ is the coefficient of N^0 in

$$m_n^{(0)}(N)=\text{total number of configurations of } n \text{ lines with only two odd vertices, one being at the origin.} \tag{7.8}$$

Consequently $m_n^{(0)}$ is made up of the total number c_n of n-step self-avoiding chains plus contributions from shorter chains with polygons. Similarly, the second moment is given by

$$\mu_2(v)=\sum_{n=0}^{\infty} m_n^{(2)}v^n, \tag{7.9}$$

where $m_n^{(2)}$ is equal to the total number of chains, and chain plus polygon configurations, in which each chain is weighted by the square of its (reduced) end-to-end distance; formally

$$m_n^{(2)}=\sum_{\mathbf{r}}(r/a)^2q_n(\mathbf{r})=\langle R_n^2\rangle m_n^{(0)}, \tag{7.10}$$

where $\langle R_n^2\rangle$ is the mean square size of the nth-order distribution. The second moment is easier to calculate than the whole distribution since a detailed breakdown of configurations is unnecessary (see below).

7.2 Range of Correlation

An expansion for the true range of correlation $\kappa_e(T)$ may be found by analyzing the expression (5.21) for the decay factor.[29] Here only the result in graphical terms is presented. For simplicity, we consider only directions **e** corresponding to a lattice axis, say the x axis. We suppose, in the first instance, that the lattice is made up of $(L+1)$ layers normal to **e**, each layer having A sites and being connected with periodic boundary conditions. A chain of L lines parallel to **e** will just reach from the origin in the zeroth layer to the corresponding site in the Lth layer. With m additional bonds in the chain the site reached in the last layer may be displaced from that corresponding to **0**. In either case, however, we may assign periodic or skew-periodic boundary conditions by identifying the end-points of the chain (which thus becomes closed) and thence all other similarly related points in the zeroth and Lth layers. With this convention for "periodic boundary conditions" we define

$$w_n(L;N)=\text{number of configurations of } L+n \text{ lines on a lattice of } N \text{ sites } (L>n \text{ and } N>Ln^{d-1}) \text{ in which (a) each lattice bond is used at most once, (b) an even number of lines meet at each site, and (c) a chain of bonds reaches around the lattice in the direction } \mathbf{e} \text{ and passes through the origin;} \tag{7.11}$$

and, formally setting $L=1$,

$$w_n=\text{coefficient of } N^0 \text{ in } w_n(L=1;N). \tag{7.12}$$

(The special boundary conditions imposed are needed to ensure the correctness of this definition.) Then we have for the range of correlation

$$\omega_x=\exp(-\kappa_x a)=v\sum_{n=0}^{\infty} w_nv^n. \tag{7.13}$$

To illustrate the use of this expansion (and incidentally to provide a check on the prescription) we calculate the leading terms of ω_x for the square lattice. Clearly $w_0(L;N)=w_0=1$. With one extra bond we may insert a "kink" in the chain, i.e., a step parallel to the positive or negative y axis. Since this may be inserted in L

[36] In the terminology of Sykes [see M. F. Sykes, J. W. Essam, B. R. Heap, and B. J. Hiley, J. Math. Phys. 7, 1557 (1966)] a theta graph has the topology of the letter Θ.

places we have

$$w_1(L;N)=2L. \tag{7.14a}$$

With $n=2$ extra bonds, there might be two separated unit kinks, or a double kink of two consecutive positive or negative y bonds; consequently

$$w_2(L;N)=4\binom{L}{2}+2L. \tag{7.14b}$$

Similarly for $n=3$ the possibilities are (i) three separated unit kinks, (ii) a double kink and a separated unit kink, or (iii) a treble kink, so that

$$w_3(L;N)=8\binom{L}{3}+4L(L-1)+2L. \tag{7.14c}$$

Combining these results in (7.12) and (7.13) and distinguishing the interactions along the two axes yields

$$\omega_x=v_x[1+2v_y+2v_y^2+2v_y^3+\cdots], \tag{7.15}$$

which illustrates that terms due to the separated kinks drop out.

More interesting behavior occurs in the fourth-order term. The different combinations of simple kinks yield the contribution

$$16\binom{L}{4}+8L\binom{L-1}{2}+4\binom{L}{2}+4L(L-1)+2L \quad \text{to } v_y^4. \tag{7.16a}$$

However, one may also construct a "hook" by using a retrograde x step as illustrated in Fig. 1. Evidently this contributes

$$2L \quad \text{to} \quad v_x^2v_y^2. \tag{7.16b}$$

Finally it is possible to have a separated square which must not have a line in common with the now straight chain. This yields the extra contribution

$$(N-2L) \quad \text{to} \quad v_x^2v_y^2. \tag{7.16c}$$

On applying (7.12) these last two terms cancel precisely and we are left with only the term $2v_y^4$ from (7.16a). In fifth order a similar cancellation of the terms in $v_x^2v_y^3$ takes place between three types of hook and a chain with a unit kink and a separated square. In total we reproduce just the expansion of the rigorous result (5.23) generalized to two interactions.[31]

For the simple cubic lattice we see similarly that the leading terms due to kinks are

$$w_0=1, \quad w_1=4, \quad w_2=12, \quad w_3=36, \tag{7.17}$$

which correspond simply to the first few self-avoiding walks in one of the square layers. In fourth order the corresponding contribution is $w_4^{(i)}=100$. The hook now makes a contribution of $w_4^{(ii)}=12$ since it may be bent, whereas the chain and separated square yield only $w_4^{(iii)}=-4$. In total therefore $w_4=108$.

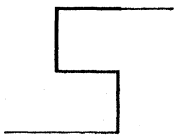

FIG. 1. A "hook" of four extra bonds arising in the graphical expansion of the true range of correlation on the square lattice.

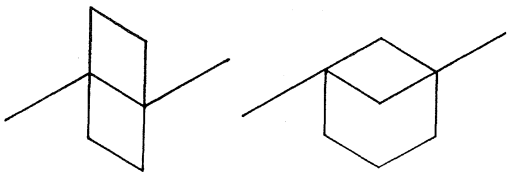

FIG. 2. Configurations contributing to the range of correlation series for the simple cubic lattice in order 7.

In higher order the complications ramify. The "in-layer" self-avoiding walk terms may be obtained from known work.[37] The hooks and other retrograde configurations may be classified according to the number of retrograde steps and may be enumerated by projection onto a layer. Most then reduce to lower-order self-avoiding walks decorated with two or more "dots." However, the possibilities of multiple lines and intersections in the projected configurations must not be overlooked. Interference between separated retrograde configurations and kinks must be carefully examined since they yield a nonvanishing net contribution unlike sets of separated kinks alone. Configurations with separated polygons have to be studied mainly by considering the various space types, e.g., on the simple cubic the flat, bent, and twisted hexagons. Special care must be taken not to overlook *or* overcount configurations such as those in Fig. 2 which can be decomposed into a chain and polygon in various different ways. The completeness of the enumeration of possibilities can be checked by reproducing the exact square lattice expansion to higher order. Full details of the necessary configurations and their weights have been given elsewhere.[14b] The final result for the simple cubic lattice is

$$\omega_x=v+4v^2+12v^3+36v^4+108v^5+356v^6+1204v^7+4420v^8+16124v^9+\cdots. \tag{7.18}$$

Its behavior will be analyzed in Sec. 8.1.

The corresponding expansions may be obtained for the bcc and fcc lattices but owing to the increased complexity these have only been carried to the first few terms (see also later discussions).

7.3 Enumeration and Counting Problem

In the remainder of this section we explain in more detail the techniques used to calculate the first n terms of the second-moment series $\mu_2(v)$ and hence of $\Lambda_2(v)$ for the square ($n=11$), triangular ($n=8$), simple cubic ($n=10$), bcc ($n=8$), and fcc ($n=6$) lattices and to calculate the complete set of correlation functions to order $n=11$ on the square lattice and to order $n=10$ on the simple cubic. The resulting series are

[37] M. E. Fisher and M. F. Sykes, Phys. Rev. **114**, 45 (1959).

tabulated fully in Appendix B. The reader uninterested in the technical details of the enumeration and counting problem should proceed directly to Sec. 8 where the various series are analyzed.

We consider firstly the evaluation of the second-moment series (7.9) and start by expressing the coefficients more concisely in graphical terms. Now a *weak embedding* of an abstract linear graph Υ_n of n lines (connected or otherwise) in a lattice $\mathcal{L}$ is defined by the conditions (a) that each line of the graph lies on a distinct bond of $\mathcal{L}$ and (b) that each vertex of the graph lies on a distinct site of $\mathcal{L}$. Let $\mathfrak{N}(\Upsilon_n; \mathcal{L}, N)$ be the number of such distinct weak embeddings of Υ_n in a lattice $\mathcal{L}$ of $N > n^d$ sites with periodic boundary conditions. Then the (weak) *lattice constant* of Υ_n in $\mathcal{L}$ is defined by[11]

$$(\Upsilon_n) = \text{coefficient of } N \text{ in } \mathfrak{N}(\Upsilon_n; \mathcal{L}, N). \quad (7.19)$$

If now Ω_n denotes a graph of n lines (connected or otherwise) with precisely two vertices of odd degree we have from (7.2), (7.3), and (7.10)

$$m_n^{(2)} = 2 \sum_{\Omega_n} \langle R^2(\Omega_n) \rangle (\Omega_n), \quad (7.20)$$

where $R^2(\Omega_n)$ denotes the square of the distance between the odd vertices of Ω_n in a particular embedding (using units of a lattice spacing) and the angular brackets denote an average over all embeddings. The factor 2 arises from the choice of origin on either of the odd vertices.

From this expression it is clear that the task of calculating $m_n^{(2)}$ may be split into three parts: (i) the enumeration of all the required graphs Ω_n; (ii) the determination of the corresponding lattice constants (Ω_n); (iii) the calculation of the mean square sizes $\langle R^2(\Omega_n) \rangle$.

As regards (i) the graphs Ω_n are also needed for the calculation of the susceptibility $\chi_0 = 1 + \mu_0$. Since the latter series are known to high order[33] it might be thought that a list of the required Ω_n would be already available. However, the existing series were obtained with the aid of a counting theorem proved by Sykes[38] which, by means of a recurrence relation, bypasses the need for a complete graphical breakdown. However, since the susceptibility coefficients verify

$$a_n = m_n^{(0)} = \sum_{\Omega_n} (\Omega_n), \quad (7.21)$$

a useful check on steps (i) and (ii) is provided by the known coefficients.[38]

It may be remarked that the counting theorem is not readily generalized to the calculation of $m_n^{(2)}$ since the information on the separation of the odd vertices must now be carried through. The symbolic methods of analysis used in proving the theorem may, however, be applied to those graphs Ω_n in which the two odd vertices

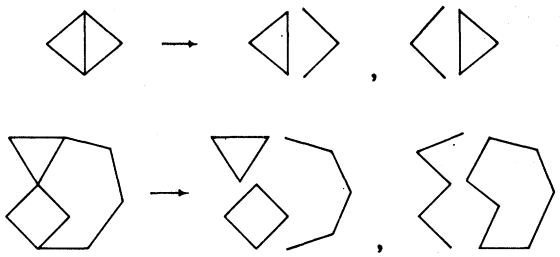

FIG. 3. Two graphs which may be decomposed into a longest chain and polygons in $\delta = 2$ distinct ways.

are on a common line since the mean square size is then trivial.

To proceed further we classify the graphs Ω_n into simple chains C_n, and composite graphs of chains and one, two, $\cdots$ polygons which we write $C_l \oplus P_m$, $C_l \oplus P_m \oplus P_{m'}, \cdots$ where the total number of lines is n. The graphs $C_l \oplus P_m$ include (a) a chain and a (completely) separated polygon written as C_l, P_m, (b) a chain with a polygon touching at one vertex, and (c) a chain with a polygon touching at two or more vertices subject to the restriction that such graphs, which can be decomposed in more than one way, must always be regarded as formed from the largest possible chain and the smallest possible polygon. The composite graphs of type $C_l \oplus P_m \oplus P_{m'}$, etc. are defined similarly. However, there is still the possibility that some composite graphs may be formed in a number of distinct ways (as illustrated in Fig. 3). Such rather highly connected graphs must be classified separately and will be denoted by Ξ_n while $\delta(\Xi_n)$ will denote the number of their allowed decompositions. With this notation we have

$$\tfrac{1}{2} m_n^{(2)} = \langle R^2(C_n) \rangle (C_n) + \sum_{l+m=n} \langle R^2(C_l \oplus P_m) \rangle (C_l \oplus P_m) + \sum_{l+m+m'=n} \langle R^2(C_l \oplus P_m \oplus P_{m'}) \rangle (C_l \oplus P_m \oplus P_{m'}) + \cdots - \sum [\delta(\Xi_n) - 1] \langle R^2(\Xi_n) \rangle (\Xi_n), \quad (7.22)$$

where the last term corrects for overcounting in the earlier summations.

The first term in (7.22) is numerically the largest and may be obtained from studies on the lattice "excluded volume problem."[37] Specifically the number of self-avoiding walks $c_n = 2(C_n)$ is known to high order.[37,38] Fisher and Hiley[39] calculated the mean square sizes $\langle R^2(C_n) \rangle$ by a recursion method to order 8 and 10 on the simple cubic and square lattices. Martin[40] calculated with an electronic computer the distribution $c_n(x)$ of self-avoiding walks which terminate on a given plane for the simple cubic to order 10 and the bcc and fcc lattices to orders 8 and 7, respectively. Martin also obtained the complete distributions for the square and triangular lattices to orders 12 and 9, respectively. The

[38] M. F. Sykes, J. Math. Phys. **2**, 52 (1961).

[39] M. E. Fisher and B. J. Hiley, J. Chem. Phys. **34**, 1253 (1961).

[40] J. L. Martin, Proc. Cambridge Phil. Soc. **58**, 92 (1962).

corresponding square-size series were published (and analyzed) by Domb.[41] More recently Domb, Gillis, and Wilmers[42] have computed the complete distributions of self-avoiding walks on the square lattice to order 18 and on the simple cubic to order 13. These latter data are ample for our present purposes, but for the bcc and fcc lattices we have ourselves programmed a computer to obtain the complete distributions (and additional data, see below) to orders 9 and 6, respectively.

7.4 Analysis of Composite Graphs

The composite graph $C_l \oplus P_m$ first enters at order $n=l+3$, or $l+4$ on a loose-packed lattice. From the definition of the lattice constant of a separated graph one finds that to calculate $(C_l \oplus P_m)$ one need only examine "disallowed graphs," $C_l \bigstar P_m$, formed by superimposing a C_l and P_m with one or more *multiple lines* (such overlapping configurations not contributing *directly* to the Ising-model series). By further noticing that the two odd vertices must belong to the same connected component, we see that

$$\langle R^2(C_l \oplus P_m)\rangle(C_l \oplus P_m) = -\langle R^2(C_l \bigstar P_m)\rangle(C_l \bigstar P_m). \quad (7.23)$$

In applying this expression, however, we must bear in mind the restriction (c) on the definition of the graphs $C_l \oplus P_m$ when C_l and P_m touch at two or more points. Such configurations will be overcounted when (7.23) is eventually summed over l and m, and must be subtracted. Thus in fifth order the graph θ_5, a square with diagonal, may be formed either from a triangle and a two-chain (in two ways as discussed above) or from a square and a unit chain, which combination must be removed from the corresponding reduction formula.

To calculate the lattice constants of overlapping or multiple-line graphs $C_l \bigstar P_m$ we use both the method of direct counting of possibilities, which needs no further explanation, and the following method which employs data obtained with the aid of a computer. To illustrate what is involved consider the most numerous case (on a loose-packed lattice) of a square P_4 and a chain C_{n-4}. The number of squares passing through a given bond is $8p_4/q$, where $p_4=(P_4)$. Hence, in first order there will be $(n-4)8p_4/q$ overlapping configurations. However, in some of these, two or more bonds of the chain will coincide with the square and, clearly, these cases will be overcounted. Most frequently the double bonds will lie consecutively along the chain as illustrated in Figs. 4(a) and (b). The occurrence of such cases may be determined once the relative orientations of successive pairs of bonds along the chain are known. On the square and simple cubic lattices we need only distinguish the junction types (i) "straight on," and (ii) "bent."

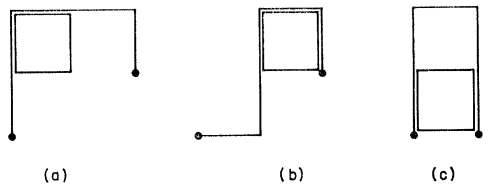

FIG. 4. Various overlapping configurations of a square, P_4, and a five-chain, C_5, on the square lattice.

If j_2 is the number of bent junctions in a particular embedding of C_{n-4}, we must have in second order $[(n-4)(8p_4/q)-j_2]$ overlapping configurations. Finally cases of two or more *non*consecutive overlaps, such as illustrated in Fig. 4(c) must be subtracted separately. Notice, however, that three or more consecutive overlaps *are* correctly accounted for by the second-order expression.

The method may be extended to arbitrary polygons and lattices by defining weights $\rho_i(P_m)$ equal to the number of polygons P_m which pass through a pair of consecutive bonds forming an ith type of junction. If $J_i(C_l)=\sum j_i$ is the total numbers of junctions of the ith type in all embeddings of C_l, the second-order correction is generally $-\sum_i \rho_i(P_m)J_i(C_l)$. Once again configurations with *non*consecutive overlaps must be corrected for separately. However, these are generally much fewer in number and cannot, in any case, arise until relatively high order.

The weights $\rho_i(P_m)$ may be ascertained fairly easily by examining the various "space types" of embedding of P_m. The numbers $J_i(C_l)$, on the other hand, are conveniently found by programming a computer to generate all self-avoiding walks and recording the numbers of the various types of junction and, for the complete correlation distributions, the end-to-end distances and vectors. An outline of the program, which is not entirely straightforward if an unreasonable amount of computing time is not to be used, has been presented elsewhere.[14b] The complete distributions with junction counts have been obtained for the square simple cubic, bcc and fcc lattices to order 7, 6, 6, and 5, respectively. These are sufficient to yield the appropriate data for the correlation functions to orders 11, 10, 10, and 8, respectively.[14b]

The analysis of the composite configuration $C_l \oplus P_m \oplus P_{m'}$ with two polygons is similar but appreciably more involved. Indeed the complications increase so rapidly that without an extension of technique it would be difficult to count correctly configurations of a chain with three or more polygons. This sets a limit of $n \leqslant 12$ on the loose packed lattices and $n \leqslant 9$ on a general lattice. So far, however, these limits have not quite been attained, principally because of the difficulties already arising in high order with two polygons or one polygon and a relatively long chain.

We have mainly considered the second-moment series but it is clear that the same general techniques apply to the derivation of the complete correlation function

[41] C. Domb, J. Chem. Phys. 38, 2957 (1963). Domb extended the values for the square lattice to $n=16$.

[42] C. Domb, J. Gillis, and G. Wilmers, Proc. Phys. Soc. (London) 85, 625 (1965).

distribution if full account is kept of the separation vectors of the odd vertices in all configurations.

The second-moment expansions and, for convenience, the zeroth-moment or susceptibility expansions (to comparable order) are listed in Table XV of Appendix B. The complete correlation expansion coefficients $q_n(\mathbf{r})$ for the square and simple cubic lattices are given in Tables XVI and XVII of Appendix B while the fourth- and sixth-moment expansions for these lattices are presented in Table XVIII. The detailed configurational data for the second-moment series are available[14b] but are not given here in the interests of space economy.

8. ANALYSIS OF SERIES

In this section we study the high-temperature series expansions in powers of v whose derivation was explained in the previous section. In the analysis we use the exact critical points (5.1) for the plane lattices and the estimates

$$\begin{aligned} v_c &\simeq 1/4.5840 \simeq 0.218150, \quad \text{(simple cubic)} \\ &\simeq 1/6.4032 \simeq 0.156172, \quad \text{(bcc)} \\ &\simeq 1/9.8260 \simeq 0.101771, \quad \text{(fcc)} \end{aligned} \tag{8.1}$$

for the three cubic lattices. The estimates for the sc and bcc are those of Sykes, Domb, and Fisher[33,35]; they differ by less than 5 parts in 10^5 from the estimates of Baker[34] and are probably correct to 1 part in 10^4 or better. The estimate adopted for the fcc lattice lies close to Baker's estimate[34] and is 2 parts in 10^4 larger than the original estimate of Domb and Sykes.[33] We have adopted it here because it seems to give rather more consistent results. For all three lattices the uncertainties in v_c are so small (relative to the available length of series) as to make very little difference to our conclusions. In particular, they only affect the third decimal place in estimates of the various exponents ν, η, etc.

In analyzing the series we will employ the ratio and Padé approximant techniques. These methods have been discussed in detail elsewhere[5,33–35,43,44] and we will not, therefore, give further general explanations.

8.1 Correlation Range

We start by studying the series (7.18) for the decay factor $\omega_x = \exp(-\kappa_x a)$ for the simple cubic along a lattice axis. The last five ratios $\mu_n = w_n/w_{n-1}$ are

$$3.000,\ 3.296,\ 3.382,\ 3.671,\ 3.648, \tag{8.2}$$

while the square roots of alternate ratios, $(w_n/w_{n-2})^{1/2}$, are

$$3.000,\ 3.1447,\ 3.3389,\ 3.5236,\ 3.6595. \tag{8.3}$$

These sequences are increasing roughly linearly with $1/n$ and extrapolation indicates a limit of about $4.6 \simeq 1/v_c$ (the second sequence being far more regular). This indicates that $\omega_x(T)$ is nonanalytic at $T=T_c$ for the simple cubic lattice in contrast to the plane square lattice [see Eq. (5.23)] but as would be expected on the basis of the mean field or Bethe approximations [see Eq. (4.12)]. The limiting slope of the sequences (8.2) and (8.3) on a plot versus $1/n$ should yield the exponent ν. The sequences are not sufficiently regular, however, to yield more than the rough estimate $0.60 \leqslant \nu \leqslant 0.70$; this is consistent with our expectations but says nothing significant about the value of η.

To obtain a more well-behaved function we use the fact that $\omega_x \to 1$ as $T \to T_c$ and examine the function

$$\begin{aligned} (1-\omega_x)^{-1} = 1 &+ v + 5v^2 + 21v^3 + 89v^4 + 377v^5 + 1629v^6 \\ &+ 7061v^7 + 30977v^8 + 135993v^9 + \cdots, \end{aligned} \tag{8.4}$$

which must diverge at the critical point as $(T-T_c)^{-\nu}$. The ratios of this series are found to behave quite regularly and from the sequence of ratios μ_n we may form successive estimates

$$\nu_n\{(1-\omega_x)^{-1}\} = 1 - n(1-\mu_n v_c) \tag{8.5}$$

for the exponent ν. We find

$$\nu_n = 0.6204,\ 0.6557,\ 0.6191,\ 0.6563,\ 0.6194. \tag{8.6}$$

These are oscillating regularly (a consequence of the loose-packed structure of the lattice) so we examine the sequence of means

$$\bar{\nu}_n = \tfrac{1}{2}(\nu_n + \nu_{n-1}), \tag{8.7}$$

which yields

$$\bar{\nu}_n = 0.6593,\ 0.6380,\ 0.63740,\ 0.63769,\ 0.63782. \tag{8.8}$$

These are rising slightly and accordingly we estimate

$$\nu = 0.641 \pm 0.004. \tag{8.9}$$

Through the relation (6.9) and the result[33–35] $\gamma = 1.250$ this provides us with our first estimate of η in three dimensions, namely,

$$\eta = 0.050 \pm 0.012, \tag{8.10}$$

which is clearly greater than zero. In fact our further analysis will lead us to a somewhat higher estimate of greater precision.

We may also employ the Padé approximant technique to study the function $(1-\omega_x)^{-1}$. If this function has a pure branch point at $v=v_c$ then the logarithmic derivative

$$D(v) = (d/dv)\ \ln(1-\omega_x)^{-1} \tag{8.11}$$

will have a pole at $v=v_c$ but will otherwise be analytic there. In these circumstances, the Padé approximants should converge rapidly and the residues of the approximants to $D(v)$ or the values of the generalized exponent function

$$\nu^*\{v;\ 1-\omega_x\} = (v-v_c)(d/dv)\ \ln(1-\omega_x)^{-1} \tag{8.12}$$

[43] J. W. Essam and M. E. Fisher, J. Chem. Phys. 38, 802 (1963).
[44] G. A. Baker, Jr., in *Advances in Theoretical Physics*, edited by K. A. Brueckner (Academic Press Inc., New York, 1965), Vol. I.

at $v=v_c$ should yield accurate estimates for ν. In fact, it is found that the Padé approximants to $D(v)$ or $\nu^*(v)$ converge very slowly at v_c and do *not* yield useful estimates for ν.[45] The structure of the approximants indicates a singularity more complex than a simple branch point in $(1-\omega_x)$, of the form, for example,

$$(1-\omega_x)=A(v-v_c)^{\nu}[1+b(v-v_c)^{\zeta}+\cdots], \quad (8.13)$$

with $0<\zeta<1$ and a significant value of b. It is easily checked that the functions $D(v)$ and $\nu^*(v)$ following from (8.13) still have branch points at $v=v_c$. Furthermore, the behavior of the expansion coefficients of $D(v)$ themselves is also consistent with (8.13). The occurrence of such a strong "coincident branch point" is perhaps not very surprising since reference to Eqs. (4.13) and (4.14) shows that the same thing happens even in the mean field approximation (where $\zeta=\frac{1}{2}$) and it remains in the Bethe approximation.

To complete the analysis of ω_x we form the *effective* reduced second moment $\Lambda_2'(\omega)$ of the inverse scattering as defined in Eq. (4.17) [see also the discussion in Sec. 5.4]. Substituting with (7.18) we find

$$\Lambda_2'(v)=v+6v^2+31v^3+156v^4+765v^5+3714v^6 +17827v^7+85144v^8+404081v^9+\cdots. \quad (8.14)$$

From its definition we see that this function should diverge as $(T-T_c)^{-2\nu}$.

The ratios are again found to be quite smoothly behaved and from the analog of (8.5) and (8.7) we find the sequence of estimates

$$2\bar{\nu}_n\{\Lambda_2'\}=1.2738,\ 1.2862,\ 1.2873,\ 1.28907,\ 1.28802,\ 1.28813. \quad (8.15)$$

These are a little irregular but suggest a limit fairly close to $2\nu=1.2875$ or

$$\nu=0.6437\pm0.0015. \quad (8.16)$$

We may now reapply the Padé approximant method to the function $\Lambda_2'(v)$. In the mean field and Bethe approximations (where $\Lambda_2'=\Lambda_2$) the correction factor at $T=T_c$ is now quite analytic so we might hope more generally that $\Lambda_2'(v)$ will have a *simple* branch point at v_c. This guess is borne out by the rapid convergence of approximants to the logarithmic derivative of $\Lambda_2'(v)$ and to the generalized exponent $2\nu^*\{\Lambda_2'/v\}$ defined in analogy to (8.12). In Table I we display some of the higher-order Padé approximant estimates for 2ν.[46] These suggest a limit in the range $2\nu=1.290\pm0.003$ or

$$\nu=0.645\pm0.0015, \quad (8.17)$$

TABLE I. Padé approximant estimates (Ref. 45) of ν from $2\nu^*\{\Lambda_2'/v\}=-[(v-v_c)(d/dv)\ \ln(\Lambda_2'/v)]_{v=v_c}$ for the simple cubic lattice.

L, M	$2\nu^*\{\Lambda_2'\}$	L, M	$2\nu^*\{\Lambda_2'\}$
1, 2	1.2850	1, 6	1.2886
2, 1	1.2845	2, 5	1.2921
		3, 4	1.2929
2, 2	1.3058	4, 3	1.2916
		5, 2	1.2913
2, 3	1.2910	6, 1	1.2886
3, 2	1.2908		
2, 4	1.2906		
3, 3	1.2899		
4, 2	1.2904		

which is consistent with (8.16) and (8.9) although somewhat higher.

It may be appropriate at this juncture to stress that the uncertainties quoted here and elsewhere represent an indication of the apparent precision of the procedure used and are not in any sense rigorous bounds. The consistency between different procedures gives an indication of the probable over-all accuracy and precision.

We may summarize our analysis of the true range of correlation of the simple cubic lattice with the combined estimate

$$\nu=0.644\pm0.002, \quad (8.18)$$

which yields

$$\eta=0.059\pm0.006. \quad (8.19)$$

With the aid of these estimates we can construct approximation formulas for the numerical evaluation of ω_x and κ_x for all $T>T_c$; but we defer consideration of this task to Sec. 9.

8.2 Second-Moment Expansion

The expansion coefficients $m_n^{(2)}$ of the second moment $\mu_2(v)$ of the correlations are listed in Appendix B. We examine these firstly by the ratio method to estimate the exponent of divergence at T_c which, by the definitions (3.16), (3.20), and (3.23), will be $\gamma+2\nu_1$. The ratios $\mu_n=m_n^{(2)}/m_{n-1}^{(2)}$ are found to behave regularly on a plot versus $1/n$ and linear extrapolation yields the known critical points quite accurately. Accordingly we proceed directly to estimate ν_1 from the sequence

$$2\nu_{1,n}\{\mu_2\}+\gamma-1=(n-\delta)(v_c\mu_n-1), \quad (8.20)$$

where δ represents an "n shift" which has no effect asymptotically but yields different sequences for finite n. This is a useful aid to over-all extrapolation. Various sequences for all the lattices are presented in Table II.

The sequences $2\nu_{1,n}$ for the two plane lattices are fairly slowly varying but are significantly curved on a $1/n$ plot. However, the corresponding sequence of linearly extrapolated *intercepts*

$$2\nu_{1,n}'=(n+1)(2\nu_{1,n+1})-n(2\nu_{1,n}) \quad (8.21)$$

[45] The near diagonal approximants to $\nu^*(v)$ yield the mainly increasing sequence 0.565, 0.555; 0.565, 0.574; 0.583, 0.592; see R. J. Burford's thesis [Ref. 14(b)].

[46] We adhere to the notation of Ref. 43 in which $[L,M]$ denotes an approximant with a polynomial of degree L in the numerator and degree M in the denominator. Baker (Refs. 34 and 44) and other authors use the opposite convention.

TABLE II. Estimates $2\nu_{1,n}$ derived from the ratios of the expansion coefficients for the second moment $\mu_2(v)$ through Eq. (8.20).

Square			Triangular			sc			bcc			fcc		
n	$\delta=0$	$\delta=\frac{1}{2}$	n	$\delta=0$	$\delta=\frac{1}{2}$	n	$\delta=1$	$\delta=\frac{1}{2}$	n	$\delta=1$	$\delta=\frac{1}{2}$	n	$\delta=1$	$\delta=\frac{1}{2}$
5	2.2165	1.9200	3	2.7478	2.1648	4	1.2839	1.5396	3	1.2053	1.5691	2	1.1925	1.9138
6	2.1486	1.9070	4	2.4542	2.0537	5	1.2777	1.4687	4	1.2393	1.4875	3	1.2187	1.5859
7	2.1028	1.8990	5	2.3151	2.0087	6	1.2837	1.4371	5	1.2400	1.4262	4	1.2349	1.4824
8	2.0765	1.8999	6	2.2367	1.9878	7	1.2819	1.4096	6	1.2513	1.4014	5	1.2446	1.4314
9	2.0561	1.9003	7	2.1871	1.9773	8	1.2845	1.3941	7	1.2526	1.3777	6	1.2509	1.4010
10	2.0435	1.9038	8	2.1532	1.9718	9	1.2835	1.3794	8	1.2583	1.3661			
11	2.0329	1.9064				10	1.2849	1.3702						

for the triangular lattice, and

$$2\nu_{1,n}''=\tfrac{1}{2}(n+1)(2\nu_{1,n+2})-\tfrac{1}{2}(n-1)(2\nu_{1,n}) \quad (8.22)$$

for the square lattice vary almost linearly with $1/n$ and may be extrapolated with greater confidence. In this way we estimate

$$\begin{aligned}\nu_1&=1.000\pm0.010, \quad \text{square}\\ &=1.005\pm0.010, \quad \text{triangular}.\end{aligned} \quad (8.23)$$

We note in the first place that the two values are essentially identical as expected. Secondly, within the uncertainties of $\pm1\%$ we also have $\nu=\nu_1$ in agreement with the conclusions of Sec. 6.1.

For the three-dimensional lattices the values of $2\nu_{1,n}$ are found to vary more linearly with $1/n$. Indeed the $\delta=1$ sequence for the simple cubic lattice is almost constant (see Table II). Allowing for the slight rate of increase of this sequence suggests a limit of $2\nu_1\simeq1.287$. The successive intercepts (8.22) of the $\delta=\frac{1}{2}$ sequence are 1.2834, 1.2907, 1.2866, 1.2886, and 1.2866. In view of these results we estimate

$$\nu_1=0.6435\pm0.0010, \quad \text{sc}. \quad (8.24)$$

This agrees closely with the final estimate (8.18) for ν so that, well within the uncertainties of extrapolation, we have $\nu=\nu_1$ for the simple cubic lattice also.

The sequences for the bcc lattice are shorter but also fairly regular. The intercepts (8.22) for the $\delta=\frac{1}{2}$ sequence are 1.2833, 1.2723, 1.2807, and 1.2779 which seem to be increasing. The most constant intercepts for the $\delta=1$ sequence are obtained by replacing the factors $(n+1)$ and $(n-1)$ in (8.22) by $(n+3)$ and $(n+1)$ and are 1.3094, 1.2813, 1.2904, and 1.2828. From these figures we conclude

$$\nu_1=0.6425\pm0.0015, \quad \text{bcc}. \quad (8.25)$$

Evidently, within the precision obtainable this agrees with the value for the simple cubic confirming the expected independence of lattice structure.

Finally for the fcc only very short sequences are available although they are fairly linear. The intercepts calculated for $\delta=1$ from (8.21) are 1.2711, 1.2835, 1.2834, and 1.2824. We feel able to estimate

$$\nu_1=0.6415\pm0.0025, \quad \text{fcc}. \quad (8.26)$$

This is slightly lower than the values for the bcc and sc lattices but allowing for the increased uncertainty due to the shorter length of the series there seems little

TABLE III. Padé approximant estimates of ν from $2\nu^*\{\mu_2/v\}=-[(v-v_c)(d/dv)\ln(\mu_2/v)]_{v=v'}-\gamma$.

Square		Triangular		sc		bcc		fcc	
L, M	$2\nu^*$	L, M	$2\nu^*$	L, M	$2\nu^*$	L, M	$2\nu^*$	L, M	$2\nu^*$
2, 2	1.9531	1, 1	1.9835	1, 2	1.2766	1, 1	1.2139	0, 2	1.2812
				2, 1	1.2753			1, 1	1.2931
2, 3	1.8990	1, 2	1.9822			1, 2	1.2782	2, 0	1.2798
3, 2	2.0140	2, 1	1.9821	2, 2	1.3594	2, 1	1.2747		
								0, 3	1.2822
3, 3	2.2266	2, 2	1.9835	2, 3	1.2951	2, 2	1.2833	1, 2	1.2823
				3, 2	1.2943			2, 1	1.2821
2, 5	2.0038	2, 3	2.0094	2, 4	1.2935	2, 3	1.2812	3, 0	1.2812
3, 4	1.9334	3, 2	2.0069	3, 3	1.2900	3, 2	1.2808		
4, 3	2.0291							1, 3	1.2816
		2, 4	2.0003	2, 5	1.2790	2, 4	1.2813	2, 2	1.2805
2, 6	1.9958	3, 3	2.0017	3, 4	1.2876	3, 3	1.2813	3, 1	1.2812
3, 5	1.9995	4, 2	1.9998	4, 3	1.2873	4, 3	1.2812		
4, 4	2.0037								
5, 3	1.9983			2, 6	1.2868				
				3, 5	1.2879				
2, 7	1.9994			4, 4	1.2879				
3, 6	2.0007			5, 3	1.2879				
4, 5	2.0011								
5, 4	2.0007								

TABLE IV. Padé approximant estimates of ν from $2\nu^*\{\Lambda_2/v\} = -[(v-v_c)(d/dv)\ln(\Lambda_2/v)]_{v=v_c}$.

Square		Triangular		sc		bcc		fcc	
L, M	$2\nu^*$	L, M	$2\nu^*$	L, M	$2\nu^*$	L, M	$2\nu^*$	L, M	$2\nu^*$
3, 3	2.0000	1, 1	2.0181	2, 4	1.2906	1, 1	1.2420	0, 2	1.2787
				3, 3	1.2899			1, 1	1.2844
2, 5	2.0234	1, 2	2.0018	4, 2	1.2904	1, 2	1.2787	2, 0	1.2775
3, 4	1.9927	2, 1	2.0008			2, 1	1.2769		
4, 3	2.0025			2, 5	1.2919			0, 3	1.2811
		2, 2	2.0000	3, 4	1.2926	2, 2	1.2830	1, 2	1.2816
2, 6	1.9972			4, 3	1.2915			2, 1	1.2815
3, 5	1.9952	2, 3	2.0019	5, 2	1.2912	2, 3	1.2816	3, 0	1.2806
4, 4	1.9954	3, 2	2.0009			3, 2	1.2814		
5, 3	1.9923			2, 6	1.2823			1, 3	1.2810
2, 7	1.9956	2, 4	1.9981	3, 5	1.2891	2, 4	1.2818	2, 2	1.2808
3, 6	1.9958	3, 3	1.9881	4, 4	1.2858	3, 3	1.2819	3, 1	1.2810
4, 5	1.9960	4, 2	1.9944	5, 3	1.2894	4, 3	1.2814		
5, 4	1.9959			6, 2	1.2825				

reason to doubt that the true value of ν_1 is the same for all the cubic lattices and equal to ν.

We have also used the Padé approximant technique to estimate ν from the μ_2 series. Table III presents various approximants formed by evaluating $2\nu^*\{\mu_2/v\}$ defined in analogy to (8.12). For both plane lattices, the approximants converge very rapidly and we would estimate

$$\nu_1 = 1.000 \pm 0.003, \quad (d=2) \tag{8.27}$$

which is a significant improvement on the result (8.23) obtained by the ratio method and confirms closely the equality $\nu_1 = \nu$. Convergence for the three-dimensional lattices seems less rapid. Nevertheless the values for the simple cubic confirm (8.24) quite closely although perhaps suggesting a somewhat higher value for ν_1 near 0.6440. The bcc values have a tendency to increase but by themselves would lead to the rather low estimate 0.641 which is just consistent with (8.25). The very short fcc series lead to a similar estimate.

8.3 Reduced Second Moments and Other Series

In Appendix C are tabulated the expansion coefficients $\lambda_n^{(2)}$ of the reduced second moment $\Lambda_2(v)$ defined by (3.16). [The coefficients have been multiplied by $(2d/q)$ to remove fractions.] We first notice, by comparison with (5.34), (5.55), and (8.14), that $\Lambda_2(v)$ is equal to $\Lambda_2'(v)$, derived from the true correlation range, correct to order v^8 for both the square and simple cubic lattices and correct to v^6 for the triangular lattice. In fact the differences are

$$\begin{aligned} \Lambda_2'(v) - \Lambda_2(v) &= 4v^9 + 0v^{10} + 32v^{11} + \cdots, \quad \text{square} \\ &= 4v^7 + 24v^8 + \cdots, \quad \text{triangular} \\ &= 8v^9 + \cdots, \quad \text{sc.} \end{aligned} \tag{8.28}$$

These are so small even at $v \simeq v_c$ that we may conclude immediately that the critical behavior of Λ_2' and Λ_2, and hence of κ and κ_1, is almost identical. This is probably the strongest indication that $\nu = \nu_1$. Nevertheless, as demonstrated in Sec. 5.4, the differences are not without significance for the behavior of the scattering at T_c as a function of k^2. Indeed the positiveness of the difference is in agreement with the analysis of Secs. 6.2 and 6.3 which indicates that the critical-point ratio $\psi_c = (\Lambda_2'/\Lambda_2)_c$ should be slightly greater than unity [see Eqs. (6.25) and (6.29)].

The Λ_2 series for the bcc and fcc lattices agree precisely with the few initial terms known for Λ_2' on these lattices. There are reasons to believe, however, that the differences will be of order v^6 for the bcc lattice and possibly the same for the fcc (see Sec. 10.4).

For the simple cubic lattice the difference (8.28) and the additional term in Λ_2 leads to estimates for ν_1 slightly different to those found for ν. Thus from the last five ratios we find

$$2\bar{\nu}_{1,n}\{\Lambda_2\} = 1.2873,\ 1.28907,\ 1.28802,\ 1.28785,\ 1.28680, \tag{8.29}$$

in place of (8.15). The last few estimates are falling fairly rapidly and suggest a limit for ν_1 between 0.6420 and 0.6430 which is somewhat lower than the direct estimate (8.24) from μ_2. Similarly the last sets of Padé approximant estimates differ from those in Table I. The modified values and further values are presented in Table IV. These lead to essentially the estimate (8.24) if not to a slightly higher value. The slight disparity between the two approaches and the spread of the approximants indicates the magnitude of the uncertainty. It is worth remarking that in estimating ν_1 from Λ_2 we do *not* need to know (or assume) a value for γ.

The evidence for the bcc lattice in Table IV also suggests a lower value than (8.25) obtained from the μ_2 series, say, $\nu \simeq 0.641$ or slightly higher. The fcc estimates are again similar but as before do not deserve much weight in view of the few terms available.

The value of ν_1 may also be estimated in various other ways such as by evaluating the terms of the logarithmic derivative series for Λ_2 at $v = v_c$ (see below) or by studying the sequence of coefficients $\langle R_n^2 \rangle$ defined in (7.10) which are analogous to the mean square size of a self-avoiding lattice walk of n steps.[37–42] These coefficients have the theoretical advantage that the ratio

of successive terms must approach *unity*, with a slope versus $1/n$ proportional to ν_1. Consequently we need neither the exponent γ *nor* the value of the critical point v_c to make estimates.

From the series for the higher moments $\mu_4(v)$ and $\mu_6(v)$ for the square and simple cubic lattices given in Appendix B one may check (6.14) for $t>2$ and obtain further estimates for ν_1. The check proves quite satisfactory although, as might be expected, the approach to simple asymptotic behavior is somewhat slower for the higher moments.

These methods, and others, lead to essentially the same conclusions regarding the value of ν_1 (and with comparable precision) as those already described. Consequently we omit further details.

8.4 Values of ν and η

To summarize the above analysis we may state: (a) that we have verified that $\nu=\nu_1$ for the square and simple cubic lattices to well within the uncertainties of extrapolation (we will assume the equality holds for all lattices and drop the distinction henceforth); (b) that to within the uncertainties, the value of ν for the lattices studied depends only on dimensionality. In as far as there is any evidence to the contrary the value of ν for the simple cubic lattice might be some 0.001 to 0.003 higher than for the bcc and fcc lattices. We do not, however, believe these apparent differences are real and they will be ignored in the subsequent analysis; (c) bearing in mind the relative length of series and the precision of different extrapolation procedures we estimate for all three-dimensional lattices that

$$\nu=0.6430\pm0.0025\,,\quad (d=3) \tag{8.30}$$

while for plane lattices we have the result (fully rigorous for the square lattice)

$$\nu=1\,,\quad (d=2)\,. \tag{8.31}$$

Through the relation (6.9) we have the corresponding estimates

$$\eta=0.056\pm0.008\,,\quad (d=3) \tag{8.32}$$

with better precision and a slightly higher value for the simple cubic, while for the plane lattices

$$\eta=\tfrac{1}{4}\,,\quad (d=2)\,. \tag{8.33}$$

We might be tempted to conjecture that the exponent η in three dimensions should also be a simple fraction and we might note that powers of two seem to be favored in the Ising model. The conjecture[3] $\eta=\frac{1}{16}=0.062500$ which implies $\nu=20/31=0.64516\cdots$ cannot, perhaps, be ruled out but is definitely high on present evidence. The next simplest possibility is

$$\eta=1/18=0.055555\cdots\,, \tag{8.34}$$

implying

$$\nu=9/14=0.642857\cdots\,. \tag{8.35}$$

These values are in the center of the range of uncertainty (and the fraction for ν is less repulsive). For the sake of definiteness we shall adopt them in subsequent analysis. In any event probable deviations from these conjectures will cause negligible changes in other numerical estimates.

9. EVALUATION OF SERIES

To calculate the range of correlation $\kappa(T)$ and other functions through the critical region one needs closed extrapolation formulas that are consistent with the values of the critical exponents γ, ν, and η. Such formulas are derived in this section.

9.1 Effective Correlation Range

The effective correlation range $\kappa_1(T)$, related to $\Lambda_2(T)$ by (3.20), may be evaluated by various routes. We follow a procedure used successfully for evaluating the susceptibilities.[35] From the series for Λ_2 tabulated in Appendix C we form the expansion of the logarithmic derivative

$$(d/dv)\ln[2d\Lambda_2/qv]=\sum_{n=1}^{\infty} l_n v^{n-1}\,, \tag{9.1}$$

already used in the Padé approximant studies. We then examine the coefficients

$$j_n=l_n v_c{}^n-2\nu\,, \tag{9.2}$$

using the values $\nu=1$ and $9/14$ for $d=2$ and 3. If the value of ν is correct (and the dominant singularity is at $v=v_c$) the coefficients j_n should approach zero; this is observed to be so. We can then write

$$\ln(\kappa_1 a)^2=-\ln|\Lambda_2|=2\nu\ln[1-(v/v_c)]$$

$$+\ln(2d/qv_c)+\ln|t|+\sum_{n=1}^{m} d_n t^n+\mathfrak{R}_m(t)\,, \tag{9.3}$$

where

$$t=v/v_c \tag{9.4}$$

and

$$d_n=-j_n/n\,, \tag{9.5}$$

and where $\mathfrak{R}_m(t)$ is the remainder resulting from the truncation of the series with coefficients d_n. [Note $\Lambda_2(v)$ changes sign with v so that (9.3) extends to negative as well as positive v.]

For the loose-packed lattices the coefficients d_n alternate in sign (see Table V) and the partial sums even at $t=1$ are quite rapidly convergent. For the triangular and fcc lattices, the d_n are apparently of one sign (see Table V) but the partial sums again converge rather rapidly. Consequently, it would not be unreasonable to neglect the remainder $\mathfrak{R}_m$ altogether. To improve the accuracy, however, expecially near the antiferromagnetic singularity of the loose packed lattices at $t=-1$ we examine the coefficients j_n in an attempt to choose a reasonable form for $\mathfrak{R}_m$. Previous work on the suscepti-

TABLE V. Coefficients d_n and amplitudes A for the calculation of $\kappa_1(T)$ from Eqs. (9.3), (9.4), and (9.8). [Note t must be replaced by $-v/v_c$ in the remainders for the triangular and fcc lattices.]

n	Square	Triangular	sc	bcc	fcc
1	0.343146	0.392305	−0.023186	0.036338	0.064465
2	0.142136	0.066642	0.024195	0.033110	0.011062
3	0.003367	0.012579	−0.007457	−0.008193	0.002727
4	0.014285	0.002564	0.003231	0.007045	0.001271
5	0.000060	0.000552	−0.004312	−0.003126	0.000953
6	0.001675	0.001604	0.001711	0.003445	
7	0.000001	0.000028	−0.002372	−0.001690	
8	0.003683		0.001485		
9	−0.005743		−0.001463		
10	0.006572				
A	−0.80	−0.001	−0.120	−0.150	−0.027
$\mathfrak{R}_m(1)$	−0.0033	0.0001	0.00060	0.00116	0.0045

bility[35] and the known behavior of the plane lattice correlation functions at T_c suggests that $(\kappa_1 a)^2$ might have a logarithmic (or near logarithmic) branch point at the antiferromagnetic singularity corresponding to $d_n \sim (-)^n/n(n+1)$. Accordingly, we have examined the sequences $(n+1)j_n$. For the simple cubic lattice we find

$$(-)^n(n+1)j_n = 0.090,\ 0.065,\ 0.129,\ 0.072,\ 0.133,\ 0.107,\ 0.132. \quad (9.6)$$

These values seem to be oscillating around a limit of about 0.120. Similarly for the bcc we find

$$(-)^n(n+1)j_n = 0.199,\ 0.098,\ 0.141,\ 0.094,\ 0.145,\ 0.095, \quad (9.7)$$

which suggests a limit of about 0.150. In view of this behavior, a reasonable approximation for the remainder should be

$$\mathfrak{R}_m(t) \simeq A \sum_{n=m+1}^{\infty} (-)^{n+1} t^n/n(n+1) = A[t^{-1}(1+t)\ln(1+t) - 1 - \sum_{n=1}^{m} (-)^{n+1} t^n/n(n+1)], \quad (9.8)$$

with the amplitudes $A_{sc} = -0.120$ and $A_{bcc} = -0.150$. For the square lattice the coefficients d_n exhibit only one cycle of oscillation so that a firm value of A cannot really be estimated. Nevertheless, the value $A_{sq} = -0.80$ should yield a fairly accurate estimate. Alternatively, because of the relatively small difference $\Lambda_2 - \Lambda_2'$ displayed in Eq. (8.28) one might almost as well adopt the approximation $\kappa_1 = \kappa_1'$ and use the exact expression (5.33).

For the fcc lattices the constant sign of the coefficients d_n means that the expression (9.8) for $\mathfrak{R}_m$ is only appropriate if t is replaced by $-t$ on the right-hand side (or equivalently if t is defined as $-v/v_c$ in the remainder). The sequence 0.066, 0.0327, 0.0254, and 0.0286 for $(n+1)j_n$ indicates that $A_{fcc} = -0.027$ should then yield a satisfactory approximation to the remainder. The available coefficients d_n for the triangular lattice are also all positive and if they remain so, the same modified form of remainder would be appropriate. The penultimate term, however, represents rather a large irregularity [associated with the difference $\Lambda_2' - \Lambda_2$; see Eq. (8.28)] so that it is difficult to estimate a reliable value of A. The value $A_{tri} = 0.001$ should, however, be satisfactory pending the calculation of further terms. [Comparison with the square lattice series even suggests that subsequent terms might alternate in sign which would indicate a small remainder near $v = v_c$ in agreement with the value of A chosen. Further confirmation of this value is obtained by comparison with the true value of F, equation (5.44), and from the estimation of $r_1(T)$ in the next subsection.]

The selected values of A and the consequent (maximum) values of the remainder $\mathfrak{R}_m$ at the ferromagnetic critical point $v = v_c$ $(t = 1)$ are also included in Table V. The additional logarithmic branch point at $v = v_c$ implied by the modified form of remainder is probably spurious but because of the small amplitude it will be numerically insignificant. Other forms of remainder might be chosen for the fcc and triangular lattices but until longer series are available they are probably not justified. Notice, however, that this remainder [and the equation (9.3)] predict *no* singularity at $v = -v_c$ which is correct as the close packed lattices will not sustain simple antiferromagnetic order and have no transition of any kind near $v = -v_c$.

9.2 Behavior of $\kappa_1(T)$ and $\kappa(T)$

With the data in Table V and Eqs. (9.3), (9.2), and (9.8), the effective correlation range may be calculated accurately at all temperatures exceeding T_c. Very close to T_c the dominant error for $d = 3$ will arise from the uncertainty in the value of ν (unless the adopted value proves to be exact). However, even at $(T - T_c)/T_c = 10^{-3}$ the error in $\kappa_1 a$ for the simple cubic lattice is probably only a fraction of a percent while for higher temperatures the errors will be 0.1% or less.

Figure 5 compares the variation of $\kappa_1 a$ with temperature for two- and three-dimensional lattices and for the

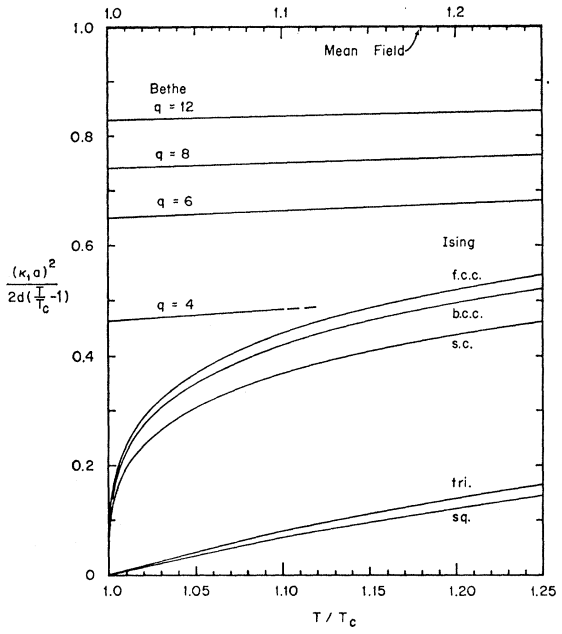

FIG. 5. Plot showing the variation of the effective correlation range $\kappa_1(T)$ for the mean field and Bethe approximations and for two- and three-dimensional Ising lattices (see also Fig. 14).

corresponding mean field and Elliott-Marshall-Bethe approximations. A marked dependence on dimensionality and a relatively small dependence on lattice structure are evident. The errors of the approximate theories are significant even for $T/T_c=1.1$ where the correct value of $(\kappa_1 a)^{-2}$ in three dimensions is about twice as large as the Bethe value. At $T/T_c=1.001$, the corresponding error factor has increased to about 7.

It transpires that one may write

$$\log_{10}\kappa_1 a \simeq \nu \log_{10}[(T/T_c)-1] + B_0 + B_1[(T/T_c)-1], \quad (9.9)$$

with quite high accuracy for $T/T_c<1.4$ on all lattices and for both approximations (see also Fig. 14 below). Appropriate values of B_0 and B_1 are given in Table VI.

In terms of the amplitude F_1 defined as in (6.13) and (6.5), we have

$$B_0=\log_{10}F_1. \quad (9.10)$$

Comparison with the exactly known value of F for the square lattice [Eq. (5.25)] yields

$$\Delta_2=(F_1/F)^2\simeq 1.00097, \quad (9.11)$$

where the last two figures must be considered somewhat uncertain. This estimate may be compared with that obtained in Sec. 6, Eq. (6.30), in quite a different manner by using a simple approximant to the total scattering and an estimate of the susceptibility amplitude C. Although in one case the deviation from unity is 9.7×10^{-4} and in the other only 1.1×10^{-4}, the agreement in sign and in order of magnitude must be considered very satisfactory in view of the approximations necessarily incurred in both calculations. For the triangular lattice we similarly find, using (5.44), that $(F_1/F)^2\simeq 1.0016$, although in view of the shorter series this value is less certain than (9.11).

TABLE VI. Critical-point parameters for the calculation of $\kappa_1(T)$ according to Eq. (9.9). Note that for the three-dimensional Ising models $F_1=F$ to within the precision available.

Model	Lattice	ν	$B_0=\log_{10}F_1$	B_1
Ising	Square	1	0.24640	−0.299
	Triangular		0.27975	−0.32
	sc	9/14	0.31989	−0.053
	bcc		0.35092	−0.080
	fcc		0.36219	−0.100
Elliott-Marshall-Bethe approximation	Square	½	0.133397	0.109
	Triangular		0.207061	0.055
	sc	½	0.295113	0.055
	bcc		0.323619	0.037
	fcc		0.348285	0.022
Mean field approximation	$d=2$	½	0.301030	0
	$d=3$	½	0.389076	0

For the simple cubic lattice only one term of the difference $\Lambda_2-\Lambda_2'$ is available and consequently no significant estimate of the difference between F_1 and F can be made at present this way although it is clearly very small. The *true* inverse range κ may thus be calculated quite accurately via (4.17) by replacing Λ_2' by Λ_2 and using (9.3).

9.3 Effective Interaction Range

To use the various expressions for the total scattering developed in Sec. 6 one needs, in addition to the effective range $\kappa_1(T)$, the zero-angle scattering (or susceptibility) $\chi_0(T)$ or, alternatively, the effective interaction range $r_1(T)$ which remains finite at the critical point. This was defined in Eq. (6.24) via $(r_1\kappa_1)^{2-\eta}=1/\chi_0$. Consequently it can be calculated by evaluating the formulas of the last section for $\kappa_1(T)$ and using previously obtained approximant expressions to calculate $\chi_0(T)$.[34,35] It is of interest, however, to analyze the function $r_1(T)$ directly and this we now undertake along the lines already followed for $\kappa_1(T)$.

From the series for χ_0 and Λ_2, we may form the expansion

$$\ln(r_1/a)=-\tfrac{1}{2}\ln(2d/qv_c)+\tfrac{1}{2}\ln|v/v_c|+\sum_{n=1}\rho_n v^n. \quad (9.12)$$

The coefficients ρ_n may be examined to determine the singularities of $\ln(r_1/a)$. Both from the behavior of the ratios ρ_n/ρ_{n-1} and the direct Padé approximants, one concludes that $r_1(T)$ is *nonsingular* at the ferromagnetic critical point $v=v_c$. For the triangular lattice the evidence suggests strongly that there are no singularities on the real axis in the whole physical range $-1\leqslant v\leqslant 1$. For the fcc, the corresponding singularity-free region seems to be $-0.7\leqslant v\leqslant v_1\simeq 1.3v_c$. Consequently, evalua-

tion of direct Padé approximants to the ρ_n series will be a very satisfactory method of summation, i.e., we replace the truncated sum in (9.12) by

$$\Sigma_{L+M}(v)\simeq[\sum_{n=1}^{L} a_n v^n]/[1+\sum_{n=1}^{M} b_n v^n]. \quad (9.13)$$

Appropriate coefficients are tabulated in Appendix D. By expanding the approximants in powers of v to order $m=L+M$, the exact coefficients ρ_n are, of course, recaptured to the order available.

For the sc and bcc lattices, the regular region of the positive real axis extends to $v_1\simeq 1.4v_c$ and $2v_c$, respectively. On the negative axis there seems to be a singularity at $v_2\simeq -1.4v_c$ in both cases, but this might well correspond to a weak logarithmic branch point at the antiferromagnetic critical point $v_a=-v_c$ of the form found in $\kappa_1(T)$. For the square net the evidence for such a singularity is rather stronger. The nearest positive real singularity, however, still seems to lie beyond the critical point at $v_1\geqslant 2v_c$. Since we are mainly interested in the numerical values near v_c and since any singularity at v_a is undoubtedly rather weak, direct Padé approximants of the form (9.13) will again be quite satisfactory for the range $|v|\leqslant v_c$. Appropriate coefficients a_n and b_n are included in Appendix D.

By evaluating a variety of approximants with different L and M one may gauge the probable accuracy of the extrapolation for $r_1(T)$. Even at the ferromagnetic critical point, the accuracy appears to be better than 0.1% for all the lattices. [In fact the remainder of the series in (9.12) makes a very small contribution relative to the other terms.] A plot of $r_1(T)$ versus T/T_c for different lattices is presented in Fig. 6. The grouping by dimensionality is again evident. Near the critical point we have

$$r_1(T)/a=(r_1/a)_c\{1-c[(T/T_c)-1]+\cdots\}. \quad (9.14)$$

The critical-point values $(r_1/a)_c$ and c are given in Table VII. The values of $(a/r_1)_c^{2-\eta}$ which enter in the expression for the zero-angle scattering are also tabulated along with the corresponding Bethe approximation, namely, $2d(q-2)/(q-1)$, which follows from (4.22). The mean field approximation yields simply $2d$.

As indicated above, the last two figures given for $(r_1/a)_c$ and $(a/r_1)_c^{2-\eta}$ are uncertain to within 10 to 40 digits. The precision and consistency here may be cross-checked by computing the susceptibility amplitude from

$$C=(a/r_1)_c^{2-\eta}/F_1^{2-\eta}, \quad (9.15)$$

using the results of Tables VI and VII. [This equation follows from (6.24), (6.8), and the analog of (6.7).] The values of C found this way for the square and simple cubic lattices agree to within 0.04 and 0.02%, respectively, with those found directly from χ_0.[35] For the other lattices, the agreement is within 0.15% or better which is the expected precision of C.

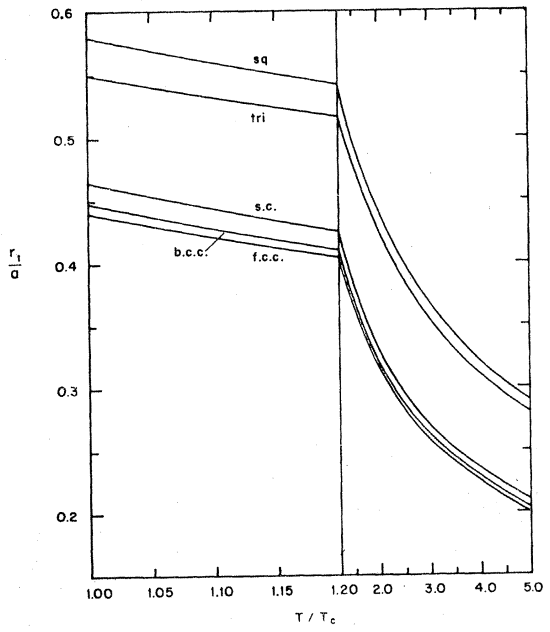

FIG. 6. Variation of the effective range of interaction $r_1(T)$ with temperature for various lattices.

TABLE VII. Critical-point parameters for $r_1(T)$.

Lattice	$(r_1/a)_c$	c	$(a/r_1)_c^{2-\eta}$	$2d(q-2)/(q-1)$
Square	0.57959	0.350	2.5974	2.6666
Triangular	0.54962	0.311	2.8503	3.2000
sc	0.46448	0.491	4.4418	4.8000
bcc	0.44761	0.467	4.7733	5.1429
fcc	0.44027	0.457	4.9292	5.4545

10. ANALYSIS OF THE DISTRIBUTIONS

In the previous two sections the second moments of the correlation functions $\Gamma(\mathbf{r};T)$ have been studied for all lattices. For the square and simple cubic lattices, however, the high-temperature expansions of the complete correlation function distribution have been calculated (Appendix B) so that a more detailed discussion is possible. In this section we study, in particular the angular symmetry of the critical-point scattering, and the values of the individual correlations functions for small $\mathbf{r}$ near and at T_c.

10.1 Symmetry of Scattering

At high temperatures the scattering necessarily displays anisotropy related to the lattice axes, as is clear from Secs. 5.4, 6, and 7.1. Since the sum $\sum_{\mathbf{r}}\Gamma(\mathbf{r},T)$ diverges as $T\rightarrow T_c$, the behavior of the scattering near T_c is determined by the asymptotic form of the expansion coefficients $q_n(\mathbf{r})$, defined in (7.1), as $n\rightarrow\infty$. If these distributions approach spherical symmetry so will the critical-point scattering (and vice versa). To examine the symmetry of the coefficient distributions

we adopt a method devised by Domb in another connection.[42] Consider the *Cartesian moments* of the correlations, $\mu_{f,g,h}(v)$, defined in (3.10), and their expansion coefficients

$$m_n(f,g,h)=\sum_{\mathbf{r}}(x/a)^f(y/a)^g(z/a)^h q_n(\mathbf{r}), \quad (10.1)$$

which are just the corresponding moments of the coefficient distributions. (For definiteness we consider the simple cubic lattice.) One may then define symmetry coefficients

$$\sigma_n(f,g,h)=m_n(f,g,h)/m_n{}^{(f+g+h)}, \quad (10.2)$$

where $m_n{}^{(t)}$ are the expansion coefficients of the *spherical* moments [see Eqs. (3.7) and (7.9)]. A similar definition of $\sigma_n(f,g)$ applies to the square lattice.

Now it is not difficult to show[42] that for a spherically symmetric distribution one has

$$\sigma_n(f,g,h)=\sigma^0(f,g,h)$$
$$=\frac{\Gamma[\frac{1}{2}(f+1)]\Gamma[\frac{1}{2}(g+1)]\Gamma[\frac{1}{2}(h+1)]}{2\pi\Gamma[\frac{1}{2}(f+g+h+3)]}, \quad (10.3)$$

where $\Gamma(z)$ is the gamma function. Similarly for a circularly symmetric two-dimensional distribution one finds

$$\sigma_n(f,g)=\sigma^0(f,g)$$
$$=\Gamma\left(\frac{f+1}{2}\right)\Gamma\left(\frac{g+1}{2}\right)\Big/\pi\Gamma\left(\frac{f+g+2}{2}\right). \quad (10.4)$$

If one calculates the reduced symmetry coefficients $\sigma_n(f,g,h)/\sigma^0(f,g,h)$ for lattice distributions of unrestricted random walks (which correspond to the mean field approximation) or for random walks restricted

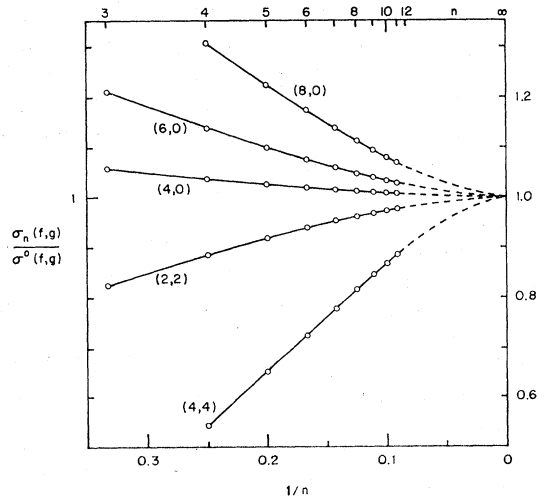

FIG. 7. Plot of the reduced symmetry coefficients of the nth-order correlation distributions on the square lattice versus $1/n$. The value unity corresponds to a symmetrical distribution.

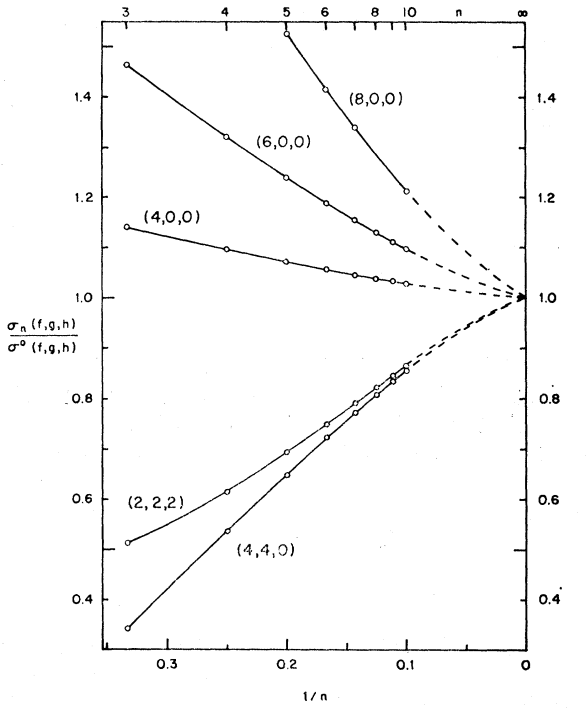

FIG. 8. Plot of the reduced symmetry coefficients for the simple cubic lattice versus $1/n$ demonstrating the asymptotic approach to full spherical symmetry.

to make no immediate reversals[22] (which correspond to the Bethe approximation) one finds that for all combinations of f, g, and h the values approach the symmetric limit unity as $n\to\infty$. Furthermore the approach may be expressed as a power series in $(1/n)$.[42]

Accordingly we have computed various reduced symmetry coefficients (up to order $f+g+h=8$) for the square and simple cubic lattices and examined their behavior versus $1/n$. To economize space we do not tabulate the values (it is only a matter of labor to obtain them from the tables in Appendix B but the plots are displayed in Figs. 7 and 8. [Note that the coefficients $\sigma_n(4,0)$ and $\sigma_n(2,2)$ are linearly related. All the other coefficients selected for both figures are linearly independent.] Examination of these figures leaves no reasonable doubt regarding the full asymptotic symmetry of the distribution coefficients and hence of the scattering intensity as $T\to T_c$. Indeed the approach to full symmetry is *more* rapid than for the corresponding mean field or Bethe approximations—presumably owing to the more rapid divergence of the mean square size $\langle R_n{}^2\rangle$ as $n\to\infty$ or, correspondingly, of the second moment $\Lambda_2(T)$ as $T\to T_c$.

An alternative approach would be to examine the reduced symmetry functions

$$\mathcal{S}(f,g,h)=\mu_{f,g,h}(v)/\mu_{f+g+h}(v)\sigma^0(f,g,h). \quad (10.5)$$

These will remain finite at the critical point and, in view of the conclusions drawn above, should approach the

TABLE VIII. Critical-point behavior of the correlation functions of the simple cubic lattice compared with some results for the square lattice. Note $\mathbf{r}=(ka,la,ma)$, the indicated uncertainties refer to the last decimal place, and $E(\mathbf{r})$ is defined in Eq. (5.2).

		Simple cubic				Square	
k, l, m	r/a	$\Gamma_c(\mathbf{r})$	$E(\mathbf{r})$	$(r/a)^{1+\eta}\Gamma_c/D$	$E(\mathbf{r})/E_1$	$(r/a)^{1/4}\Gamma_c/D$	$E(\mathbf{r})/E_1$
1, 0, 0	1	0.3284±8	0.332±4	1.026	1	1.0053	1
1, 1, 0	1.4142	0.2070±10	0.472±7	0.933	1.423	0.9870	1.4142
1, 1, 1	1.7321	0.1630±15	0.568±8	0.910	1.656	···	···
2, 0, 0	2	0.1585±20	0.623±8	1.030	1.88	1.0055	1.8006
2, 1, 0	2.2361	0.137±3	0.72±1	1.001	2.17	0.9965	2.000
2, 1, 1	2.4495	0.120±4	0.75±2	0.966	2.26	···	···
2, 2, 0	2.8284	0.11±1	0.76±3	1.031	2.29	0.9963	

symmetric value unity as $T \to T_c$. In principle, these functions could be measured experimentally by studying the anisotropy of the k^4, k^6, $\cdots$ terms in the low-angle scattering. Should this prove feasible it would be a straightforward matter, along the lines of Sec. 9, to obtain accurate extrapolation formulas for $\mathcal{S}(f,g,h)$ valid up to the critical point.

10.2 Correlations at the Critical Point

The rows in Tables XVI and XVII of Appendix B represent the expansion coefficients of the individual correlation functions $\Gamma(\mathbf{r})$. The values for low $\mathbf{r}$ on the square lattice may indeed be checked against the exact expressions for the correlation functions (Sec. 5). The nearest-neighbor correlation function is proportional to the energy U and hence two further terms are known for the simple cubic.[35,47] To estimate the critical values of the correlation functions from the truncated series, the remainders must be estimated. For the energy this problem has been studied in detail.[11,35,47,48] To a reasonable first approximation the specific heats of the three-dimensional lattices appear to have logarithmic singularities as for the plane lattices. Consequently, the behavior of the energy of $\Gamma(\mathbf{r})$ near T_c should again be given by (5.2). The $(T-T_c)\ln(T-T_c)$ singularity in that formula implies that the remainders $\mathcal{R}_m(v_c)$ of the truncated energy expansion evaluated at $v=v_c$ will decrease asymptotically as $1/m$. Accordingly, linear extrapolation of the partial sums versus $1/m$ [or versus $1/(m-\delta)$ for small δ] should yield estimates of the critical energy and Γ_c. Equally the slopes of the plot will give an esimate for the amplitude E of the singular term [see Eq. (5.2)]. The reliability of this method may be tested on the plane lattices where it is found to yield the exact values of Γ_c to within 1% or better and the amplitudes to comparable or slightly lower accuracy.[35]

We expect in three dimensions, as in two, that all correlation functions will exhibit a singularity of similar type at T_c. The behavior of the partial sums for $\Gamma_c(\mathbf{r})$ bears out this hypothesis with reasonable precision. Accordingly, all the $\Gamma_c(\mathbf{r})$ and $E(\mathbf{r})$ may be estimated by linear extrapolation of the partial sums versus $1/(m-\delta)$.

The results of this extrapolation are displayed in Table VIII for small k, l, and m with $\mathbf{r}=(ka,la,ma)$. For $|k|+|l|+|m| \leqslant 4$, four or five nonvanishing terms of each series are available, but for $(r/a) \geqslant 3$ the estimated remainders are greater than the largest partial sums and the uncertainties are consequently rather large. (When $|k|+|l|+|m| \geqslant 5$ only three nonzero terms are available and worthwhile extrapolation is not really possible.) Note that the indicated uncertainties in Table VIII refer to the last decimal place and the uncertainties quoted for the amplitudes $E(\mathbf{r})$ do not take full account of the possible errors in $\Gamma_c(\mathbf{r})$.

By multiplying the estimated critical values by $(r/a)^{1+\eta}$ with $\eta=1/18$, we may test for consistency with the expected decay law

$$\Gamma_c(\mathbf{r}) \simeq D/(r/a)^{1+\eta}, \quad (d=3, r \to \infty) \qquad (10.6)$$

and estimate the amplitude D [see Eqs. (5.29)]. In this way we conclude that

$$D \simeq 0.320 \pm 0.010, \quad \text{(simple cubic)}. \qquad (10.7)$$

This value of D has been used to compute the fifth column in Table VIII. The constancy of the entries to within 3 to 6% indicates that (10.6) is quite accurately followed even for small $\mathbf{r}$, as on the square lattice. [Indeed the values of $\Gamma_c(\mathbf{r})$ would by themselves indicate that η has quite a small value, although with relatively low precision.] The penultimate column of the table contains the corresponding figures for the square lattice (where they exist). The variation above or below unity for the two lattices is very similar except that square lattice deviations are of somewhat smaller amplitude.

The sixth column of Table VIII contains the simple cubic singularity amplitudes normalized by $E_1=E(a,0,0)$. The last column gives the corresponding figures for the square lattice. The correspondence between the two sequences is quite remarkable. Although a general similarity is to be expected it is not clear why the behavior should be so close numerically.

The estimates of Table VIII rest on the assumption that the specific-heat singularity of the three-dimensional lattices is logarithmic. Actually careful analysis and other theoretical arguments suggest that it is probably slightly sharper, diverging as $(T-T_c)^{-\alpha}$

[47] C. Domb and M. F. Sykes, Phys. Rev. **108**, 1415 (1957).
[48] M. E. Fisher, Phys. Rev. **136**, A1599 (1964).

TABLE IX. Values and estimates of the correlation amplitude D [see Eq. (10.6) and Eqs. (6.18) and (6.22)].

Lattice	$\Gamma_c(a,0,0)/D$	D	C/C'
Square	1.00530	0.703380	0.63917
Triangular	0.99703	0.66865	0.63919
sc	1.026	0.320	1.129
bcc	1.026	0.263	1.138
fcc	0.984	0.248	1.145

with $\alpha \simeq \frac{1}{8}$ or even as large as $\frac{1}{5}$.[47,48,43,11] If $\alpha \neq 0$ the estimates of Γ_c should be obtained by extrapolating the partial sums linearly with $1/(m-\delta)^{1-\alpha}$ which leads to slightly higher values. For the shortest vectors $\mathbf{r}$ the boost is only about 1.5% but it increases with r to 6 or 7% at $r/a \simeq 3$. Because of the distribution of values, however, the estimate for D increases only about 1.3% to 0.325 ± 0.010 so that $\Gamma_c(a,0,0)/D$ remains close to 1.025.

The data in Table VIII describe the individual correlation functions close to T_c while the truncated series expansions will suffice at high temperatures. To cover all temperatures above T_c we may easily extend the analysis slightly to derive explicit extrapolation formulas as in the original discussion of the energy.[35] Since the individual functions are not, however, really accessible to experiment we do not give such formulas here. (Approximate theoretical calculations might well be compared with the previously given accurate expressions for the energy.)

The fact that $D \simeq \Gamma_c(a,0,0) = U_c/U_0$, where U_0 is the zero-point energy, enables us to estimate D for the other three-dimensional lattices. Table IX shows the values of D and the ratio $\Gamma_c(a,0,0)/D$ for the square and triangular lattices.[24] The ratios deviate about 0.5% above unity and 0.3% below, respectively. As we have seen, the corresponding deviation for the simple cubic is about +2.6%. It seems reasonable to assume a similar deviation for the bcc lattice, whereas for the fcc, which is close packed, we assume a proportional deviation of −1.6% as shown in the table. The previously estimated values[35,49] of U_c can then be used to obtain the estimates of D shown in Table IX. These should be accurate to within a few percent.

The last column in this table gives the ratio of the approximate susceptibility amplitude C' calculated via (6.22) using these values of D and the values of $F \simeq F_1$ (Table VI), to the "true" amplitude C as found by the best numerical estimates.[34,35] (For the plane lattices the exact value of F has been used.) These figures validate the arguments of Sec. 6.2.

[49] Longer series for the fcc lattice indicate that $\Gamma_c(a,0,0)$ might be slightly higher than the original estimate of Ref. 35 [M. F. Sykes (private communication)].

10.3 Metamagnetic Susceptibilities

For the normal antiferromagnetic Ising model contemplated in Secs. 2.2 and 3.1 the sign of the interaction energy J is negative for all nearest-neighbor bonds and the ground state is one of strictly alternating spin alignment. As explained, antiferromagnets are included in all our analysis simply by changing v to $-v$ and $\mathbf{k}$ to $\mathbf{k}+\mathbf{k}_0$. One may, however, also contemplate "metamagnetic" or "layer" models in which the ordered state consists of sheets of ferromagnetically aligned spins, alternate sheets being oriented antiferromagnetically. The simplest such two-dimensional model is obtained on the square lattice by taking $J_x = |J|$ and $J_y = -|J|$. Then alternate columns of spins in the lattice will tend to align all up or all down. By using the symmetry of the correlation functions under change of sign of v_x and v_y it is easy to see that the initial susceptibility of this model is given by

$$\begin{aligned}(k_B T/m^2)\chi_T = 1 &+ 4[\Gamma(2a,0)-\Gamma(a,a)] \\ &+ 4[\Gamma(4a,0)-2\Gamma(3a,a)+\Gamma(2a,2a)] \\ &+ 4[\Gamma(6a,0)-2\Gamma(5a,a)-2\Gamma(4a,2a) \\ &+ \Gamma(3a,3a)]+\cdots, \quad (10.8)\end{aligned}$$

where the $\Gamma(\mathbf{r},v)$ are the standard ferromagnetic correlation functions with $v = \tanh(|J|/k_B T)$. On reflection it will be clear that the right-hand side of (10.8) is also equal to $\hat{\chi}(\mathbf{k},v)$ at the symmetric point $k_x a = \pi$ and $k_y a = 0$ in the Brillouin zone. From Appendix B we then find the expansion

$$(k_B T/m^2)\chi_T = 1 - 4v^2 + 4v^4 - 12v^6 - 12v^8 - 84v^{10} \cdots. \quad (10.9)$$

The absence of a term in v shows that the susceptibility at high temperatures appears to be "paramagnetic" over a greater temperature range than for a normal antiferromagnet.

By the same arguments one may construct the susceptibility expansions for simple cubic metamagnets with layer ordering in sheets ($J_x = J_y = |J|$, $J_z = -|J|$) or ordering in ferromagnetic chains ($J_x = J_y = -|J|$, $J_z = |J|$). These again correspond to $\hat{\chi}(\mathbf{k},v)$ at simple points in the Brillouin zone. More complex situations in which the aligned sheets are two or more lattice layers thick, etc. may be handled similarly. We defer detailed analysis and discussion of these models until a future occasion. (Although it might be remarked that in real metamagnetic materials the in-lattice and between-lattice interactions are normally significantly different, this case is not covered by our present data.) We may, however, anticipate that as for the simple antiferromagnets,[35,50] the susceptibility $\chi_T(T)$ will have a maximum slightly *above* T_c and be decreasing rapidly *at* the critical point.

[50] M. E. Fisher, Phil. Mag. 7, 1731 (1962).

10.4 Direct Correlation Function

To characterize the correlation distributions more generally it is of interest to compute the direct correlation function $H(\mathbf{r})$ defined in Sec. 3 1. We consider the square lattice initially and proceed in two stages: Firstly we attempt to express the correlation expansion coefficients $q_n(\mathbf{r})$ in terms of the unrestricted random walk distributions and then we invert the resulting expression for $\hat{\chi}(\mathbf{k},v)$ to obtain $\hat{H}(\mathbf{k})$.

The distribution of unrestricted random walks of n steps has the Fourier transform $[\hat{q}(\mathbf{k})]^m = q^m[\hat{\gamma}(\mathbf{k})]^m$. With the aid of the binominal expansion, the corresponding distribution on the square lattice is found to be

$$p_m(r) = \binom{m}{\frac{1}{2}(m-i-j)}\binom{m}{\frac{1}{2}(m-i+j)}, \quad (x=ia,\ y=ja). \tag{10.10}$$

By repeated subtraction of the distributions $p_m(\mathbf{r})$ from $q_n(\mathbf{r})$, starting with $m=n$, one may find the coefficients u_{nm} in the relation

$$\hat{q}_n(\mathbf{k}) = \sum_{m=0}^{n} u_{nm}\hat{q}^m(\mathbf{k}), \tag{10.11}$$

provided such a relation holds. It is to be stressed that this expression is not obvious. There are many distributions with the full symmetry of the square lattice which cannot be so expressed. [An example is $P_2(\mathbf{r})=1$ if $|x|=|y|=a$ but $P_2(\mathbf{r})=0$ otherwise.] In fact one discovers that (10.11) *is* valid for the square lattice, at least to order eleven, with the coefficients given in Table X. (Owing to the sublattice structure $u_{nm}\equiv 0$ unless m and n have the same parity.)

From (10.11) follows the double power series expansion

$$\hat{\chi}(\mathbf{k},v) = \sum_{n=0}^{\infty}\sum_{m=0}^{n} u_{nm}v^n\hat{q}^m, \tag{10.12}$$

which may be inverted algebraically via (3.11) to yield

$$\hat{H}(\mathbf{k}) = \sum_{m=0}^{\infty} H_m(v)\hat{q}^m(\mathbf{k}). \tag{10.13}$$

Although proved only to order v^{11} for the square lattice we conjecture that such an expansion may be generally valid for all two-dimensional nearest-neighbor Ising lattices.

For the square lattice we find explicitly

$$H_0(v) = -4v^2-12v^4-44v^6-188v^8-852v^{10}-O(v^{12}), \tag{10.14}$$

$$H_1(v) = v+v^3+5v^5+21v^7+93v^9+401v^{11}+O(v^{13}), \tag{10.15}$$

$$H_2(v) = 4v^{10}+O(v^{12}), \tag{10.16}$$

$$H_3(v) = O(v^{13}), \quad H_4(v) = O(v^{12})\cdots. \tag{10.17}$$

Correct to v^9 the transform of the direct correlation function evidently has the simple form $H_0+H_1\hat{q}(\mathbf{k})$, which is the most obvious generalization of the mean field and Bethe approximation formulas. By considering the limit $\mathbf{k}\to 0$, we see that the leading coefficients of $H_0(v)$ and $H_1(v)$ are merely proportional to the corresponding coefficients of the expansion of $1/\chi_0(v)$. In fact we may write

$$1-H_0(v) = \mathcal{E}\{1/\chi_0(v)\}+O(v^{10}), \tag{10.18}$$

$$-qH_1(v) = \mathcal{O}\{1/\chi_0(v)\}+O(v^{13}), \tag{10.19}$$

where $\mathcal{E}\{f\}$ and $\mathcal{O}\{f\}$ denote the even and odd parts of the function f. We remark that the smallness of $H_3(v)$, $H_4(v),\cdots$ might have been guessed from the smallness of the difference $\Lambda_2'-\Lambda_2$ already noticed (although it does not follow from this). Indeed by comparing (10.13) with the definitions (3.11) and (3.14) we find

$$2d\Lambda_2 = \chi_0(v)\mathcal{O}\{-1/\chi_0(v)\}+2q^2\chi_0(v)H_2(v)+\cdots. \tag{10.20}$$

For the square lattice, the second- and higher-order terms are of order v^{10}. Thus to a very good approximation (as may be checked directly) the second correlation moment may be calculated from the zeroth-moment χ_0 alone.

One may ask for the graph-theoretical significance of the "deviations" found in tenth order. This turns out to be the fact that the smallest theta graphs on the square lattice in which the odd vertices can reach beyond the first coordination shell are $(2,2,6)_\theta$ and $(2,4,4)_\theta$ as is easily verified.[36] Both these graphs have ten lines and hence enter at v^{10}. Their relative weights (lattice constants) are 2:1 which is the same as the number of two-step random walks to the corresponding points (a,a) and $(2a,0)$, respectively. For this reason only a multiple of $\hat{q}^2(\mathbf{k})$ is introduced. The same thing happens on the triangular lattice with the theta graphs $(2,2,4)_\theta$ and $(2,3,3)_\theta$ which would enter in a corresponding way in eighth order.

When we undertake the corresponding calculations for the coefficients u_{nm} for the simple cubic, we find that (10.11) remains valid up to the eighth order with the

TABLE X. Coefficients u_{nm} for the expansion of $\hat{\Gamma}(\mathbf{k})$ on the square lattice in powers of $\hat{q}(\mathbf{k})$.

	m					
n	1	3	5	7	9	11
1	1					
3	−7	1				
5	21	−13	1			
7	−51	82	−19	1		
9	77	−354	179	−25	1	
11	−199	1175	−1137	312	−31	1

	m					
n	0	2	4	6	8	10
2	−4	1				
4	4	−10	1			
6	−12	47	−16	1		
8	−12	−156	126	−22	1	
10	−84	393	−672	241	−28	1

TABLE XI. Coefficients for the expansion of $\hat{\Gamma}(\mathbf{k})$ in powers of $\hat{q}(\mathbf{k})$ and for the excess distributions $y_n(\mathbf{r})$ at $\mathbf{r}=(\pm ja, \pm ka, \pm la)$ for the simple cubic lattice.

			m			(j,k,l)	
n	1	3	5	7	9	1, 1, 1	2, 1, 0
1	1						
3	−11	1					
5	45	−21	1				
7	−359	198	−31	1			
9	129	−1574	451	−41	1	104	32

			m				(j,k,l)		
n	0	2	4	6	8	10	1, 1, 0	2, 1, 0	2, 2, 0	3, 1, 0
2	−6	1								
4	6	−16	1							
6	−174	109	−26	1						
8	−1146	−784	321	−36	1		16			
10	−22 038	3337	−2854	615	−46	1	152	256	96	48

coefficients given in Table XI.[51] At that stage, however, the relation (10.11) breaks down since the residual distribution in the second coordination shell [obtained by subtracting the fourth and higher powers of $\hat{q}(\mathbf{k})$] is *not* proportional to $\hat{q}^2(\mathbf{k})$. This leaves an ambiguity in the definition of u_{nm} which we remove generally by requiring that the value of $q_n(\mathbf{r})$ at $\mathbf{r}=(ma,0,0)$ be correctly given by (10.11). This in turn serves to define an "excess correlation distribution" $y_n(\mathbf{r})$ whose Fourier transform $\hat{y}_n(\mathbf{k})$ must be added to the right-hand side of (10.11) to ensure its validity. The coefficients of the excess distributions, which have of course full cubic symmetry, are also presented in Table XI. The first deviation at $n=8$ and $\mathbf{r}=(a,a,0)$ corresponds to the theta graph $(2,2,4)_\theta$. It may be verified that the odd vertices can be placed only on sites equivalent to $\mathbf{0}$ and $\mathbf{r}=(2a,0,0)$ and that there are no other theta graphs on the simple cubic lattice of this order. Similarly the leading term of the excess in ninth order is associated with the new theta graph $(3,3,3)_\theta$ which will only reach to $\mathbf{r}=(a,a,a)$ or equivalent points.

The inversion of (10.12) with the addition of the excess transform $\hat{Y}(\mathbf{k},v)$ may be accomplished with just a little more labor than before. [What is involved is the convolution of the excess distributions $y_n(\mathbf{r})$ with the lower-order $q_n(\mathbf{r})$ and corresponding $h_n(\mathbf{r})$ distributions.] We may generalize (10.13) by writing

$$\hat{H}(\mathbf{k},v)=\sum_{m=0}^{\infty} H_m(v)\hat{q}^m(\mathbf{k})+\hat{Z}(\mathbf{k},v), \qquad (10.21)$$

which defines the direct correlation excess distributions $z_n(\mathbf{r})$ uniquely, provided, as before, we choose $H_m(v)$ in case of ambiguity so that $z_n(\mathbf{r})=0$ at $\mathbf{r}=(ma,0,0)$. The resulting nonvanishing expansion coefficients for the $H_m(v)$ and $z_n(\mathbf{r})$ are tabulated in Table XII. Evidently the excess distributions are initially very small but their relative magnitude probably increases for larger n. Although their existence is of theoretical significance they probably do not play an appreciable role numerically.

TABLE XII. Expansion coefficients in powers of v for the partial direct correlations $H_m(v)$ and corresponding excess distributions $z_n(\mathbf{r})$ on the simple cubic lattice.

n	H_0	H_2	$z_n(a,a,0)$	n	H_1	$z_n(a,a,a)$
2	−6			1	1	
4	−30			3	1	
6	−318			5	9	
8	−3918		16	7	121	
10	−54 582	24	312	9	1609	8

The relations (10.18), (10.19), and (10.20) hold again but with correction terms of order v^8, v^9, and v^8, respectively. On checking (10.20) for the bcc lattice, one finds "deviations" of order v^6 presumably related to the theta graph $(2,2,2)_\theta$ which can be realized on this lattice. This might suggest that the difference $\Lambda_2'-\Lambda_2$ will be of order v^6 or v^7 on the bcc lattice. However, the deviations in the expression (10.20) for Λ_2 on the simple cubic enter in order v^8 *in contrast* to v^{10} for the square net but for both lattices the difference $\Lambda_2'-\Lambda_2$ is of order v^9. The reason for this behavior must be in the rather different basic expansions of the true and effective correlation ranges so that too close an analogy should not really be expected. [Note that (10.20) cannot be expected to hold for the triangular and fcc lattices because of their close-packed structure.]

11. BEHAVIOR OF THE SCATTERING

11.1 Recapitulation

In this section we return to the general discussion of Sec. 6 concerning the form of the critical scattering in order to test the formulas advanced there against the detailed knowledge of the correlation series and to review the results which follow for the Ising model.

[51] The appropriate pure random walk distributions $p_m(\mathbf{r})$ follow from the generating function $(x+x^{-1}+y+y^{-1}+z+z^{-1})^m$ but cannot be expressed as compactly as in (10.10). They are readily calculated, however, by recursion. We are indebted to F. T. Hioe for assistance with the related calculations.

Firstly we restate the exponent values $\eta=\frac{1}{4}$, $\nu=1$ and $\eta=1/18$, $\nu=9/14$ for two and three dimensions, respectively (Sec. 8), and recall that precise extrapolation formulas for the effective range of correlation $\kappa_1(T)$ [or equivalently the second moment $\Lambda_2=1/(\kappa_1 a)^2$] on all the lattices were developed in Sec. 9; specifically, Eqs. (9.3) to (9.5), (9.8), and Table V. Near the critical point the simpler formula (9.9) with the data in Table VI should suffice. Similarly explicit formulas have been developed for the effective interaction range $r_1(T)$, namely, equations (9.12), (9.13) with the coefficients listed in Appendix D, while near T_c the approximate formula (9.14) with the data of Table VII applies. Alternatively, the zero-field reduced susceptibility $\chi_0(T)=1/(\kappa_1 r_1)^{2-\eta}$ may be calculated directly from previously developed expressions.[34,35]

With this information one may evaluate the simple "first-order" approximation formula (6.23) for the scattering, namely,

$$\hat{\chi}(\mathbf{k},T)\simeq\chi_0(T)/[1+K^2(\mathbf{k})/\kappa_1^2(1-\tfrac{1}{2}\eta)]^{1-(\eta/2)} \simeq(a/r_1)^{2-\eta}[(\kappa_1 a)^2+a^2K^2(\mathbf{k})/(1-\tfrac{1}{2}\eta)]^{-1+(\eta/2)}. \tag{11.1}$$

For small k and $T>T_c$ this is always correct to order k^2 while the behavior at T_c is correct in form. However, the amplitude of the $k^{-(2-\eta)}$ dependence at $T=T_c$ is too large by about 12% for the sc lattice (and about the same for the bcc and fcc lattices) and by a factor of about 2.4 for plane lattices. This does, of course, imply a similar inaccuracy for larger values of k near T_c. Indeed at the zone edge $\mathbf{k}=\mathbf{k}_0$, corresponding to the antiferromagnetic susceptibility (Sec. 3.1), the approximation (11.1) yields a value for $\hat{\chi}(T_c)$ on the sc lattice 13.6% higher than the best estimate.[35] For the square lattice the corresponding ratio is 2.39. Thus (11.1) is fairly satisfactory for three-dimensional lattices but much less so for plane lattices. To remedy these defects we examine critically the "second-order" approximation formula of Sec. 6 in the following subsections.

11.2 Square Lattice Scattering

The improved, "second-order" scattering approximant (6.27) may be written

$$\hat{\chi}(\mathbf{k},T)\simeq\left(\frac{a}{r_1}\right)^{2-\eta}\frac{[(\kappa_1 a)^2+\phi^2 a^2K^2(\mathbf{k})]^{\eta/2}}{[(\kappa_1 a)^2+\psi a^2K^2(\mathbf{k})]}, \tag{11.2}$$

where, in recapitulation $K(\mathbf{k})$ is defined in (2.2) and (2.1) and

$$\psi(T)=1+\tfrac{1}{2}\eta\phi^2(T), \tag{11.3}$$

which ensures that the behavior for small $\mathbf{k}$ is always given correctly to order k^2 (for T above T_c). As explained in Sec. 6 we may then fix the critical value $\phi_c=\phi(T_c)$ by requiring that (11.2) reproduce the correct amplitude $\hat{D}$ of the $1/k^{2-\eta}$ small-k behavior at T_c. This yields the values (6.31).

As a test of the accuracy of (11.2) at $T=T_c$ for higher values of k we may, as above, evaluate (11.2) at the extreme point of the Brillouin zone, i.e., at the antiferromagnetic point $\mathbf{k}=\mathbf{k}_0$. In d dimensions we obtain

$$\xi_c=(k_B T/m^2)\chi_{\text{anti}}(T_c)=\hat{\chi}(\mathbf{k}_0,T_c) \simeq\xi_c^{\times}=\left(\frac{a}{r_1}\right)_c^{2-\eta}\frac{(\phi_c^{\eta}/\psi_c)}{(4d)^{1-(\eta/2)}}. \tag{11.4}$$

For the square lattice the estimates of $(a/r_1)_c$ and ϕ_c yield $\xi_c^{\times}=0.1743$ which should be compared with the best direct estimate for ξ_c, namely 0.1570 [obtained by studying the lengthy series expansion for $\chi_{\text{anti}}(v)$[35,52]]. Since the approximation (11.2) was optimized for small k (rather than for small $|\mathbf{k}-\mathbf{k}_0|$), this comparison is a stringent test. Consequently the 11% deviation of $\xi_c^{\times}$ from ξ_c is not too unsatisfactory [and in particular represents a major improvement over the consequences of the first-order expression (11.1)]. To obtain more accurate values near $\mathbf{k}_0$, allowance would have to be made for the nonanalytic drop in $\chi_{\text{anti}}(T)$ [essentially of the form $(T-T_c)|\ln(T-T_c)|$] which occurs as T_c is approached from above.[35] Without further detailed analysis the simplest method of improvement is to add to the right-hand side of (11.2) the k-independent correction term

$$(k_B T/m^2)[\chi_{\text{anti}}(T)-\chi_{\text{anti}}^{\times}(T)], \tag{11.5}$$

where $\chi_{\text{anti}}^{\times}(T)$ is the approximation to $\chi_{\text{anti}}(T)$ implied by (11.2). [The accurate extrapolation formula given in Ref. 35 can be used in evaluating (11.5).] This correction term decreases rapidly from its critical value 0.017, as T increases. Furthermore, for $|\mathbf{k}a|\simeq\frac{1}{2}\pi$ the magnitude of $\hat{\chi}$ reaches unity so that the correction is then only of order 1 or 2%. For the smaller values of k where the enhanced critical scattering is observed it will be relatively smaller by a factor of a tenth or less.

To determine the form of $\phi(T)$ at high temperatures we impose (6.28) which ensures that the pole of the denominator in (11.2) corresponds to the true correlation range κ. This yields

$$\phi^2(T)=32v^8[1-4v+11v^2+\cdots]. \tag{11.6}$$

With this series for ϕ we may expand (11.2) in powers of K and check the accuracy of the coefficient of a^4K^4 (or equivalently Λ^4) by comparison, most easily, with (10.13) to (10.17). This reveals the surprising fact that (11.2) with (11.6) yields the *exact* fourth-order k dependence as far as it is known, i.e., correct to order v^{11}.

Finally to obtain an expression for $\phi(T)$ valid at all temperatures above T_c, we extract the square root of (11.6) and form a Padé approximant for $\phi(v)$ subject to the extra ("second point") condition that $\phi(v_c)=\phi_c$

[52] These estimates have been closely confirmed by W. Marshall and J. L. Gammel (private communication) using Padé approximant techniques.

$=0.02940$. We thus adopt the expression

$$\phi(T)=4\sqrt{2}v^4(1+a_1v)/(1+b_1v+b_2v^2), \quad (11.7a)$$

with

$$a_1=-2.360217, \quad b_1=-0.360217,$$
$$b_2=-4.220435, \quad \text{(square lattice)}. \quad (11.7b)$$

This function is regular and without zeros in the interval $|v|<1.02v_c$. It exhibits a maximum about $1.64\phi_c$ at $T\simeq 1.086T_c$ (for v positive).

In summary, Eqs. (11.2), (11.3), and (11.7), together with (9.3), (9.12), and (9.13), constitute our best approximant to the square lattice scattering function. They embody the k^0, k^2, and k^4 behavior exactly to order v^{11} and the exact small k dependence at $T=T_c$. For ferromagnetic interactions the over-all expressions should be accurate to better than 1 or 2% for all $T\gtrsim T_c$ and all $|\mathbf{k}a|\leq\frac{1}{2}\pi$. With the added correction (11.5), this accuracy will probably be retained for all $\mathbf{k}$. For smaller values of ka the accuracy will improve further, approaching 0.1% or better. Figures 9 and 10 contain plots of the scattering intensity according to (11.2). They will be discussed below.

11.3 Simple-Cubic-Lattice Scattering

To test the second-order approximant for the simple cubic lattice we first use the critical-point scattering amplitude

$$\hat{D}=12.0917\left(\frac{a^3}{v_0}\right)D\simeq\left(\frac{a}{r_1}\right)_c^{2-\eta}\frac{\phi_c{}^{\eta}}{1+\frac{1}{2}\eta\phi_c{}^2}, \quad (11.8)$$

as determined by the estimate (10.7) for D, to fix the value of ϕ_c as previously. [The numerical coefficient in (11.8) follows from (6.5) with $\eta=1/18$.] The central value for D gives

$$\phi_c=0.084, \quad \psi_c=1.00020, \quad \text{(sc lattice)} \quad (11.9)$$

which may be compared with the square lattice values (6.31).

The accuracy for large k may again be assessed by evaluating $\hat{\chi}$ at $\mathbf{k}=\mathbf{k}_0$ via (11.4) which yields $\xi_c{}^{\times}=0.3456$. The best estimate[35,52] for ξ_c is 0.3397 which is only 1.7% lower. In view of the 3% uncertainty in D (see Sec. 10.2) this agreement is excellent and indicates that the second-order approximant should be accurate to 1 or 2% for all $\mathbf{k}$ [without need of the correction (11.5)].

The high-temperature behavior obtained by imposing (6.28), using (8.13) and (8.27), is

$$\phi(T)=12\sqrt{2}v^4[1+\cdots]. \quad (11.10)$$

Only the leading term of ϕ can be found since Λ_2' is known only to order v^9 (even though Λ_2 is known to order v^{10}). By expanding (11.2) in powers of K^2 we can again determine the approximation for Λ_4 to order v^{10} and compare it with the exact series. We discover that when $\mathbf{e}=\mathbf{k}/|\mathbf{k}|$ is parallel to a lattice axis the agreement is exact to this order (as for the square lattice). However, this equivalence does *not* hold for general directions of $\mathbf{k}$; small deviations occur in the v^8 and higher terms. This discrepancy is a direct reflection of the existence of the "excess distributions" found in Sec. 10.4. These cannot be expressed as powers of $\hat{\gamma}(\mathbf{k})$[or $K(\mathbf{k})$] and are therefore necessarily overlooked by (11.2). (The excess distributions do not apparently arise on the square lattice.) One might modify the numerator of the approximant (11.2) so as to represent the angular variation more accurately (or to match the spherically averaged value of Λ_4 rather than its value on an axis) but this does not seem worthwhile since the differences are quite small, the value along an axis *is* given correctly, and the form of (11.2) is, in any case, not exact.

For use at all temperatures we adopt the simple Padé approximant

$$\phi(T)=12\sqrt{2}v^4/(1+b_1v), \quad (11.11a)$$

with

$$b_1=-0.4026, \quad \text{(sc)}. \quad (11.11b)$$

This function is regular and monotonic in the interval $|v|<1.8v_c$ and reproduces the desired value at the critical point. Together with (11.2), (11.3), (9.3), (9.12), and (9.13) it constitutes our best over-all approximant for the simple cubic lattice scattering. These formulas should be accurate to within 1 or 2% for all $\mathbf{k}$ and all $T\gtrsim T_c$ but appreciably more accurate for $T>T_c$ and k moderately small. If $\phi(T)$ is simply replaced by its critical value ϕ_c accuracy suffers very little. The deviation in $\hat{\chi}$ never exceeds 0.6% and is always less than 0.1% for $ka<1$ and less than 0.01% for $ka<0.2$. Plots of the scattering are given in Figs. 11, 12, and 13, and are discussed below.

11.4 Other Lattices

Table XIII collects together the values of $\hat{D}$ following from Table IX and (6.5) and the corresponding values of ϕ_c and ψ_c for the square, sc, and other lattices. (In three dimensions the uncertainties in D correspond to uncertainties in ϕ_c of about 20% but owing to the small value of η this evidently corresponds to only 1 or 2% in $\hat{\chi}$.)

For the triangular lattice two leading terms of the expansion of ϕ may be determined from (8.27). The Padé approximant

$$\phi(T)=4\sqrt{2}v^3/(1+b_2v^2), \; b_2=37.633, \; \text{(triangular)} \quad (11.12)$$

reproduces the critical value; it is monotonic and regular for all real v and should yield a satisfactory approximation for $\hat{\chi}$. It is not possible to check the accuracy at $\mathbf{k}=\mathbf{k}_0$ by comparison with the antiferromagnetic case since the symmetry relation applies only to the loose-packed lattices. There is little reason to doubt, however, that the accuracy will be nearly comparable with that obtained on the square lattice, i.e., within 1 or 2% for all $T\gtrsim T_c$ for $|\mathbf{k}a|\leq\frac{1}{2}\pi$.

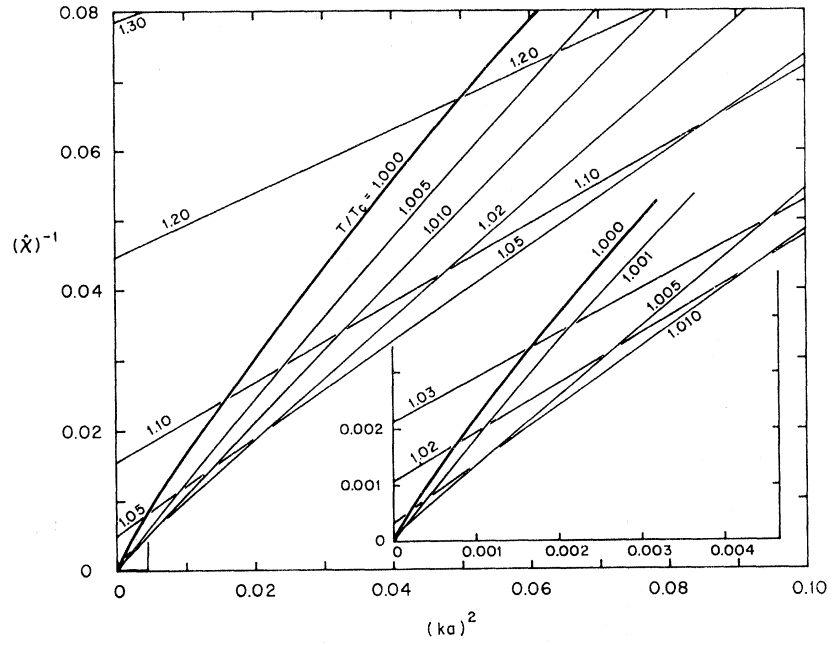

FIG. 9. Inverse scattering intensity of the square lattice versus $(ka)^2$ for $\mathbf{k}$ parallel to a principal diagonal and for various values of T/T_c. Note change of scale for inset.

For the bcc lattice evaluation of the approximant to $\hat{\chi}$ at $\mathbf{k}=\mathbf{k}_0$ yields $\xi_c^{\times}=0.3686$ compared with the best estimate[35] of $\xi_c=0.3692$. The very close agreement (within 0.2%) is probably fortuitous in view of the uncertainties of the estimate for D but it does again suggest that the second-order approximant should be accurate to 1 or 2% for all $\mathbf{k}$ in three dimensions. For the fcc lattice this check is again impossible but quite comparable accuracy should obtain.

TABLE XIII. Values of the critical-point scattering parameters.

Lattice	$\hat{D}$	ϕ_c	$(\psi_c-1)\times10^3$
Square	1.07499	0.02940	0.108
Triangular	1.18100	0.02940	0.108
sc	3.87	0.084	0.20
bcc	4.13	0.073	0.15
fcc	4.24	0.065	0.12

For both these lattices the high-temperature expansion of ϕ cannot be computed since the series expansions for κ or Λ_2' are not yet derived. However, the graph-theoretical arguments at the end of Sec. 10.4 suggest that $\phi(v)$ is probably of order v^3 for both lattices. For this reason we propose the simple expressions

$$\phi(T)=\Phi v^3 \tag{11.13a}$$

with

$$\Phi=19.191 \text{ (bcc)}, \quad \Phi=62.045 \text{ (fcc)}. \tag{11.13b}$$

The amplitude Φ is of the order of magnitude expected by analogy with the simple cubic result (11.10). The still simpler alternative of setting $\phi\equiv\phi_c$ should be almost as accurate as verified on the simple cubic lattice.

11.5 Discussion

The accuracy of the formula (11.2) for the scattering having been assessed above, we may examine its consequences graphically. Figure 9 shows a conventional plot of inverse scattering intensity versus $(ka)^2$ for $\mathbf{k}$ parallel to a main diagonal of the square lattice. The curvature

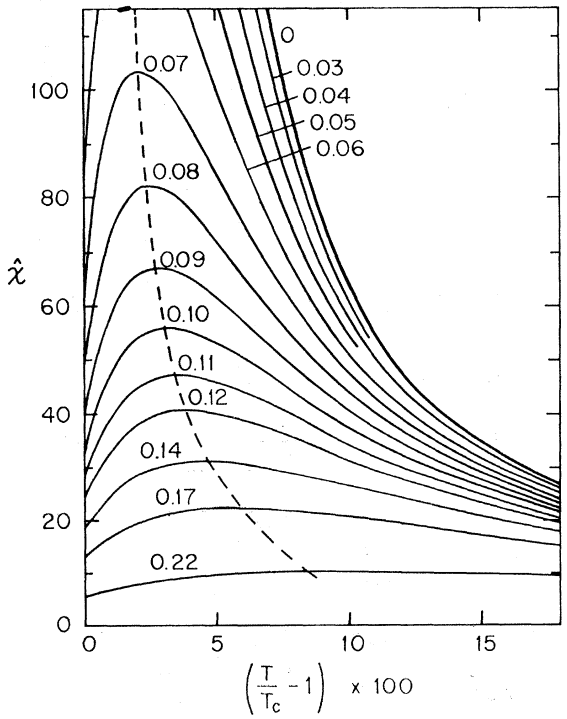

FIG. 10. Variation of the scattering intensity of the square lattice with temperature for fixed wave number. (The curves are labeled by the values of $k_x a=k_y a$.)

of the critical-point isotherm (marked $T/T_c=1.000$) corresponding to the value $\eta=\frac{1}{4}$ is clearly seen and the vertical tangent as $(ka)^2\to 0$ can easily be imagined. Surprisingly, perhaps, the isotherms appear at first to *fall* as the temperature increases. This is quite contrary to expectations based on the approximate theories. The large scale inset (of the region marked off near the origin) shows that this fall occurs, as it must, only for large enough values of k, since the plots for $T>T_c$ intersect the critical isotherm at small k. The meaning of this strong "line-narrowing" behavior becomes more apparent from Fig. 10 where the intensity is plotted versus temperature for fixed wave number. (The curves are labeled by the values of $k_xa=k_ya$.) Evidently the scattering intensity at a fixed angle goes through a *maximum above* T_c and then falls as the critical point is approached more closely.[53] There can be no doubt as to the reality of this maximum since for moderately large ka it occurs so far above T_c as to be predicted by the truncated series expansions without any extrapolation. For $T/T_c<1.05$ the relative temperature of the maximum $T_{\max}/T_c$, is linearly related to ka with a moderately large coefficient so that the difference $T_{\max}-T_c$ should be readily detectable in experiments on two-dimensional

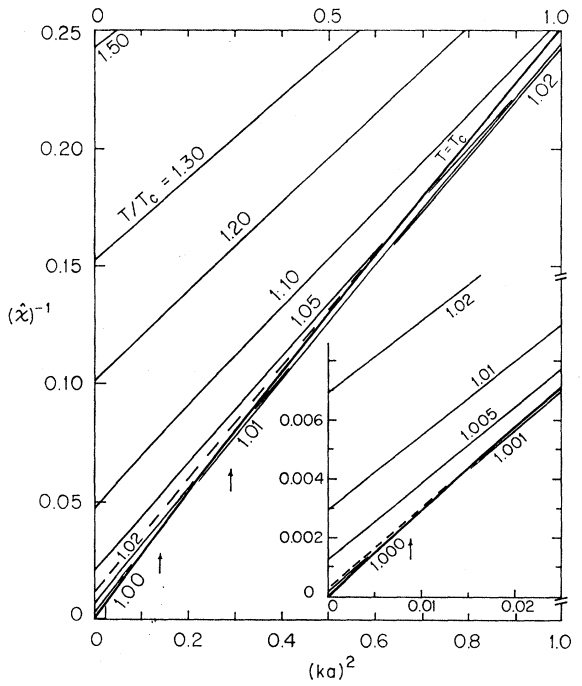

FIG. 11. Inverse scattering intensity of the simple cubic lattice versus $(ka)^2$ for **k** parallel to a principal diagonal and for various values of T/T_c. The dashed straight lines are tangent to the critical isotherms at the high ka values. The arrows indicate intersections with isotherms for higher T.

[53] According to (11.2) the intensity displays a point of inflection much closer to T_c and finally approaches the critical point with rather small slope. It may be doubted, however, whether the present extrapolation formulas can be relied on for such a subtle point so relatively close to T_c. The effect is quite invisible on the scale of these figures.

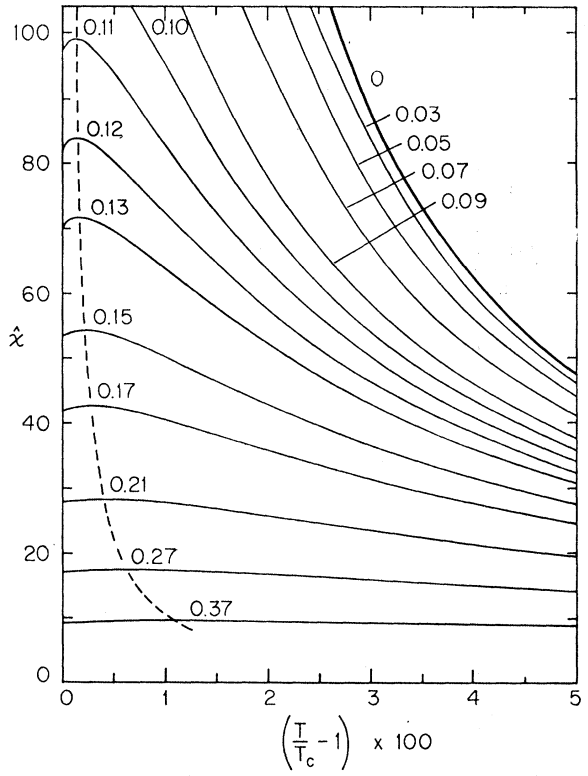

FIG. 12. Scattering intensity of the simple cubic lattices versus temperature. (The curves are labeled by the values of $k_xa=k_ya=k_za$.)

systems (e g., scattering from foreign absorbed atoms in equilibrium on a crystalline face). Depending on the scale, the curvature of the isotherms of $\hat{\chi}^{-1}$ versus $(ka)^2$ persists to 1 or 2% above T_c but thereafter the plots become rapidly very linear.

On the scale of Figs. 9 and 10, the scattering for k parallel to a lattice axis, instead of a diagonal, is indistinguishable, i.e., the scattering is quite isotropic. Numerically the intensities at $T=T_c$ for axis and diagonal differ by 0.1% when $ka\simeq 0.17$ and by 1% when $ka\simeq 0.52$. The fractional differences at $T/T_c=1.05$ are very similar. These figures indicate the point at which the lattice structure becomes detectable.

In Fig. 11 the inverse scattering for the simple cubic lattice with **k** parallel to a principal diagonal is plotted versus $(ka)^2$. The critical isotherm is definitely curved, as can be seen by comparison with the dashed straight line which is tangent at the higher ka values. Because of the small value of η, however, the curvature is not obvious and could easily be obscured in a real system by experimental uncertainties in the data. (There is no sign graphically of the theoretically infinite divergence of the slope of the isotherm as $ka\to 0$!) Dependent on the range of $(ka)^2$, the plots examined are already very linear at only 0.5 to 1% above T_c. The line narrowing observed with the square lattice is also much less marked but each isotherm does eventually intersect the critical isotherm and thereafter lie below it. The intersections

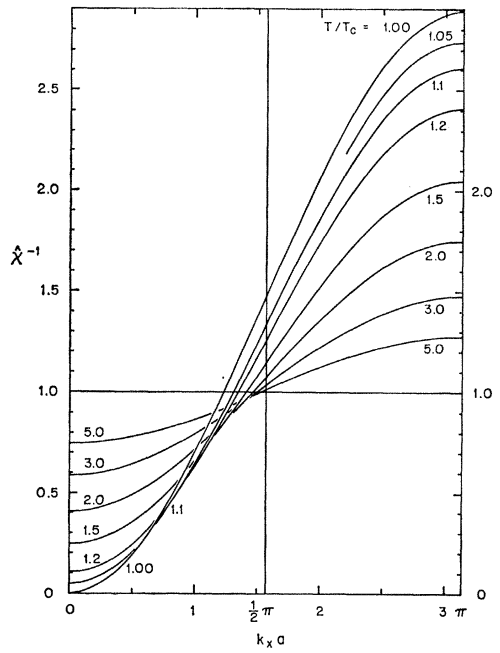

FIG. 13. Complete variation of the inverse scattering intensity for $\mathbf{k}$ parallel to a principal diagonal of the simple cubic lattice ($k_x=k_y=k_z$). Note the displacement of the "neutral point" $\hat{\chi}=1$ as T falls.

for $T/T_c=1.01$, 1.02, and 1.001 (in inset) are marked on the figure by vertical arrows. The corresponding maxima in $\hat{\chi}$ versus T at fixed ka are visible in Fig. 12. Comparison with Fig. 10 (note different temperature scales) shows that the maxima now occur far closer to the critical point. Furthermore instead of varying linearly with ka the difference $T_{\max}-T_c$ varies as $(ka)^{1/\nu}$. The general relation as T approaches T_c is

$$F\left(\frac{T_{\max}}{T_c}-1\right)^{\nu}\approx\left(\frac{\eta\psi_c-\phi_c^2}{2-\eta}\right)^{1/2}ka\{1+O[(ka)^{1/\nu}]\}, \tag{11.14}$$

so that the coefficient of proportionality is rather small. As a consequence when, for example, $ka=0.1$ the maximum occurs only 0.05% above T_c compared with 2.2% on the square lattice. Even at $ka=1$ the simple cubic maximum occurs only some 3% above T_c. Similarly the height of the maximum relative to the value of $\hat{\chi}(\mathbf{k},T)$ at the critical point is about 1.019 compared to about 1.67 for the square lattice. For this reason it may be difficult in low-angle experiments to resolve the temperature of the maximum from the critical point itself. However, in precise work the critical temperature should obviously not be determined from the position of a maximum at finite $\mathbf{k}$. Probably, as in the case of the antiferromagnetic susceptibilities,[35,50] T_c is located at the point of steepest decrease of $\hat{\chi}(\mathbf{k},T)$ with falling T, i.e., at a (mild) singularity in $\partial\hat{\chi}/\partial T$.[53a]

The degree of spherical isotropy and the influence of lattice structure may be gauged by comparison with scattering for $\mathbf{k}$ parallel to an axis. At the critical point, differences of 0.01, 0.1, and 1% are observed at $ka\simeq0.04$, 0.14, and 0.43, respectively, while when $T/T_c=1.05$ the corresponding wave numbers are $ka\simeq0.12, 0.23$, and 0.49.

Finally in Fig. 13 the inverse scattering intensity of the simple cubic lattice with $\mathbf{k}$ parallel to a main diagonal is plotted versus k_xa ($=k_ya=k_za$) over the whole range up to the antiferromagnetic point $\mathbf{k}=\mathbf{k}_0$. The displacement of the "neutral point" $\hat{\chi}=1$ from the midpoint to lower $\mathbf{k}$ values is indicative of the line narrowing near T_c and the maxima at fixed $\mathbf{k}$. Evidently the displacement is quite marked even at $T=3T_c$ although it is not, of course, predicted by mean field theory. The scattering intensity about the antiferromagnetic point $\mathbf{k}=\mathbf{k}_0$ is at a minimum but is not otherwise anomalous.

We present no figures for the bcc, fcc, or triangular lattices because of the close similarity to the sc and square lattices, respectively. Clearly, however, experimental data should be compared with the theory for the appropriate lattice so that the significance of any deviations will not be obscured. The explicit magnitude of the dependence on lattice structure can be gauged by comparing the different rows in Tables VI, VII, IX, and XIII bearing in mind that all wave vectors and distances have been scaled by the nearest-neighbor distance a (rather than by the cube edge a' or other factor).

11.6 Conclusion

We conclude by comparing our theoretical predictions with the recent experiments on pure beta-brass by Als-Nielsen and Dietrich[12] who studied the ordering transition by neutron scattering techniques making careful corrections for finite resolution and other limiting factors. (Comparisons with other relevant experiments have been discussed elsewhere.[3,5,13,15]) However, attention should also be drawn to more recent experiments on the binary fluid system perfluorheptane-iso-octane by Brady, McIntyre, Myers, and Wims[54] in which they find that $\eta\simeq0.10$ gives a good account of the observed curvature in the scattering plot close to T_c. [See also the *note added in proof* (Ref. 53a).]

Als-Nielsen and Dietrich first measured a scattering isotherm at 1.2% above $T_c(=741°\text{K}, \Delta T=8.9°K)$ in an angular range $0\leqslant|\mathbf{k}a|<0.64$. They found the k dependence could be well fitted by the Ornstein-Zernike form but on using our first-order approximant (11.1) with various values of η they found a shallow minimum in the total squared deviation at $\eta=0.03$; the fit at $\eta=1/18$ appeared to be about as good as at $\eta=0$.[55]

They then measured the peak intensity $\hat{\chi}(k=0,T)$ in the decade $T/T_c=1.003$ to 1.030 and from a least-

[53a] *Note added in proof.* Dr. L. Passel has kindly pointed out that recent neutron-scattering experiments on iron by D. Bally, B. Grabeev, A. M. Lungu, M. Popovici, and M. Totia, at Bucharest, have revealed a maximum in $\hat{\chi}$ at fixed $k\neq0$ *above* T_c, just as predicted here. Furthermore, the observed values of $T_{\max}-T_c$ seem to be of the same order of magnitude as we find, and the critical point is located on the steepest portion of the $\hat{\chi}$-versus-T curve.

[54] G. W. Brady, D. McIntyre, M. E. Myers, Jr., and A. M. Wims, J. Chem. Phys. 44, 2197 (1966); see also Proceedings of the Small Angle X-Ray Conference, Syracuse University, 1966 (to be published).

[55] In Eq. (11.1) Ka was replaced by ka. The second-order formula (11.2) has not yet been fitted to the data.

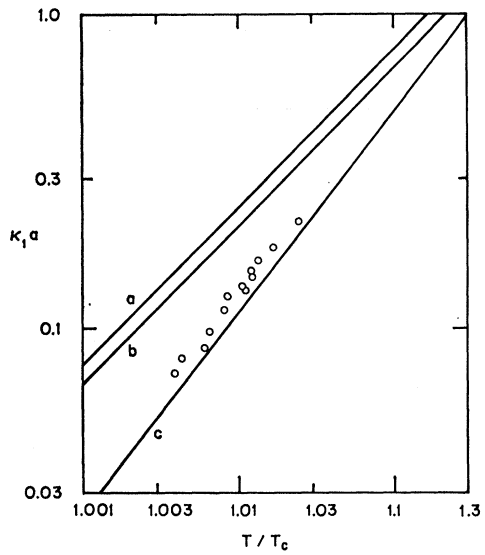

FIG. 14. Logarithmic plot of the experimental data on $\kappa_1 a$ for beta-brass as a function of temperature. The curves are the predictions of (a) mean field theory, (b) the Elliott-Marshall-Bethe approximation, and (c) the present analysis of the bcc Ising nearest-neighbor model.

squares fit on a log-log plot deduced the result $\gamma=1.252\pm0.006$ or, allowing conservatively for possible systematic errors, $\gamma=1.25\pm0.02$.[12] This value is, of course, exactly the prediction for the three-dimensional Ising models! The range of correlation κ_1 was determined in the same temperature interval by fitting the observed angular dependence.[56] These experimental results are shown on a log-log plot in Fig. 14 together with the predictions of mean field theory, the Bethe-Elliott-Marshall approximation, and the present analysis for a bcc lattice. A least-squares fit to a straight line on this plot yielded $\nu=0.647\pm0.022$ in remarkable agreement with our Ising-model estimate of $\nu=0.643\pm0.003$. Through the relation $(2-\eta)\nu=\gamma$ Als-Nielsen and Dietrich finally estimated $\eta=0.077\pm0.067$ compared with our estimate of $\eta=0.056\pm0.008$. As evident from Fig. 14, the observed amplitude F_1 for κ_1 is slightly larger than our estimate; the experimental-to-theoretical ratio was 1.17 ± 0.13.

The very close agreement of these results with our analyses of the Ising model is most satisfying. While it may be premature to draw physical conclusions (e.g., about effective higher-neighbor interactions, etc.) from observed deviations in amplitudes, it is clear that the Ising model provides an excellent detailed account of the order-disorder process in beta-brass.[57] One may in the future hope to see it tested as precisely in other real physical systems thereby increasing and deepening our insight into critical phenomena.

APPENDIX A

Values of the parameter f relating the correlation ranges in Eq. (4.17) and (4.18) are given in Table XIV.

TABLE XIV. Values of the parameter f relating the correlation ranges in Eqs. (4.17) and (4.18).

Lattice	Direction parallel to:	f^2
square	axis	1
	diagonal	$\frac{1}{2}$
triangular	normal to bond	$\frac{3}{4}$
sc	cube edge (axis)	1
	face diagonal	$\frac{1}{2}$
	major (body) diagonal	$\frac{1}{3}$
bcc	cube edge	$\frac{1}{3}$
	face diagonal	$\frac{2}{3}$
fcc	cube edge	$\frac{1}{2}$

APPENDIX B

Expansion coefficients for moments and correlations are given in Tables XV–XVIII.

TABLE XV. Coefficients for the expansion of the zeroth and second correlation moments in powers of v; see Eqs. (3.7), (7.7), and (7.9).

	Square		Triangular		sc		bcc		fcc	
n	$m_n^{(0)}$	$m_n^{(2)}$	$m_n^{(0)}$	$m_n^{(2)}$	$m_n^{(0)}$	$m_n^{(2)}$	$m_n^{(0)}$	$m_n^{(2)}$	$m_n^{(0)}$	$m_n^{(2)}$
1	4	4	6	6	6	6	8	8	12	12
2	12	32	30	72	30	72	56	128	132	288
3	36	164	138	582	150	582	392	1416	1404	4908
4	100	704	606	3912	726	4032	2648	13 568	14 652	72 096
5	276	2708	2586	23 550	3510	25 542	17 864	119 240	151 116	973 116
6	740	9696	10 818	131 640	16 710	153 000	118 760	992 768	1 546 332	12 432 096
7	1972	32 948	44 574	697 422	79 494	880 422	789 032	7 948 840	15 734 460	
8	5172	107 648	181 542	3 547 392	375 174	4 920 576	5 201 048	61 865 344	159 425 580	
9	13 492	340 916	732 678		1 769 686	26 879 670	34 268 104			
10	34 876	1 052 960	2 935 218		8 306 862	144 230 088				
11	89 764	3 185 188	11 687 202		38 975 286					
12	229 628		46 296 210							

[56] The observed temperature dependence of κ_1 is not changed if $\eta=0$ or $\eta=1/18$ is assumed in this fitting. Note also that a slightly different definition of κ_1 was used in Ref. 12.

[57] It should be remarked that Als-Nielsen and Dietrich have also made measurements below T_c which again correspond closely to Ising-model predictions although this is not the place to discuss them.

TABLE XVI. Square lattice: correlation function expansion coefficients $q_n(\mathbf{r})$ with $\mathbf{r}=(\pm la, \pm ma)$ or $(\pm ma, \pm la)$; see Eq. (7.1).

	n						n				
l, m	1	3	5	7	9	11	l, m	2	4	6	8	10
1, 0	1	2	4	12	42	164	1, 1	2	4	10	32	118
							2, 0	1	6	16	46	158
2, 1		3	11	31	97	351						
3, 0		1	12	48	152	506	2, 2		6	24	76	248
							3, 1		4	26	92	298
3, 2			10	55	201	684	4, 0		1	20	118	452
4, 1			5	52	244	885						
5, 0			1	30	250	1200	3, 3			20	120	480
							4, 2			15	118	521
4, 3				35	259	1176	5, 1			6	92	574
5, 2				21	231	1266	6, 0			1	42	474
6, 1				7	149	1215						
7, 0				1	56	826	4, 4				70	560
							5, 3				56	532
5, 4					126	1176	6, 2				28	416
6, 3					84	1026	7, 1				8	226
7, 2					36	699	8, 0				1	72
8, 1					9	326						
9, 0					1	90	5, 5					252
							6, 4					210
6, 5						462	7, 3					120
7, 4						330	8, 2					45
8, 3						165	9, 1					10
9, 2						55	10, 0					1
10, 1						11						
11, 0						1						

TABLE XVII. Simple cubic lattice: correlation function expansion coefficients $q_n(\mathbf{r})$ with $\mathbf{r}=(\pm ka, \pm la, \pm ma)$ or other permutations of k, l and m; see Eq. (7.1).

	n						n						n
k, l, m	1	3	5	7	9	k, l, m	9	k, l, m	2	4	6	8	10	k, l, m	10
1, 0, 0	1	4	40	456	6100	3, 3, 3	1680	1, 1, 0	2	16	170	2144	30 334	4, 3, 3	4200
						4, 3, 2	1260	2, 0, 0	1	12	176	2348	33 804	4, 4, 2	3150
1, 1, 1		6	54	648	8840	4, 4, 1	630							5, 3, 2	2520
2, 1, 0		3	47	649	9199	5, 2, 2	756	2, 1, 1		12	168	2424	36 088	5, 4, 1	1260
3, 0, 0		1	24	504	8368	5, 3, 1	504	2, 2, 0		6	144	2272	35 312	5, 5, 0	252
						5, 4, 0	126	3, 1, 0		4	106	1976	33 054	6, 2, 2	1260
2, 2, 1			30	540	8700	6, 2, 1	252	4, 0, 0		1	40	1156	24 136	6, 3, 1	840
3, 1, 1			20	430	7802	6, 3, 0	84							6, 4, 0	210
3, 2, 0			10	355	6981	7, 1, 1	72	2, 2, 2			90	1800	31 410	7, 2, 1	360
4, 1, 0			5	202	5006	7, 2, 0	36	3, 2, 1			60	1480	28 220	7, 3, 0	120
5, 0, 0			1	60	2300	8, 1, 0	9	3, 3, 0			20	960	21 960	8, 1, 1	90
						9, 0, 0	1	4, 1, 1			30	936	21 474	8, 2, 0	45
3, 2, 2				210	5250			4, 2, 0			15	748	18 647	9, 1, 0	10
3, 3, 1				140	4340			5, 1, 0			6	344	11 050	10, 0, 0	1
4, 2, 1				105	3507			6, 0, 0			1	84	4140		
4, 3, 0				35	2219										
5, 1, 1				42	1806			3, 3, 2				560	16 240		
5, 2, 0				21	1407			4, 2, 2				420	13 440		
6, 1, 0				7	541			4, 3, 1				280	11 060		
7, 0, 0				1	112			4, 4, 0				70	5600		
								5, 2, 1				168	7392		
								5, 3, 0				56	4564		
								6, 1, 1				56	3184		
								6, 2, 0				28	2432		
								7, 1, 0				8	802		
								8, 0, 0				1	144		

TABLE XVIII. Expansion coefficients for fourth and sixth moments on the square and simple cubic lattices [see Eqs. (3.7)].

	Square		sc			Square		sc	
n	$m_n^{(4)}$	$m_n^{(6)}$	$m_n^{(4)}$	$m_n^{(6)}$	n	$m_n^{(4)}$	$m_n^{(6)}$	$m_n^{(4)}$	$m_n^{(6)}$
1	4	4	6	6	7	693 940	16 836 020	12 868 422	224 595 942
2	96	320	192	576	8	2 805 120	84 131 072	85 697 280	1792 799 232
3	932	5924	2742	14 694	9	10 743 220	388 949 684	546 306 582	13 397 954 550
4	6208	62 336	28 032	225 792	10	39 400 288	1690 053 440	3364 458 048	95 064 939 840
5	33 684	480 788	239 382	2632 230	11	139 444 004	6980 530 084		
6	160 160	3046 080	1824 960	25 803 072					

APPENDIX C

Expansion coefficients for the reduced second moments $(2d/q)\Lambda_2^{(v)}$ are given in Table XIX.

TABLE XIX. Expansion coefficients for the reduced second moments $(2d/q)\Lambda_2(v)$.

n	Square $\lambda_n^{(2)}$	Triangular $\frac{2}{3}\lambda_n^{(2)}$	sc $\lambda_n^{(2)}$	bcc $\frac{3}{4}\lambda_n^{(2)}$	fcc $\frac{1}{2}\lambda_n^{(2)}$
1	1	1	1	1	1
2	4	6	6	8	12
3	13	31	31	57	133
4	40	148	156	400	1424
5	117	673	765	2729	14 949
6	332	2962	3714	18 472	154 980
7	921	12 731	17 827	123 597	
8	2512	53 776	85 144	823 632	
9	6757		404 073		
10	18 004		1 912 222		
11	47 493				

APPENDIX D

Padé approximant coefficients for evaluating $r_1(T)$ from Eqs. (9.12) and (9.13) are given in Table XX.

TABLE XX. Padé approximant coefficients for evaluating $r_1(T)$ from Eqs. (9.12) and (9.13).

	Square	Triangular	sc	bcc	fcc
a_1	−0.285714	−0.428571	−0.085714	−0.114286	−0.171429
a_2	−0.652146	0.139989	0.523635	2.543144	1.218250
a_3	−0.384998	−6.587258	−1.168644	1.230130	···
a_4	−1.879136	···	−0.689180	−4.907585	···
a_5	−0.981609	···	6.724875	···	···
b_1	3.032511	−1.159975	−2.275743	−20.877508	−9.189792
b_2	1.288541	16.003582	−2.089506	−53.803544	9.478733
b_3	5.342517	−12.366329	43.544196	312.393280	25.878960
b_4	11.019412	4.094098	−47.883490	···	···
b_5	−6.536274	···	···	···	···

APPENDIX E

Glossary of principal symbols is given in Table XXI.

TABLE XXI. A glossary of principal symbols.

Symbol	Meaning	Introduced in[a]
a; a'	Lattice spacing; edge of cubic cell	2.1
B_0, B_1	Temperature coefficient for $\log_{10}\kappa_1 a$	(9.9)VI
b	Temperature coefficient for κa	(5.24)
C, C'	Susceptibility amplitudes at T_c	(6.8)(6.17)IX
$C(\mathbf{r})$	Direct correlation function for fluid	(3.13)
c	Temperature coefficient for r_1/a	(9.14)VII
c_n	Number of n-step self-avoiding walks	7.1(7.8)
D	Amplitude for correlation decay at T_c	(5.8)(5.29)(10.6)IX
$\hat{D}$	Amplitude of scattering at T_c	(3.19)(5.10)(6.5)XIII
d	Dimensionality	
$E(\mathbf{r})$, E_1	Amplitude of logarithmic singularity in $\Gamma(\mathbf{r},T)$	(5.2)VIII
$\mathbf{e}$	Unit vector	(3.24)
$\mathcal{E}\{\ \}$	Even part of	
F, F_1	Amplitudes for κa and $\kappa_1 a$ at T_c	(5.24)(6.7)(6.13)(9.10)
$G(\mathbf{r})$, $g_2(\mathbf{r})$	Fluid pair correlation functions	(2.17)
$\hat{G}(\mathbf{k})$	Fourier transform of $G(\mathbf{r})$	(2.18)
$\mathcal{G}_t(p)$	Spectral density of transfer matrix	(5.18)
$H(\mathbf{r})$, $\hat{H}(\mathbf{k})$	Lattice direct correlation function and its transform	(3.11)
$H_n(v)$	Expansion coefficient for $\hat{\mathbf{H}}(\mathbf{k})$	(10.13)(10.21)
I, I_0	Scattering intensity	(2.9)
$\mathrm{Im}\{\ \}$	Imaginary part of	
J, J_x, J_y	Exchange integrals	(2.3)(2.13)
J_i, j_i	Junction orders	7.4
K_T	Isothermal compressibility	(2.16)
$K(\mathbf{k})$	Effective wave vector for lattice	(2.2)
$\mathbf{k}$, $k=\lvert\mathbf{k}\rvert$, k_x, k_y, k_z	Wave vector, modulus, and components	2.2
$\mathbf{k}_0$	Superlattice wave vector	(3.2)
$k_\alpha(\mathbf{e};T)$	Complex singularity of $\hat{\chi}(\mathbf{k})$	(3.25)
k_B	Boltzmann's constant	
l	Length in units of lattice spacing	(5.5)(5.14)
M, m	Magnetization, magnetic moment	(2.7)
$m_n^{(t)}$, $m_n(f,g,h)$	Expansion coefficients for the moments $\mu_t(v)$ etc.	(7.7)(7.9)(10.1)
N	Total number of lattice sites	2.1
$O(\ )$	Term of order	
$\mathcal{O}\{\ \}$	Odd part of	
$Q(x)$	Term in asymptotic scattering function	(5.30)

[a] Decimals 2.1, 9.3, ··· denote subsections; numerals in parentheses (9.3), (3.27), ··· denote equations; Roman numerals IX, VI, ··· denote tables.

TABLE XXI. (*continued*).

Symbol	Meaning	Introduced in[a]
q	Coordination number	2.1
$q(\mathbf{k})$	Lattice generating function	(2.1)
$q_n(\mathbf{r})$, $\hat{q}_n(\mathbf{k})$	Expansion coefficients of $\Gamma(\mathbf{r})$ and $\hat{\Gamma}(\mathbf{k})$	(7.1)(7.4)
R^2	Squared distance between vertices	(7.10)(7.20)
$\mathbf{r}$, $r=\|\mathbf{r}\|$	Position vector and its modulus	
r_1, $r_1(T)$	Effective range of direct interaction	(6.24), (4.5)–(4.7)
$\mathcal{R}_m$	Remainder after m terms	(9.3)
s, s_0, s_i, $s_\mathbf{r}$	Spin variables ($=\pm 1$)	(2.3)
T, T_c	Temperature, critical temperature	
t	Index; temperature variable$=v/v_c$	
U	Configurational energy	(2.12)
v	Temperature variable$=\tanh(J/k_BT)$	(2.4)
v_0	Volume of lattice cell (per site)	2.1
α	Label of singularities of $\hat{\chi}(\mathbf{k})$	(3.25)
γ	Exponent of divergence of susceptibility	(3.22)
$\hat{\gamma}(\mathbf{k})$	Normalized lattice generating function	(2.1)
$\Gamma(\mathbf{r})$	Lattice (spin pair) correlation function	(2.5)(2.6)(2.11)
$\hat{\Gamma}(\mathbf{k})$	Fourier transform of lattice correlation function	(2.10)(2.18)
$\mathbf{\Gamma}(z)$	Gamma function of argument z	
δ	Increment or shift to n	(8.20)
$\boldsymbol{\delta}$, $\|\boldsymbol{\delta}\|=a$	Nearest-neighbor lattice vector	2.1
Δ_2	Coefficient in scattering function	(6.3)(6.13)
η	Exponent of correlation decay and scattering at T_c	(3.19)(5.29)(10.6)
θ; ϑ	Angles; subscript denoting a theta graph	7.1, Ref. 36
κ, $\kappa_e(T)$	True inverse range of correlation	(3.24)(3.27)
κ_1, $\kappa_1(T)=1/\Lambda$	Effective inverse range of correlation	(3.20)
Λ_2, Λ_4, $\bar{\Lambda}_4$, $\cdots$	Reduced correlation moments and expansion coefficients of $1/\hat{\chi}(\mathbf{k})$	(3.14)
Λ'_2	Effective reduced second moment of correlation	(4.16)
μ_t, $\mu_{f,g,h}(v)$	Moments of the correlation function	(3.7)(3.10)
ν, ν_1	Exponent of vanishing of κ, κ_1 at T_c	(3.29)(3.23)
$\nu^*\{v,W\}$	Generalized exponent function for ν	(8.12)
ξ_t, $\xi(T)$	Band edges of transfer matrix	(5.26)
ξ_c, $\xi_c^\times$	Reduced critical-point antiferromagnetic susceptibilities	(11.4)
ρ, ρ_c	Density, critical density	(2.14)(2.15)
τ	$(T/T_c)-1$	(4.11)
$\varphi(\mathbf{r})$	Pair potential energy	(2.13)
ϕ, $\phi(T)$	Component of scattering function	(6.27)(6.29)
ψ,$\psi(T)$	Related to Λ_2, Λ_2', and ϕ	(6.23)(6.25),(6.28)(6.29)
χ_T	Isothermal susceptibility	(2.7)(2.16)
χ_0	Reduced susceptibility/compressibility	(2.8)(2.11)
$\hat{\chi}(\mathbf{k},T)$	Scattering function (reduced scattering intensity)	(2.9)
ω	Decay factor	(4.8)(4.18)

ACKNOWLEDGMENTS

We are much indebted to colleagues and associates at King's College, London, where much of this work was performed, for their interest, advice, and help. In particular Professor C. Domb and Dr. M. F. Sykes kindly made available extensive data on self-avoiding walks and other lattice configurations while Dr. D. S. Gaunt assisted most expertly with many of the numerical calculations. It is also a pleasure to thank Professor L. P. Kadanoff and Dr. J. Als-Nielsen for stimulating correspondence and reports of their work, and Professor B. Widom and Dr. J. F. Nagle for comments on the manuscript. The encouragement and comments of many other colleagues over a course of some years have been most welcome. The partial support of the U. S. Department of the Army through its European Research Office, of the Advanced Research Projects Agency through the Materials Science Center at Cornell University, and of the Science Research Council (for a maintenance grant to R. J. B.) is gratefully acknowledged.